Characterization of pH-Dependent Poly(Acrylic Acid)-Vesicle Interaction and its Application in Cellular Drug Delivery

Thesis by

Mitsuko Fujiwara

In Partial Fulfillment
of the Requirements for
the Degree of Doctor of Philosophy

California Institute of Technology
Pasadena, California

1993

(submitted February 26, 1993)

Acknowledgments

I would like to thank both of my advisors, John D. Baldeschwieler and Robert H. Grubbs, for allowing me to pursue an interdisciplinary project, in which I had the opportunity to study both polymer science and biophysics of liposomes along with some cell biology. It was both an interesting and challenging project. I could not have asked for a better learning experience.

I would also like to thank the past and present members of both JDB and RHG research groups for their company and support. To name a few, Tracy Handel first got me interested in studying polymer-liposome interaction. Ray Goodrich has provided many enlightening discussions in the initial phase of the project. Chris DiSimone was a reliable and helpful member of the Bio group. I would like to thank Van for his help with cell culture, especially looking after my cells while I was out of town and for reading part of my thesis. Both Chris and Joon were great for bouncing off ideas and for asking questions in biochemistry. Roxanne, the social coordinator of the group, kept the JDB group close and friendly. Since I spent most of my time in the JDB lab, Elizabeth offered a lot of help finding my way around in the RHG lab. I wish Steve and Tom good luck with the rest of their stay in the JDB group and Mike and Bob with their new jobs.

I'm grateful to my friends from Cornell, who are now scattered all over the world, for keeping in touch with me to bring happiness and fond memories back and for listening to my gripes during my graduate life at Caltech.

My deepest gratitude goes to my family for their support throughout my life and to Richard for his company for the last four years.

Abstract

Polymers can be used to control drug targeting and drug release from phospholipid vesicles through changes in pH. Understanding the effect of polymers on vesicle properties is important in obtaining a better control over drug delivery using phospholipid vesicles. The pH-dependent interaction of poly(acrylic acid) (PAA) with phosphatidylcholine (PC) vesicles (bilayers) and monolayers was investigated to elucidate the mechanism of PAA-induced vesicle destabilization. PAA induced aggregation of vesicles below pH 4.6 and lipid intermixing of vesicles below pH 4.1. Mixing of aqueous contents was not observed, indicating that the process is not a true membrane fusion. An increase in the membrane permeability accompanied lipid intermixing of vesicles. Both the hydrocarbon chain and phospholipid headgroup packing was more disordered from polymer association as evidenced by the increase in the CH_2 asymmetric stretching peakwidth and peak position and by the increase in the binding of potential-sensitive dye to the vesicle surface, respectively. Polymer binding to vesicles at pH 3.8 showed a negative cooperativity with a K_b of 1.5×10^6 M^{-1}. The driving force for PAA adsorption on vesicles is the formation of hydrogen-bonds between the protonated carboxyl groups of the polymer and the phospholipid molecule. The polymer mobility was restricted upon complexation with vesicles as evidenced by the anisotropy measurements of polymer-associated fluorophore. The polymer-associated vesicles exhibited fused vesicles and tubular structures in freeze-fracture images. Formation of nonbilayer phases or phase separation was not detected in freeze-fracture images or ^{31}P-NMR powder spectra of PC vesicles. PAA induced expansion of PC monolayers at low pH, and the extent of expansion was dependent on the monolayer surface pressure and on the pH of the subphase. Polymer-induced expansion became more difficult at increasing monolayer

packing density and increasing pH. Therefore PAA-induced destabilization of vesicles is believed to be initiated by partial penetration of PAA on vesicle surface. The stress on the membrane created by PAA association presumably resulted in the rupture of bilayer and lipid intermixing of vesicles.

Table of Contents

Chapter 1

Introduction

The understanding of polymer interaction mechanisms with phospholipid vesicles is an area of growing importance, which has application to drug delivery. Phospholipid vesicles have been studied as possible candidates for drug delivery vehicles with some success. The use of polymers have been introduced as a way to improve the stability and the targeting ability of vesicles for selective drug delivery. Certain polymers have been shown to interact with vesicles and alter the membrane permeability. Understanding the effects of polymer adsorption on phospholipid membranes will give insight into how polymers could be used to control drug release from vesicles by altering lipid membrane properties. Systematic study of polymer-membrane interactions may result in the design of polymers with enhanced abilities to regulate drug release.

Vesicles. Phospholipid vesicles, or liposomes, are closed concentric phospholipid bilayer membranes with an aqueous compartment separating each bilayer (Fig. 1A). Spacing between the membrane is determined by a balance of the van der Waals forces of attraction and the electrostatic and hydration forces of repulsion. These microcapsules have the potential to envelop and protect a myriad of drugs, diagnostic agents, and biological molecules. Hydrophilic materials can be encapsulated in its aqueous compartment or conjugated to vesicle surface while lipophilic agents can be incorporated in the phospholipid bilayer. Potential uses of liposomes include therapeutic applications such as the delivery of drugs to treat cancer, parasitic diseases, and heart diseases. As the possible areas of application have grown, the need for better understanding of the structure and properties of different types of liposomes has increased.

There are three general categories of vesicles that have been used (Fig. 1B). Multilamellar vesicles (MLV) are made of multiple concentric bilayer spheres and range in size from 1 to 5 μm. MLV form spontaneously upon hydration of phospholipid films above the lipid phase transition temperature (Tm).[1] Large unilamellar vesicles (LUV) and small unilamellar vesicles (SUV) have higher free energies, and some energy must be dissipated into the system in order to produce them.[2] SUV are bilayer spheres of 20-50 nm in size and are formed upon sonication of MLV or by extrusion through a French press.[3] LUV can be obtained by extrusion of MLV through a polycarbonate filter of defined pore size.[4] The size of LUV, which range from 100 to 200 nm, depends on the pore size of the filter used. LUV can also be made by other methods, such as detergent dialysis (slow dialysis of detergent from a mixed phospholipid-detergent micellar solution) and reverse phase evaporation (evaporation of organic solvent under reduced pressure from a mixture of phospholipid in aqueous buffer and organic solvent).[5,6] SUV spontaneously aggregate and fuse into LUV or MLV after few days or weeks.

Each vesicle type has unique properties and therefore has uses for different applications. SUV and LUV are composed of relatively homogeneous population of vesicles while MLV are heterogeneous in size and are more stable. MLV are used widely for physical characterization as a model cell membrane. The high surface curvature of SUV may perturb the properties of the bilayer interior making them a rather poor model of bilayer structure in general. Due to bilayer asymmetry, 60-70 % of the phospholipid molecules of SUV reside in the outer monolayer. The high ratio of available surface phospholipid render SUV suited to study vesicle surface interaction. The advantage of LUV is their large aqueous content volume.[7] The efficiency of encapsulation in MLV and SUV is generally low (1-3%). LUV have a much higher encapsulation efficiency (above 50%) and are able to entrap large molecules (MW 10^6-10^8). The efficiency of encapsulation is an important factor in drug encapsulation and delivery.

Phospholipid. Phospholipids are amphiphilic molecules composed of a hydrophilic headgroup and hydrophobic chains. Each phospholipid contains a glycerol as a backbone with a phosphate esterified at 3' position of glycerol and hydrocarbon chains esterified at 1' and 2' positions. The headgroup is esterified to the phosphate. Phospholipids are named by their headgroup structure and hydrocarbon chain length. Representative structures of phospholipids are depicted (Table). Amphiphiles can associate in solution to form micelles, bilayers, or inverted micelles in order to minimize unfavorable interactions between the aqueous phase and the hydrophobic component. Phosphatidylcholines (PC) form bilayers in aqueous solution whereas surfactants prefer to form micelles. Phospholipid membranes can exist in different phases, such as lamellar and inverted hexagonal (H_{II}), depending on the type of phospholipid and the environmental conditions such as temperature, concentration, and hydration. Transitions from one phase to another can be detected by physical techniques. One of these transitions in which the membrane passes from an ordered solid phase to a fluid phase is known as the gel to liquid crystalline (LC) phase transition and is extensively studied using PC vesicles. This chain melting transition involves the introduction of conformational disorder in the acyl chains. Liposomes prepared from pure phospholipids display a cooperative gel to LC phase transition. For MLV, preceding the main transition, there is a pretransition, during which a change in headgroup orientation occurs giving a ruffled appearance to the vesicle surface.[8] The phase transition temperature (Tm) and the corresponding heat of enthalpy (ΔH) of different phospholipids can be determined by differential scanning calorimetry (DSC). The Tm and ΔH of the transition are influenced by the acyl chain length, presence of double bonds, and the nature of headgroups, and are characteristic for each phospholipid. These parameters are also sensitive to changes in hydrogen-bonding and hydration of phospholipids and changes in the hydrocarbon chain conformation.[9] The phase behavior of liposome membranes

determines such properties as permeability, fusion, and aggregation, which affect the stability of liposomes and their behavior on interaction with cell membrane.

In biological membranes the phospholipid molecules are aligned with the glycerol backbone approximately perpendicular to the plane of membrane, with the phospholipid headgroup in a straight line parallel with the membrane surface[10] (Fig. 2). The part of the phospholipid molecules most severely restricted in its motion is the glycerol backbone. The motion of carbon atoms in the hydrocarbon chain becomes progressively less restricted further away from the glycerol backbone. The motion of the phospholipids are more restricted in the gel phase. As the temperature increases, intramolecular chain disorder increases because the hydrocarbon chains tend to adopt a *gauche* conformation from the all-t*rans* chain configuration.[11] This expands the area occupied by the chains resulting in a decrease in phospholipid packing density and an increase in the phospholipid mobility in the LC phase. Each PC molecule has a surface area of approx. 40 $Å^2$ in the gel phase, which increases to about 60 $Å^2$ in the LC phase.

Biomembrane. Phospholipids are the major components of biological membranes. Because of their similarities to biological membranes, phospholipid vesicles have been used as a model membrane system for fusion, transport, and permeability studies and for investigation of reconstituted membrane proteins. Liposomes are often used as model membrane systems to investigate the effects of biological modulators, such as fusogens, proteins, and cholesterol, directly on membrane properties. Changes in the membrane phase transition, permeability, and phospholipid structure can give quantitative and qualitative information about membrane interactions.

Liposome membranes are semi-permeable membranes in that the rate of diffusion of molecules and ions across the membrane varies considerably as a function of size and charge. Permeability of liposomes is an important factor in characterizing differences in liposome properties. Carboxyfluorescein (CF) has been widely used for studying release

of entrapped solutes from liposomes.[12] CF is a fluorescence probe which is self-quenched at high concentrations due to intermolecular resonance energy transfer (RET). Content release is determined by the dequenching of the probe as the probe is released into the surrounding buffer, resulting in increased fluorescence. Calcein is also a self-quenching fluorophore and is used as an alternative because its fluorescence is less pH-dependent.[13] Phospholipid packing defects gives rise to small exposed areas of the membrane, resulting in an increased membrane permeability.

Fusion.[14] Membrane fusion is a fundamental process involved in many cellular events such as viral-cell interaction, intracellular transport, and exocytosis. Because of the complexity associated with the study of biological systems, artificial membranes, such as vesicles and black lipid membranes, have been used as model systems to understand mechanisms of membrane fusion. Vesicle fusion is believed to occur in three steps (Fig. 3). Aggregation occurs between neutral membranes due to van der Waals interaction. The rate of fusion increases with increasing temperature and membrane fluidity.[15] Many mechanisms of vesicle fusion has been proposed including lateral phase separation induced by binding of divalent cations to negatively-charged phospholipid such as phosphatidylserine (PS),[16] formation of hexagonal phase intermediate with neutral phospholipid, such as phosphatidylethanolamine (PE), which preferentially adopt a non-bilayer phase,[17] and dehydration of membrane surface, which eliminates the hydration barrier.[18] It is proposed that the initial step in fusion is very close apposition of membranes by partial dehydration of the membrane surface, followed by alignment of packing defects. Agents promoting fusion can act at different points in a generalized mechanism.

Fusion of liposomal membranes may be detected by measuring the fluorescence RET between two fluorescent phospholipid analogues placed in the same vesicle preparations (lipid intermixing).[19] This technique depends upon an overlap in the

emission spectrum of the donor molecule and the excitation spectrum of an acceptor molecule. Excitation of the acceptor can occur by direct transfer of energy from the excited donor and this is manifest as a reduction in the emission intensity of the donor fluorescence and a corresponding increase in emission intensity of the acceptor fluorescence. Because RET decreases as the 6th power of the distance between donor and acceptor molecules,[20] it occurs only when two molecules come into close contact as in the case when they occupy the same bilayer. When fusion is induced in the presence of excess unlabelled liposomes, the dilution of the fluorophore as they disperse through the unlabelled membranes then leads to a decrease in RET.

Drug Delivery. Liposomes have therapeutic use for intracellular infection of macrophages such as leishmaniasis and fungal infections as well as diseases of liver and lung tissues and tumors. Liposomes offer the possibility of enhanced cellular uptake of the drug. Molecules as small as glucose (MW 180) or as large as plasmids (MW 10^8) can be encapsulated in the vesicles and be protected from inactivation or degradation. Because of their restricted permeability, liposomal preparations offer a controllable time-dependent release system. Because liposomes are composed of natural or synthetic phospholipids, they can be metabolized *in vivo* and are generally nontoxic and nonantigenic. Mechanisms of liposome-cell interaction include endocytosis, fusion with the plasma membrane, cell-induced leakage of liposome content, and lipid exchange[21] (Chapter 7, Fig. 5). The liposomes taken up by endocytosis goes through the endocytic pathway described below. Some liposomes fuse directly with the cell membrane to deliver their contents to the cytoplasm, or the liposomes are destabilized upon interaction with cell surface, and their contents released at the cell surface may be taken up by pinocytosis. Lipid exchange, or intermembrane transfer, can occur upon close approach of the two phospholipid bilayers, possibly via an intermediary of cell surface proteins.

Cells with phagocytic activity rapidly take up liposomes into endosomes (pH 5-6.5), which then fuse with lysosomes, where enzymatic digestion takes place at low pH (Fig. 4). The intralysosomal pH is maintained between 4 and 5 by the action of a proton translocating ATPase.[22] Liposomes are hydrolyzed and the contents of the aqueous compartments are exocytosed or passed into the cytoplasm. Entrapped materials are released into the lysosomes, and subsequently taken up into the cytoplasm or exocytosed. Adsorption is an essential prerequisite for internalization of liposomes by cells. Adsorption or binding to the cell surface could occur without internalization of liposomes. Liposomes may bind to cells via a variety of surface receptors and then be internalized via coated pits with subsequent enzymatic degradation or recycling of ligands. Factors determining the fate of liposomes in cells, once internalized, are not yet fully understood. It is believed that some of the differences in fate depend on which cell surface receptors are recognized by the liposomes. Determination of the mechanism of delivery of liposomal contents into various cells requires the use of assays to distinguish between adsorption to the cell surface and cytoplasmic versus lysosomal delivery.

Because liposomes on *in vivo* use target naturally to the reticuloendothelial system (RES), the distribution pattern in the body needs to be controlled by lipid composition, size, charge, permeability, and surface ligands. When drugs are encapsulated in liposomes, absorption and distribution can be controlled in part by varying the physicochemical properties of the liposomes and are not dependent on the properties of the drug. Another advantage of using liposomes for drug delivery is the resulting reduced toxicity of some drugs upon encapsulation (e.g., amphotericin, actinomycin D, anthracyclines).[23]

It is desirable for intracellular delivery to improve both the efficiency and the specificity of liposome interaction with cells. Efficacy of liposomes for intracellular delivery can be increased by covalent attachment of cell surface specific ligands such as

Ig G.[24] Efficiency of vesicle delivery to cells also depends on lipid composition. In addition to the influence of the composition of liposomes, drug release can be controlled by rendering liposomes sensitive to environmental parameters such as temperature, light, chemical components, and pH so that the release is site-specific in response to environmental conditions. The other goal of vesicle research is membrane stability to chemical, osmotic, and mechanical stress. Storage stability is of particular importance for the practical clinical use of liposomes.

Polymer-Vesicle Interaction. The need for increased stability and for controlled permeability and fusogenicity led to the use of polymers to alter vesicle properties. Polysaccharides, such as dextran, have been investigated in an effort to improve the stability of liposomes.[25] Poly(ethylene glycol) (PEG) has been shown to induce fusion of vesicles and cells[26] and also to sterically stabilize the membrane for prolonged *in vivo* circulation time ("stealth liposomes").[27] Cetylacetyl-imidazole-polyethylenimine (CAIPEI) is a proton sensitive polymer, which induces destabilization of vesicles at low pH.[28] Positively-charged polyethylenimine (PEI) has been shown to induce interdigitation of negatively-charged bilayer membrane.[29] Polyamines also interact with negatively-charged phospholipids due to electrostatic interaction.[30] Poly(ethacrylic acid) (PEAA) adsorption induces a vesicle to micelle transition in aqueous dispersion of DPPC below pH 6.5 due to conformational collapse of the polyelectrolyte chain upon protonation.[31,32] Immobilization of PEAA to vesicles by Michael addition of polymer-bound thiol to a N-alkylmaleimide introduced into the membrane surfaces led to the formation of pH-sensitive membranes that were subject to rapid quatitative loss of contents upon mild acidification.[33] On the other hand, PAA, which is also a poly(carboxylic acid) does not induce micelle formation upon lowering the pH.[34]

Although many polymers are known to alter liposome properties by interacting with phospholipids, the mechanisms of polymer-vesicle interaction are not well

understood. In order to better understand the interactions of polymer with vesicles, PAA has been chosen as a model pH-sensitive polymer to study the mechanism of its interaction with PC membranes. The goal of this study is to elucidate the nature and the effect of polymer adsorption on the bilayer surface and to show how it leads to bilayer disruption.

Chapters. Chapter 2 describes PAA-induced pH-dependent destabilization of PC vesicles. PAA-vesicle interaction was studied using photon correlation spectroscopy (PCS), various fluorescence fusion assays and freeze-fracture electron microscopy. PCS, or quasi-elastic light scattering, is the analysis of the time-dependent intensity fluctuations in scattered laser light due to the Brownian motion of particle in solution or suspension.[35] The rate of fluctuation of scattered light intensity varies according to particle size since small particles diffuse more rapidly than large particles. The translational diffusion coefficient (D) can be measured, which in turn can be used to determine the mean hydrodynamic radius (R_H) of the particles using the Stokes-Einstein equation,

$$D = kT/6\pi\eta R_H$$

where k is the Blotzmann's constant, T is the temperature, and η is the solvent viscosity. Particle size distribution of vesicles was obtained from PCS to determine the extent of aggregation of vesicles. The lipid intermixing assay, described previously, and content mixing assay, which determines if the aqueous contents of aggregated vesicles intermix without leakage, are known as the fusion assays. These assays were used to characterize the fusogenic ability of the polymer at low pH. The content release assay was used to determine the change in the permeability of liposomes upon PAA interaction. Freeze-fracture images of vesicles were obtained to characterize the changes in the morphology of vesicles upon polymer-induced destabilization.

Chapter 3 describes the use of various spectroscopic and calorimetric techniques, such as FT-IR, NMR, fluorescence, and DSC, to characterize the conformation, disorder, and mobility of vesicle phospholipids. Both IR and Raman spectroscopy are non-perturbing techniques for monitoring the conformation and dynamics of phospholipid molecules. Structural alterations, packing constraints, and mobilities of the polar headgroup and hydrocarbon chains result in frequency, linewidth, and intensity changes of vibrational peaks (Fig. 5). The carbon-hydrogen stretching vibrations give rise to bands in the spectral region 2800-3100 cm^{-1}.[11] The acyl chain phase transition behavior was investigated with FT-IR instead of Raman spectroscopy due to laser-induced decomposition of PC vesicles at low pH in the presence of PAA. The CH_2 antisymmetric stretching mode at 2929 cm^{-1} and the symmetric stretching mode at 2850 cm^{-1} are sensitive to conformation and the *trans/gauche* ratio in the lipid acyl chains.[11] Hydrocarbon chains assume varying degrees of conformational disorder depending on the temperature and the nature of the extrinsic and intrinsic membrane components. These peaks are particularly useful for monitoring the gel to LC phase transition. Both the frequency and the width of the peaks increase from gel to LC phase. Alteration in the headgroups were studied using FT-IR. Phosphate group vibrations occurs between 1240 and 1220 cm^{-1} and are due to the antisymmetric PO_2 stretching mode and are dependent on the amount of hydration of the phosphate group.[36] FT-IR has been extensively used to study the effect of protons on lipid phase behavior and therefore was used to study the lipid-polymer interaction.

DSC was used to study the phase transition behavior of polymer-associated PC vesicles. Fluorescence anisotropy measurements were used to determine the mobility of vesicles. ^{31}P-NMR spectra of polymer-associated MLV were taken to determine the state of lipid and the disorder in the headgroup region from chemical shift anisotropy (CSA). ^{31}P-NMR senses the behavior and the environment of the phosphorous atom in the

phospholipid headgroup. Since phosphates in part define the surface of the membrane, ^{31}P-NMR measures properties of the membrane surface. For solids the electron distribution surrounding the phosphorous nucleus is anisotropic and thus in a magnetic field, the phosphorous experiences an orientation dependent "shielding" of the chemical shift termed the CSA. The powder patterns of phosphate show three principle elements of the chemical shift tensor σ_{11}, σ_{22}, and σ_{33} (Fig. 6). In the presence of rapid axial diffusion, two chemical shift tensors ($\sigma_{\perp}$ and $\sigma_{//}$) are adequate. The upfield maximum and downfield of the PC-MLV powder pattern corresponds to the chemical shift perpendicular and parallel to the diffusion axis, respectively (Fig. 7). The width of the powder pattern ($\sigma_{\perp} - \sigma_{//}$) is sensitive to the motion of the phopsholipid headgroup.[37]

Chapter 4 describes the behavior of fluorescently-labeled PAA as studied by fluorescence anisotropy measurements and the extent binding of polymer on phospholipid vesicles. Chapter 5 describes the interaction of PAA with PC monolayers using the Langmuir-Blodgett techniques in order to study the direct polymer-phospholipid interaction. Results from monolayer experiments are compared with bilayer studies. A background on monolayers at air-water interface is given after the introduction section in the chapter. *In vitro* study of PAA-conjugated vesicle uptake by macrophages is described in chapter 6.

References

1. Bangham, A.D., Standish, M.M. and Watkins, J.C. *J. Mol. Biol.* **13**, 238 (1965).
2. Lasic, D.O. *Biochem. J.* **256**, 1 (1988).
3. Barenholzt, Y., Amselem, S. and Lichtenberg, D. *FEBS Lett.* **99**, 210 (1979).
4. Hope, M.J. et al. *Biochim. Biophys. Acta* **812**, 55 (1985).
5. Enoch, H.G. and Strittmatter, P. *Proc. Natl. Acad. Sci.* **76**, 145 (1979).
6. Szoka, F.C. and Papahadjopoulos, D. *Proc. Natl. Acad. Sci.* **75**, 4194 (1978).
7. Papahadjopoulos, D. et al. *Techniques Cell. Phys.* **P114**, 1 (1981).
8. Marsh, D. *Biochemistry* **19**, 1632 (1980).
9. Boggs, J.M., Rangaraj, G. and Kosby, K.M. *Chem. Phys. Lipids* **40**, 23 (1986).
10. Hauser, H. et al. *Biochim. Biophys. Acta* **650**, 21 (1981).
11. Levin, I.W. in Advances in Infrared and Raman Spectroscopy vol. 11, Clark , R.J.H. and Hester, R.E. eds. Wiley-Interscience, New York ,1984.
12. Weinstein, J.N. et al. in Liposome Technology vol. III Gregoriades, G. ed. CRC Press, Florida, 1984.
13. Allen, T.M. in Liposome Technology vol. III Gregoriades, G. ed. CRC Press, Florida, 1984.
14. Cell Fusion Sowers, A.E. ed. Plenum Press, New York, 1987.
15. Rupert, L.A.M. et al. *J. Phys. Chem* **92**, 4416 (1988).
16. Leventis, et al. *Biochemistry* **25**, 6978 (1986).
17. Ellens, H., Bentz, J. and Szoka, F.C. *Biochemistry* **25**, 4145 (1986).
18. Arnold, K., Pratsch, L. and Gawisch, K. *Biochim. Biophys. Acta* **728**, 121 (1983).
19. Struck, D.K., Pagano, R.E. and Hoekstra, D. *Biochemistry* **20**, 4093 (1981).
20. Lakowicz, J. R. in Principle of Fluorescence Spectroscopy Plenum Press, New York, 1983.
21. Liposomes A Practical Approach New , R.R.C. ed. IRL Press, New York, 1990.

22. Schneider, D.L. *J. Biol. Chem.* **256**, 3858 (1981).

23. Maierhofer, G. *Am. Clin. Prod. Rev.* **June**, 33 (1985).

24. Derksen, J. T-P., Morselt, W. M. and Scherphof, G.L. *Biochim. Biophys. Acta* **931**, 33 (1987).

25. Elferink, M.G.L. et al. *Biochim. Biophys. Acta* **1106**, 23 (1992).

26. Boni, L. T. et al. *Biochim. Biophys. Acta* **775**, 409 (1984).

27. Klibanov, A.L. et al. *FEBS Lett.* **268**, 235 (1990).

28. Oku, N. et al. *Biochemistry* **26**, 8145 (1987).

29. Tirrell, D.A. et al. *Macromolecules* **18**, 1512 (1985).

30. Schuler, F. *Biochem. J.* **260**,1 (1989).

31. Tirrell, D.A., Takigawa, D.Y, and Seki. K. *Ann. NY Acad. Sci.* **446**, 237 (1985).

32. Borden K.A. et al. *Makromolecules* **20**,456 (1987).

33. Maeda, M., Kumano, A. and Tirrell, D.A. *J. Am. Chem. Soc.* **110**, 7455 (1988).

34. Seki, K. Tirrell, D.A. *Macromolecules* **17**, 1692 (1984).

35. Automeasure User Manual Malvern Instruments, England, 1986.

36. Chapman, D. *Chem. Phys. Lipids* **1**, 445,1967.

37. Cullis, P.R., deKruijff, B. and Richard, R.E. *Biochim. Biophys. Acta* **426**, 433 (1976).

Figure 1. A) Cross section of liposomes, showing phospholipid bilayer and a generic structure of phospholipid. B) MLV, LUV, and SUV in aqueous buffer solution (1 mg/ml, pH 7.4).

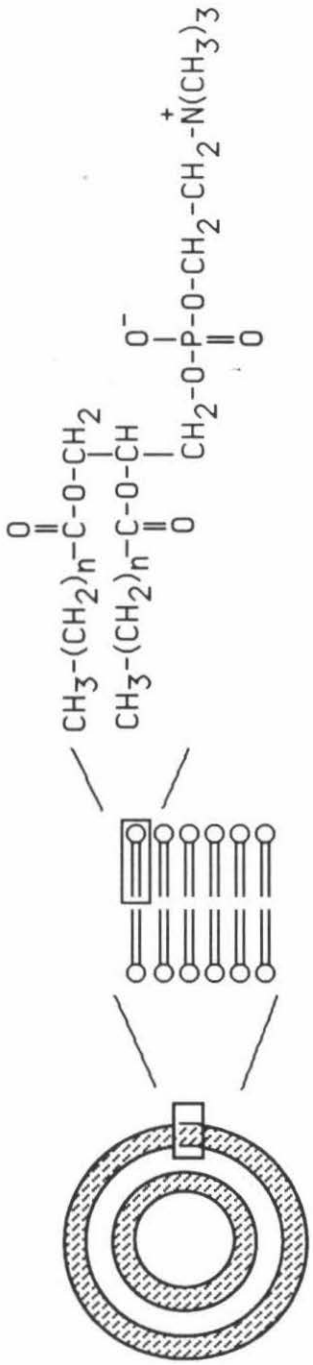
CH3-(CH2)n-C-O-CH2
CH3-(CH2)n-C-O-CH
CH2-O-P-O-CH2-CH2-N+(CH3)3
O
O
O
O-

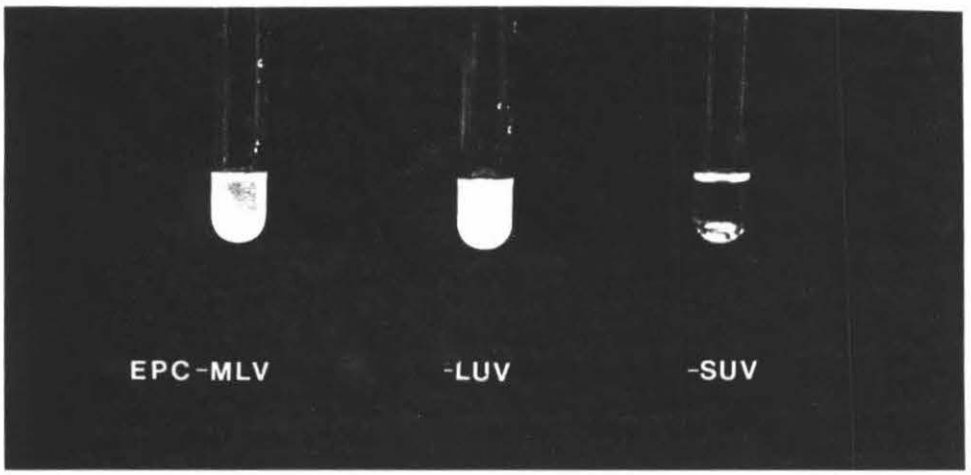

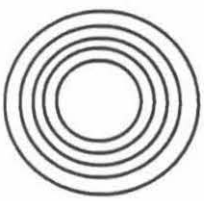

MLV

LUV

SUV

Figure 2. Orientation of phospholipid molecule in a bilayer obtained from crystal structure.

Phospholipid Orientation in a bilayer

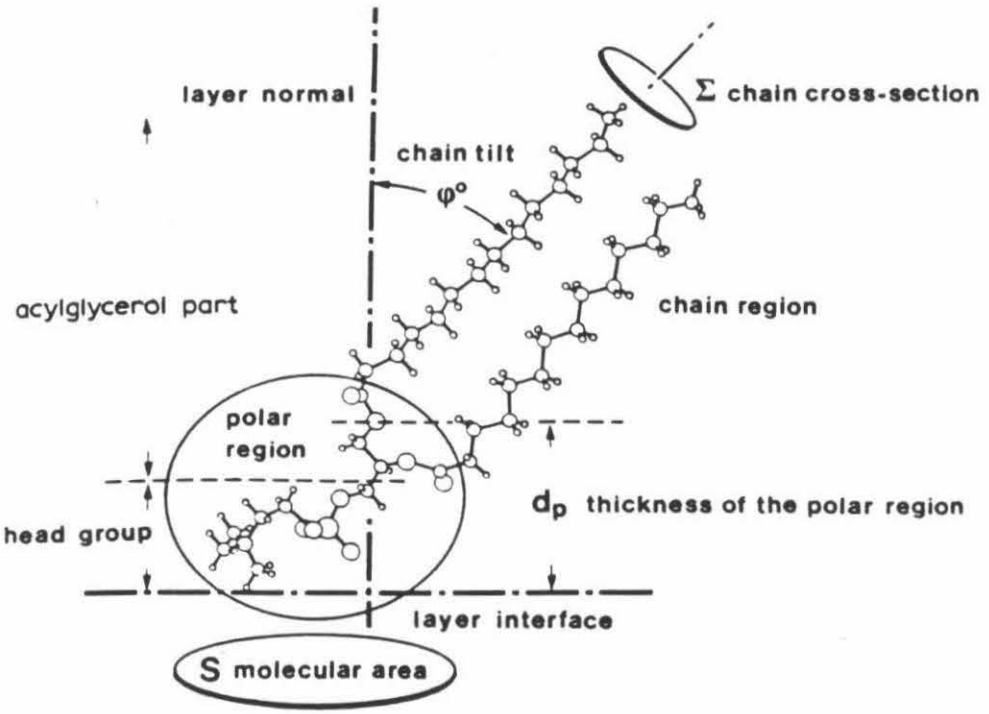

PC:
S=38.9 Å^2
dp=10.4 Å
φ=12 ^{o}

Table. Naming of phospholipid molecules, e.g, DPPC (dipalmitoyl phosphatidylcholine) has two palmitoyl chains and a choline headgroup. (top) Different headgroup names, abbreviations, its structure, and phospholipid charge. (bottom) Names of some hydrocarbon chain lengths.

name	**structure**	**charge**
choline (PC)	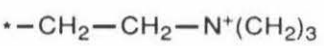	neutral
ethanolamine (PE)		neutral
serine (PS)	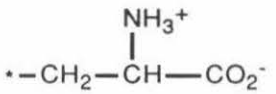	(-)
glycerol (PG, cardiolipin)	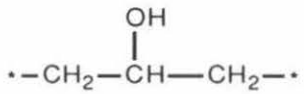	(-)
inositol (PI)	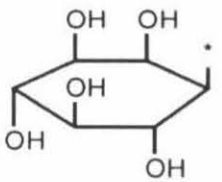	(-)

name	**notation** (chain length:unsaturation)
myristoyl (M)	14:0
palmitoyl (P)	16:0
stearoyl (S)	18:0
oleyl (O)	$18:1^{\Delta 9}$

Figure 3. Schematic drawing of membrane fusion steps: 1. aggregation of vesicles 2. destabilization at the vesicle contact point 3. lipid intermixing and content mixing of vesicles.

aggregation
rupture
merging of bilayers

Figure 4. Schematic drawing of an endocytosis pathway.

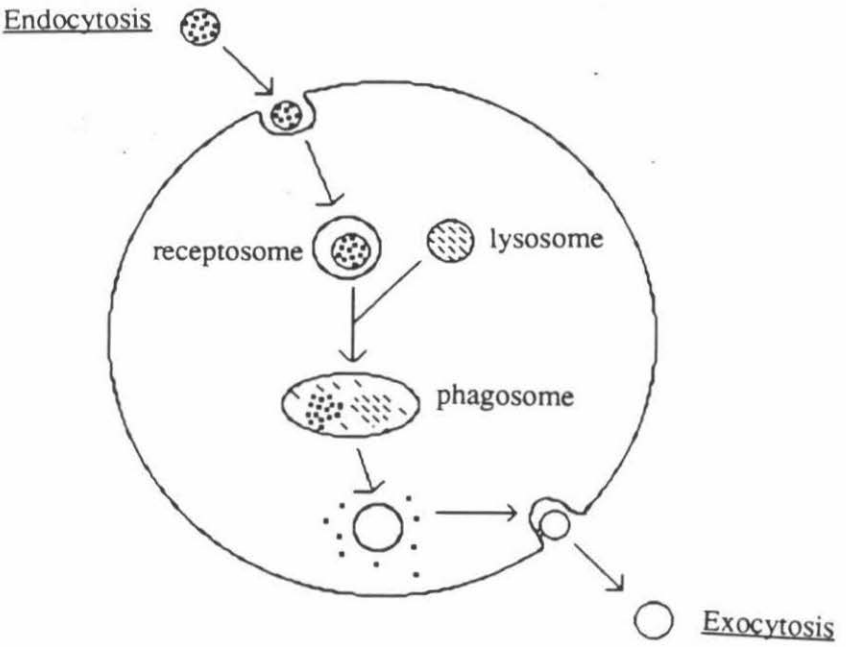

receptosome - pH 4.5, no digestive enzyme
lysosome - pH 4.5-5.5, many digestive enzymes

Figure 5. FT-IR spectra showing CH_2 symmetric and asymmetric stretching peaks of DPPC-MLV (pH 7.4) at 25 ^{o}C.

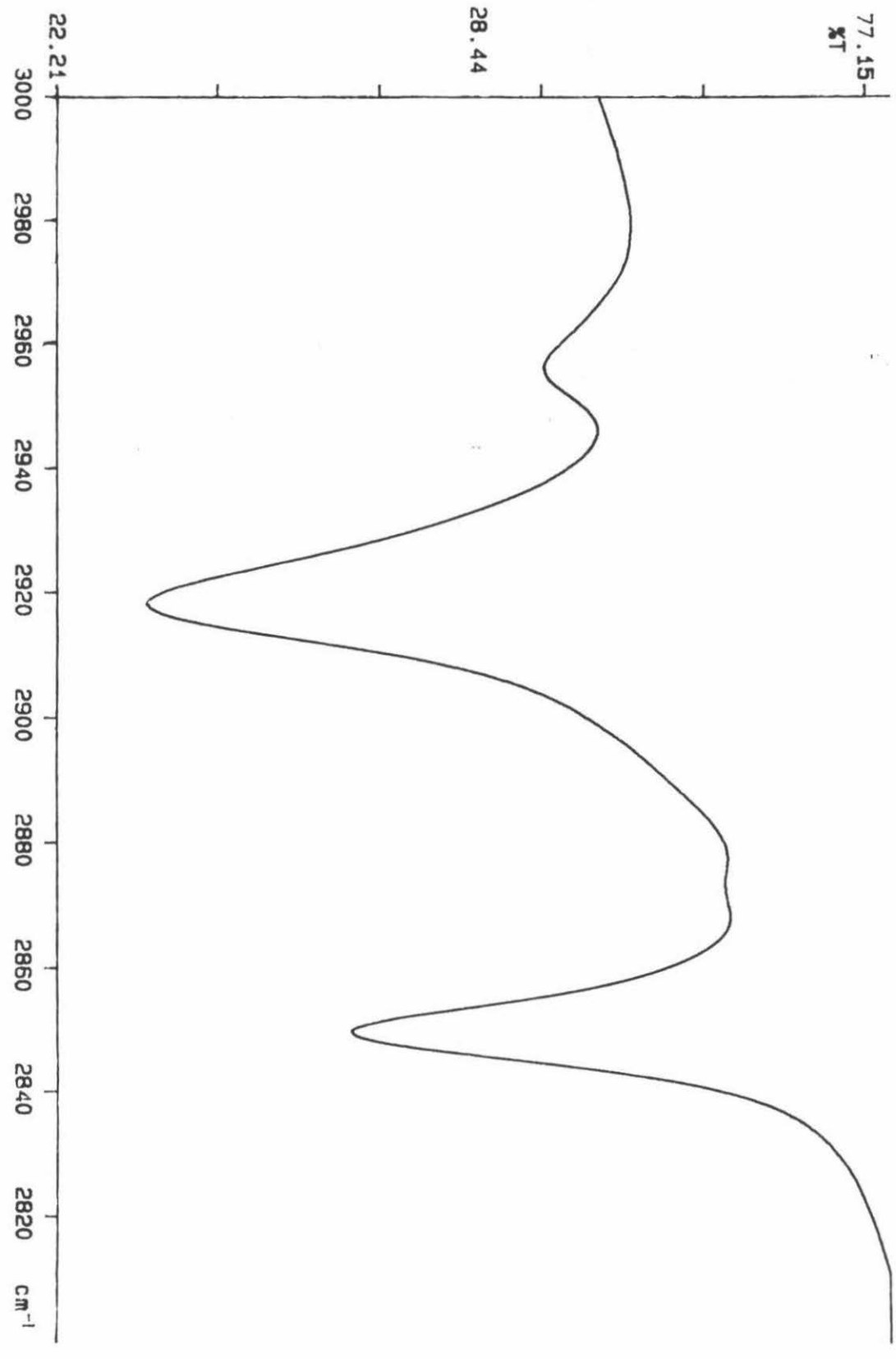
77.15
%T
28.44
22.21
3000
2980
2960
2940
2920
2900
2880
2860
2840
2820
cm⁻¹

Figure 6. Schematic drawing of the three principle chemical shift tensors of phosphate.

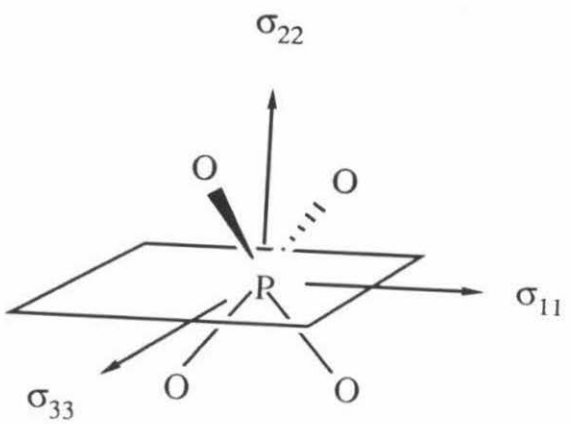
σ22
O
O
P
σ11
σ33
O
O

Figure 7. ^{31}P-NMR powder pattern of eggPC-MLV (pH 7.4) at 25 ^{o}C showing chemical shift tensors $\sigma_{\perp}$ and $\sigma_{//}$.

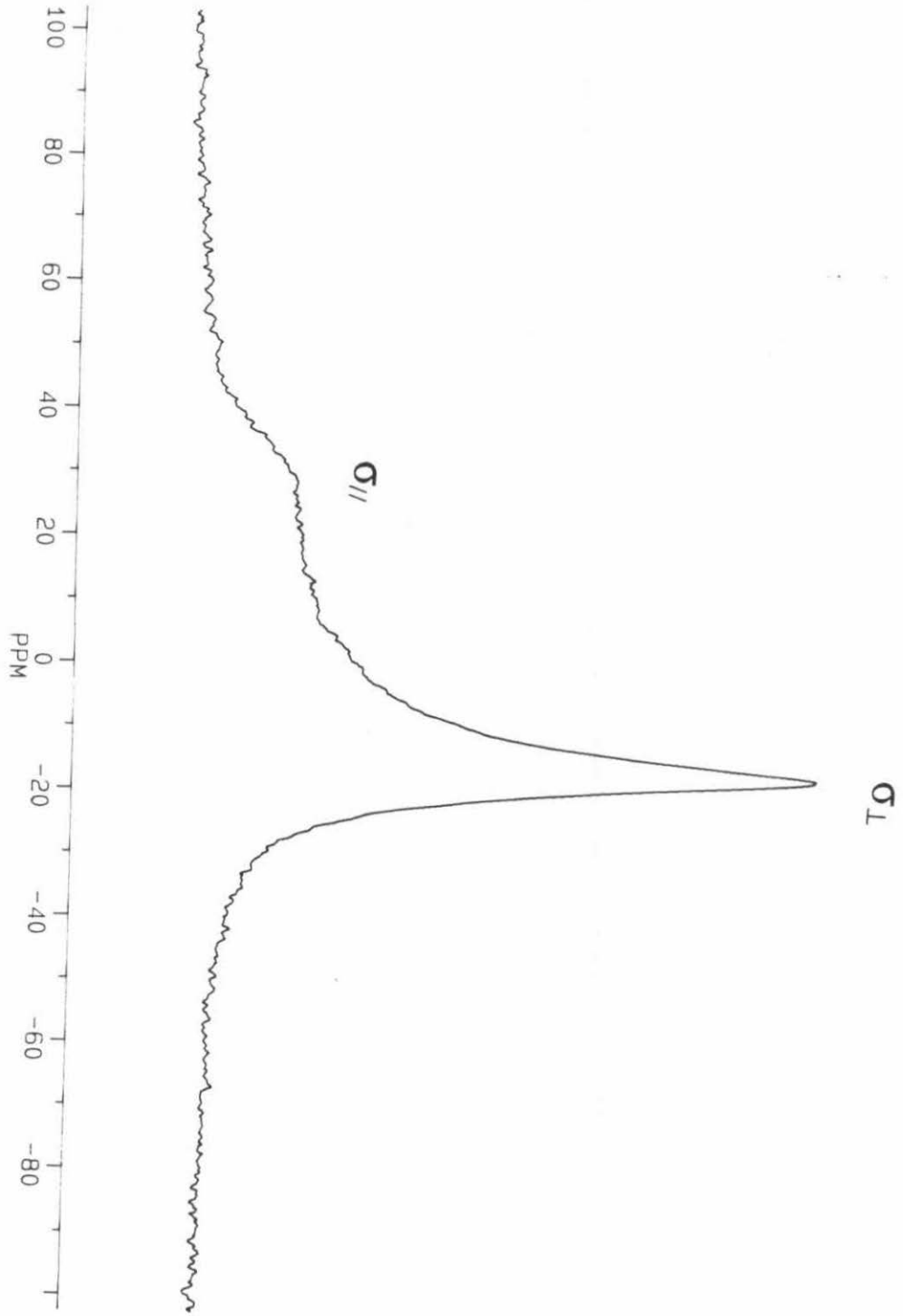
100
80
60
40
20
0
PPM
-20
-40
-60
-80
σ//
σ⊥

Chapter 2

pH-Dependent Destabilization of Phosphatidylcholine Vesicles Induced By Poly(Acrylic Acid)

Summary

pH-dependent interaction of poly(acrylic acid) (PAA)with phosphatidylcholine (PC) vesicles were investigated using techniques commonly used to study membrane fusion in order to better understand polymer-vesicle interactions for drug delivery and as models/parallels of protein-vesicle interactions. Major membrane structural changes were mediated by PAA at low pH where the protonation of the carboxylate renders the polymer more hydrophobic. PAA induced aggregation of both multilamellar and unilamellar vesicles below pH 5.0 and lipid intermixing of vesicles and release of vesicle contents below pH 4.1. Addition of PAA at low concentrations resulted in the formation of large hydrophobic flocculates, which are composed of networks of polymers and vesicles. However, in the presence of increased concentrations of PAA, vesicle aggregates stayed suspended in water due to polymer repulsion. The vesicle aggregation is believed to have resulted from dehydration of the phospholipid headgroup induced by the binding of protonated polymer. The release of vesicle contents as large as MW 10,000 was detected as a result of the collapse of vesicles into tubular structure. Increase in membrane permeability was accompanied by an increase in membrane packing disorder as indicated by merocyanine 540 (MC-540) binding. Content mixing of PAA-associated vesicles was not observed, indicating that true membrane fusion did not occur. PAA-induced vesicle alterations, which occurred above the phase transition temperature (Tm) of the lipid, were partially reversible by increasing the pH. A possible mechanism for PAA-mediated pH-dependent lipid intermixing and content release is discussed.

Introduction

Many virus-cell fusion systems require the lowering of pH to initiate the fusion process (White et al., 1981). Acid-induced fusion systems, which mimic the fusion step required for the transmission of genetic material during viral infection, have been investigated for their applications to cellular drug delivery (Lapidot & Loyter, 1990). Phospholipid vesicles, or liposomes, have been widely used as model membranes to study cell fusion mechanisms, making them candidates for cellular drug delivery vehicles. Some pH-sensitive liposomes have been developed for acid-induced cytoplasmic delivery of molecules through endosomes (Straubinger et al., 1985; Connor & Huang, 1985). These liposome formulations, which involve negatively charged lipids and phosphatidyl-ethanolamine (PE), are intrinsically unstable and are prone to leakage of their contents at low pH.

In liposomal drug delivery, it is desirable to control drug release from vesicles by altering their membrane properties. Certain polymers have been shown to render vesicles sensitive to pH by interacting with phospholipids. Cetylacetyl-imidazole-polyethylenimine causes pH-dependent lipid intermixing of negatively charged vesicles (Oky et al., 1987). Micelle formation of phosphatidyl-choline (PC) vesicles induced by poly(ethylacrylic acid) at slightly acidic pH has been extensively studied (for the most recent reference, see Eum et al., 1989). PAA, like poly(ethylacrylic acid), is sensitive to pH due to the titration of carboxylic acid groups in the side chains. Although it has been noted that PAA interacts with PC vesicles in a pH-dependent manner (Seki & Tirrell, 1984), the effect of PAA on vesicles has not been fully characterized.

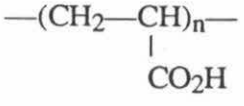

(PAA)

Studies of polymer-vesicle interactions have implications not only in drug delivery, but also in elucidating mechanisms of membrane fusion, where the importance of the

involvement of proteins in the control of biological fusion processes has been recognized. The pH-sensitive conformational change in proteins induced by the protonation of carboxylic acid is believed to play an important role in many acid-induced membrane fusion systems by exposing the hydrophobic region of the protein, which then penetrates the membrane (Parente et al., 1990a,b; Ohnishi & Murata, 1988). Understanding PAA-vesicle interaction will give an insight into the role of carboxylic acid-phospholipid interaction in membrane fusion. We have, therefore, investigated the PAA-mediated pH-dependent aggregation of PC vesicles using conventional methods, such as quasielastic light scattering spectroscopy to measure particle size, fluorescence spectroscopy for fusion assays, and electron microscopy to observe vesicle morphology (part of this work was presented previously, see Fujiwara et al., 1991).

Materials and Methods

Materials. Egg yolk phosphatidylcholine (EPC), dipalmitoyl phosphatidylcholine (DPPC), N-4-nitrobenzo-2-oxa-1,3-diazole phosphatidylethanolamine (NBD-PE), and N-(lissamine Rhodamine B sulfonyl)phosphatidylethanolamine (Rh-PE) were purchased from Avanti Polar Lipids. The purity of lipids was checked with thin layer chromatography, and the lipids were used without further purification. 8-aminonaphthalene-1,3,6-trisulfonic acid (ANTS), p-xylene-bis-pyridinium bromide (DPX), Lucifer Yellow CH (Li salt), and Lucifer Yellow-Dextran (MW 10,000) were obtained from Molecular Probes. MC-540, Triton X-100, and PAA (MW 250,000) were obtained from Aldrich. PAA solution (10 mg/ml) was dialyzed against fresh acetate buffer (10 mM NaAcetate, 100 mM NaCl, pH 7.0) through Spectra/Por membrane type 7 (MW cut-off 1,000) obtained from Spectrum. All chemicals were of reagent grade. Buffers were prepared in distilled, deionized water.

Vesicle Preparation. Multilamellar vesicles (MLV) were prepared by drying a chloroform solution of EPC or DPPC in a test tube under a stream of argon and further under vacuum

overnight. The solid film was hydrated with acetate buffer and vortexed for several minutes above the lipid Tm. For vesicles made with PAA *in situ*, lipids were hydrated with a buffer containing an appropriate amount of PAA. Large unilamellar vesicles (LUV) of 150 nm in size were made by extrusion (Lipex) of the MLV solution under nitrogen through a polycarbonate filter with a 200 nm pore size (Mayer et al., 1986). Lamellarity of LUV was determined by ^{31}P-NMR to be over 80 % unilamellar (Hope, 1985). Small unilamellar vesicles (SUV) were prepared by bath sonication or probe sonication (Heat Systems) of the MLV solution under nitrogen until vesicles of 30 - 50 nm were obtained. For probe sonicated vesicles, titanium particles were removed by centrifugation at 12,000 x g for 5 min in Microfuge 11 (Beckman). The phosphate content of the vesicle preparations was determined by the Böttcher modification of the Bartlett assay (Böttcher et al., 1961). A stock solution of vesicles (10-25 mg/ml) was added to acetate buffer of appropriate pH for each experiment. All experiments were carried out at room temperature (24.5 ^{o}C) unless otherwise stated. Data presented here are representative of at least two independent measurements or assays.

Light Scattering. Dynamic light scattering measurements were performed with a Malvern 4700c sub-micron particle analyzer using a Spectra-Physics 2020-03 argon ion laser (488 nm) operated in the current mode at 40 A. The light scattered at 90^{o} was detected using a photomultiplier. The photocount correlation function measurements were made with a Malvern K7032 correlator connected to a Malvern PC 6300 computer. Data were analyzed by a Malvern software Automeasure 3.1.

Optical Density. Absorbance at 400 nm was measured with a DU-7 spectrophotometer (Beckman).

Lipid Intermixing Assay. Resonance energy transfer assays were carried out with NBD-PE, the energy donor, and Rh-PE, the energy acceptor (Struck et al., 1981). Unlabeled vesicles were mixed in a 10:1 ratio with vesicles labeled with 2 mole% Rh-PE and NBD-

PE. The PAA solution was injected into the vesicle solution (0.7 mM) in a 1 x 1 cm quartz cuvette under constant magnetic stirring. The rate of lipid mixing was measured by following the changes in the fluorescence intensity at 530 nm with an excitation at 470 nm as a function of time. Excitation and emission slitwidths of 8 nm were used. A GG495 glass filter (Schott) was used to reduce the effect of light scattering. All fluorescence measurements were carried out with an SLM 4800 spectrofluorometer. The extent of lipid intermixing was calculated as follows,

$$\% = \frac{F(t)-F(I)}{F(T)-F(I)} \times 100$$

where F(t) is the fluorescence at time t, F(I) is the initial fluorescence and F(T) is the total fluorescence. F(T) was obtained by 1% Triton X-100 dissolution of the vesicle solution. Values were corrected for concentration changes.

Content Mixing Assay. Assays to measure the quenching of independently encapsulated ANTS and DPX probes were carried out as described previously (Ellens et al., 1985). EPC was hydrated with 25 mM ANTS and 40 mM NaCl or with 90 mM DPX, sonicated as described above, and eluted through a Sephadex G-75 (Pharmacia) column with acetate buffer. ANTS vesicles (25 μM) were mixed with DPX vesicles (25 μM), and the time-dependent fluorescence was observed at 515 nm with excitation at 384 nm using a GG475 filter.

Content Release Assay. Content release was monitored by measuring the dequenching of fluorescent probes trapped inside unilamellar vesicles as the probes were diluted upon release from the vesicles (Walter et al., 1986). Lipids were hydrated in 65 mM Lucifer Yellow or 5 mM Lucifer Yellow-dextran in acetate buffer (10 mM NaAcetate, 10 mM NaCl, pH 7.0) and run through five freeze-thaw cycles. Unilamellar vesicles were then made as described above. Nonencapsulated material was removed by passage through a Bio-Gel A-5m (Bio-Rad) column with elution buffer (10 mM NaAcetate, 100 mM NaCl,

pH 7.0). The time-dependent fluorescence of vesicles (78 μM) was observed at 530 nm with excitation at 420 nm using the GG475 filter. 100% leakage was established by solubilization of vesicles with 0.1% Triton X-100.

MC-540 Assay. A stock solution of dye (1.8 mM) was prepared in ethanol/acetate buffer mixture (2:8) and stored at 4°C in the dark. The stock solution (5 μl) was added to the vesicle solution and incubated for 30 min before ratiometric emission spectra were recorded at 540 nm excitation (Williamson et al., 1983).

Freeze-Fracture Electron Microscopy. MLV were pelleted by centrifugation at 12,000 x g for 5 min using a Beckman Microfuge 11. SUV and LUV were pelleted by centrifugation using a L5-56 Beckman Ultracentrifuge with an SW 50.1 rotor at 149,000 and 84,000 x g for 1 hr respectively. After addition of 30% (v/v) glycerol to the sample, a small pellet was sandwiched between copper hats and rapidly frozen in freon and stored in liquid nitrogen. The sample was cracked, etched, and shadowed with Pt/C using a Balzers apparatus. The replicas on formvar coated grids were then imaged on a Phillips EM 201c Transmission Electron Microscope (Zingsheim, 1972).

Results

Light Scattering

Addition of PAA (1:1 w/w) to preformed vesicles induced aggregation of vesicles below pH 5 as shown by the optical density profile of EPC-SUV solution (Fig. 1). Light scattering measurement showed that both the size and the distribution width of vesicles increased with decreasing pH; the mean diameter increased from 52 nm at pH 4.6 to 348 nm at pH 3.8. Vesicle size remained constant in the above pH range at a mean diameter of 35 nm without PAA addition (Fig. 2). Restoring the vesicle solution to pH 7.4 by the addition of 0.1 N NaOH reduced the vesicle size to 140 nm. The same trend was observed for both MLV and LUV solutions and also when vesicles were made with PAA in situ.

When varied concentrations of PAA were added, formation of large hydrophobic flocculates occurred at PAA concentrations less than 0.25 polymer/lipid (w/w) ratio. Particle size determination of these samples was not possible due to the settling of the aggregates. In addition some aggregates adhered strongly to the test tube walls. In order to determine whether the nature of the adhesive interaction is electrostatic or hydrophobic, the glass surface was hydrophobically modified with Sigmacote (Sigma) to mask any charges. Flocculate adherence to the test tube wall could not be prevented, indicating that the interaction is mainly hydrophobic.

Lipid Intermixing

To distinguish between lipid intermixing and aggregation, time-dependent lipid intermixing of vesicles was measured. No spontaneous lipid intermixing was observed within the time frame of the experiment at the pH range studied without PAA addition. PAA induced lipid intermixing of all vesicle types below pH 4.1, and the extent of lipid intermixing increased with decreasing pH (Fig. 3). Aggregation and adherence of PAA-complexed vesicles to the quartz cell made the measurements difficult to carry out after 100 s for MLV after addition of an equivalent weight of PAA. The observed extent of LUV lipid intermixing decreased with increasing PAA concentration (Fig. 4). Only a fraction of PAA is necessary to induce lipid intermixing. The rate of lipid intermixing was decreased at high polymer concentrations due to repulsive forces between the vesicles from the bound polymers. In contrast the extent of MLV lipid intermixing increased with increasing PAA concentration. This is due primarily to precipitation of flocculates at low PAA concentration. In the presence of PAA at low concentrations, the formation of large hydrophobic flocculates interfered with the lipid intermixing assay for MLV resulting in decreased lipid intermixing rate. Extra PAA present at high polymer concentrations adhered to these aggregates, making the vesicle surface hydrophilic enough to stay suspended in water to increase the rate of lipid intermixing for MLV.

Lipid intermixing of MLV occurred with phospholipid concentrations as low as 30 μM, indicating that the interaction is mediated by PAA and not by the proximity of vesicles. In order to maximize the bilayer surface available for polymer interaction, vesicles were made with PAA in situ, where the polymer is both inside and outside the vesicle. The extent of lipid intermixing was slightly enhanced compared to that when PAA was added to preformed vesicles at the same pH (Fig. 5). This suggests that polymer-surface interaction is important while membrane asymmetry does not play a major role in PAA-mediated interaction. To determine the dependence of PAA interaction on lipid phase, the extent of PAA-induced lipid intermixing of DPPC-MLV was measured at various temperatures. Lipid intermixing of vesicles was observed only above the Tm, where the lipid is in a liquid-crystalline phase (Fig. 6).

Content Mixing

Fusion is defined as the intermixing of both lipid and aqueous contents. In order to determine the nature of PAA-mediated vesicle aggregation, content mixing assays were carried out with ANTS/DPX probes. Content mixing of vesicles was not observed upon the addition of PAA at pH 3.8. Both probes were released from the vesicles and hence, did not come within quenching distance of each other.

Content Release

The release of the ANTS/DPX probes suggested that the PAA-associated vesicles were very leaky. The extent of vesicle destabilization was studied by following the release of encapsulated probes of different size. The advantage of using Lucifer Yellow instead of carboxyfluorescein or calcein for the release assay is its pH independence of the spectra and minimal spontaneous leakage of the fluorophore in the pH range studied (Walter et al., 1986). The spontaneous leakage of Lucifer Yellow from vesicles was less than 5% at pH 3.8 and less than 2% at pH 4.1 for SUV and undetectable for other pH and for LUV in the time range studied. The release of Lucifer Yellow (MW 457) occurred slowly at pH 4.1

and rapidly at pH 3.8 for both SUV and LUV in the presence of PAA (Fig. 7a). The leakage of vesicle contents and lipid intermixing occurred at the same pH. However, unlike lipid intermixing, the rate and the extent of content release were independent of vesicle concentration and lipid/polymer ratio. Release of Lucifer Yellow-dextran (MW 10,000) from LUV occurred only at pH 3.8 and at a much slower rate compared to Lucifer Yellow release likely due to its larger size (Fig. 7b).

MC-540

MC-540 is a lipophilic fluorescent molecule sensitive to membrane organization. The dye inserts preferentially into bilayers where lipids are more widely spaced (Williamson et al., 1983). Bound MC-540 exhibits a red shift of emission maximum accompanied by a large increase in fluorescence. MC-540 solution spectra were independent of the pH range studied, and the presence of PAA did not affect the spectra. Spectra of MC-540 incubated with vesicles without PAA addition were independent of pH with emission maximum at 578 nm. When vesicles in the presence of PAA were incubated with excess MC-540, most of the dye remained in solution above pH 4.6. The emission spectra at pH 4.6 showed characteristics of the dye in an aqueous environment with a slight red shift of the emission maximum from 572 nm (in H_2O) to 578 nm, similar to the spectrum of MC-540 incubated with vesicles without PAA. As the pH was decreased, a large increase in fluorescence intensity and a red shift of emission maximum to 585 nm were observed, which is indicative of dye molecules in a more hydrophobic environment (Fig. 8a). When MC-540 was titrated with vesicles, the binding curves showed that more dye was bound to polymer-associated vesicles at pH 3.8 (Fig. 8b). The increase in dye binding to vesicles is the result of the increased disorder in membrane packing.

Freeze-fracture

Freeze-fracture images were used to study morphological changes following the addition of PAA to EPC vesicles. Electron microscopy images of EPC-MLV at pH 3.8 showed a typical fracture image of multilamellar vesicles. PAA addition to above vesicles induced formation of fused multilamellar vesicles and cylindrical structures similar to those of cochleate structures (Papahadjopoulos et al., 1975) observed in Ca^{+2}-fused negatively charged vesicles (Fig. 9). Formation of cylindrical structures was also observed for unilamellar vesicles under the same conditions. It is not certain whether the tubular structures are formed from one sheet of bilayer membrane, as in the case of cochleates, or from multiple coaxial cylinders of bilayer. Subsequent increase in pH resulted in the formation of unilamellar vesicles with size ranging from 100 nm to over 1 μm. Reversion to MLV structures was not observed. This is similar to the LUV formation observed after EDTA chelation of Ca^{+2}-induced cochleates (Papahadjopoulos et al., 1975).

Discussion

Many fusion mechanisms, such as inverted hexagonal (H_{II}) phase formation (Ellens et al., 1986), lateral phase separation (Leventis et al., 1986), and membrane dehydration (Arnold et al., 1983), have been proposed depending on the types of fusogen and vesicles involved. It is postulated that there are two common barriers to overcome for a fusion process to occur: the hydration barrier and the structural barrier (Prestegard & O'Brien, 1987). Elimination of repulsive hydration forces between opposing bilayers allows intimate contact between the bilayers, resulting in vesicle aggregation.

PAA induces aggregation of both multilamellar and unilamellar PC vesicles below pH 5. As the pH is lowered, the polymer's ionic character decreases and its hydrophobic character increases due to protonation of the carboxylates. The increased hydrophobicity allows PAA to interact with vesicles at the lipid-water interface, possibly causing

dehydration of the phospholipid headgroup as indicated by the increase in Tm of PAA-complexed vesicles (Fujiwara et al., 1991). PAA overcomes the initial hydration barrier presumably by disrupting the organization of the aqueous solvent with the headgroups.

At pH less than 4.1, the hydrophobic character of PAA becomes great enough to overcome both the hydration barrier and the structural barrier such that PAA promotes lipid intermixing and content release of vesicles. Since the leakage rate is size-dependent but independent of vesicle concentration, release is most likely triggered by the loose membrane packing caused by destabilization of the membrane. Since bilayer contact-induced destabilization of vesicles would show a dependency of the leakage rate on vesicle concentration (Ellens et al., 1984), vesicle destabilization is caused most likely by polymer adsorption. MC-540 binding showed that the phospholipid packing of vesicles became disordered upon polymer interaction. The freeze-fracture electron micrographs suggest that the release of the probe is the result of bilayer rupture and subsequent reorganization to form tubular structures. Since a detergent-like action of the polymer to disrupt vesicles would result in a size-independent content release (Parente et al., 1990b), and the leakage from cochleate structures is expected to be greater than from membrane pores, the formation of cochleate-like tubular strucutre would explain the fast rate and the extent of content release from vesicles upon disruption. This apparent structural change also explains the failure to detect internal content mixing between vesicles due to the rapid dilution of the ANTS/DPX fusion probes. Since no content mixing was observed, the PAA-mediated interaction is not vesicle fusion. It is similar to the acid-induced destabilization of PE/cholesteryl hemisuccinate (CHEMS) liposomes, where a leakage and mixing of bilayer components without mixing of aqueous contents was observed (Ellens et al., 1985). One difference between the PAA system and CHEMS system is that PE/CHEMS liposomes undergo a lamellar-H_{II} phase transition (Ellens et al., 1986) while the PAA-mediated interaction does not. It is not surprising that such phase formation was

not detected in freeze-fracture images. H_{II} phase formation, an intermediate for fusion of vesicles containing PE, is highly unlikely for PC, which prefers to form a bilayer phase (Hauser et al., 1981).

Dehydration of the headgroups by PAA binding might induce a lateral phase separation, which is similar to a proposed mechanism for Ca^{+2}-induced fusion of negatively charged vesicles (Leventis et al., 1986). PAA-mediated interaction occurs only in the liquid-crystalline phase, where there is a larger spacing between the headgroups and the headgroups are more hydrated compared to that in the gel phase (Rand & Parsegian, 1989). It is possible that polymer-bound phospholipids prefer to exist in the gel phase due to dehydration of the headgroup. The phase separation between phospholipids in the liquid-crystalline phase and the polymer-bound phospholipids would provide the necessary defect in the membrane packing to overcome the structural barrier. This local perturbation would result in a destabilization of the bilayer, making vesicles prone to lysis. However, since no phase separation was observed from freeze-fracture images, this hypothesis could not be confirmed at this point.

PAA-vesicle interaction cannot be completely reversed by pH readjustment. Vesicle size was only partially reduced after an increase in the pH in the presence of PAA. Freeze-fracture images showed the formation of unilamellar vesicles of various sizes after pH readjustment. The increase in pH leads to dissociation of PAA from phospholipids due to the increased ionic character of the polymer, leaving the phospholipid bilayer to assume a vesicular structure.

Further characterization of pH-dependent PAA interaction with vesicles using spectroscopic and calorimetric techniques is in progress to support the above findings and to characterize further the perturbation in membrane structure.

Acknowledgements

We would like to thank Dr. J. P. Revel for his assistance with electron microscopy and Drs. C. DiSimone and G. Fujii for helpful comments on this manuscript.

References

Arnold, K., Pratsch, L., & Gawrisch, K. (1983) *Biochim. Biophys. Acta 728*, 121-128.

Böttcher, C. J. F.,van Gent, C. M., & Fries, C. (1961) *Anal. Chim. Acta 24*, 203-204.

Connor, J., & Huang, L. (1985) *J. Cell Bio. 101*, 582-589.

Ellens, H., Bentz, J., & Szoka, F. C. (1984) *Biochemistry 23*, 1532-1538.

Ellens, H., Bentz, J., & Szoka, F. C. (1985) *Biochemistry 24*, 3099-3106.

Ellens, H., Bentz, J., & Szoka, F. C. (1986) *Biochemistry 25*, 4141-4147.

Eum, K. M., Langley, K. H., & Tirrell, D. A. (1989) *Macromolecules 22*, 2755-2760.

Fujiwara, M., Grubbs, R. H., & Baldeshwieler, J. D. (1991) *Polym. Prepr. 32(1)*, 275.

Hauser, H., Pascher, I., Pearson, R. H., & Sundell, S. (1981) *Biochim. Biophys. Acta 650*, 21-51.

Hope, M. J., Bally, M. B., Webb, G. & Cullis, P. R. (1985) *Biochim. Biophys. Acta 812*, 55-65.

Lapidot, M., & Loyter, A. (1990) *Exp. Cell. Res. 189*, 241-246.

Leventis, R., Gagné, J., Fuller, N., Rand, R. P., & Silvius, J. R. (1986) *Biochemistry 25*, 6978-6987.

Mayer, L. D., Hope, M. J., & Cullis, P. R. (1986) *Biochim. Biophys. Acta 858*, 161-168.

Ohnishi, S., & Murata, M. (1988) in *Molecular Mechanisms of Membrane Fusion* (Ohki, S. et al., Eds), pp. 357-366, Plenum Press, New York.

Oky, N., Shibamoto, D., Ito, F., Gondo, H., & Nango, M. (1987) *Biochemistry 26*, 8145-8150.

Papahadjopoulos, D., Vail, W. J., Jacobson, K., & Poste, G. (1975) *Biochim. Biophys. Acta 394*, 485-491.

Parente, R. A., Nadasdi, L., Subbarao, N. K., & Szoka, F. C. (1990a) *Biochemistry 29*, 8713-8719.

Parente, R. A., Nir, S., & Szoka, F. C. (1990b) *Biochemistry 29*, 8720-8728.

Prestegard, J. H., & O'Brien, M. P. (1987) *Ann. Rev. Phys. Chem. 38*, 383-411.

Rand, R. P., & Parsegian, V. A. (1989) *Biochim. Biophys. Acta 988*, 351-376.

Seki, K., & Tirrell, D.A. (1984) *Macromolecules 17*, 1692-1698.

Straubinger, R. M., Düzgünes, N., & Papahadjopoulos, D. (1985) *FEBS Lett. 179*, 148-154.

Struck, D. K., Hoekstra, D., & Pagano, R. E. (1981) *Biochemistry 20*, 4093-4099.

Walter, A., Margolid, D., Mohan, R., & Blumenthal, R. (1986) *Membrane Biochem. 6*, 217-237.

White, J., Matlin, K., & Helenius, A. (1981) *J. Cell Biol. 89*, 674-679.

Williamson, P., Mattocks, K., & Schlegel, R. A. (1983) *Biochim. Biophys. Acta 732*, 387-393.

Zingsheim, H. P. (1972) *Biochim. Biophys. Acta 265*, 339-366.

FIGURE 1: Effect of pH on optical density of EPC-SUV (65 μM) in the presence of PAA (1:1 w/w). Optical density scale is normalized to EPC-SUV absorbance (400 nm) at pH 7.0.

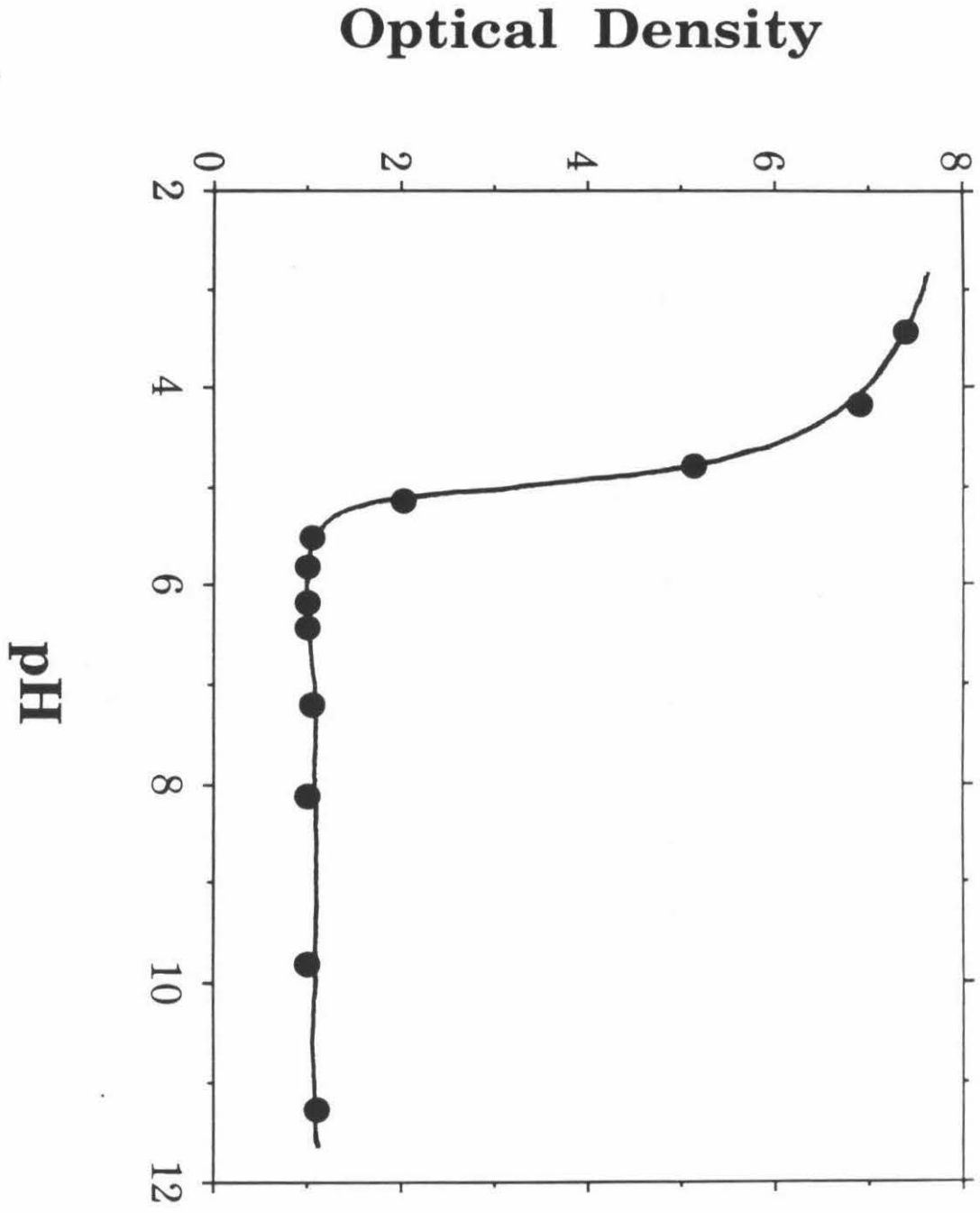
Optical Density
0
2
4
6
8
pH
2
4
6
8
10
12

FIGURE 2: (top) Dependence of EPC-SUV size distribution on pH. (bottom) EPC-SUV size distribution after addition of PAA (1:1 w/w). The solution pH is given in the figure.

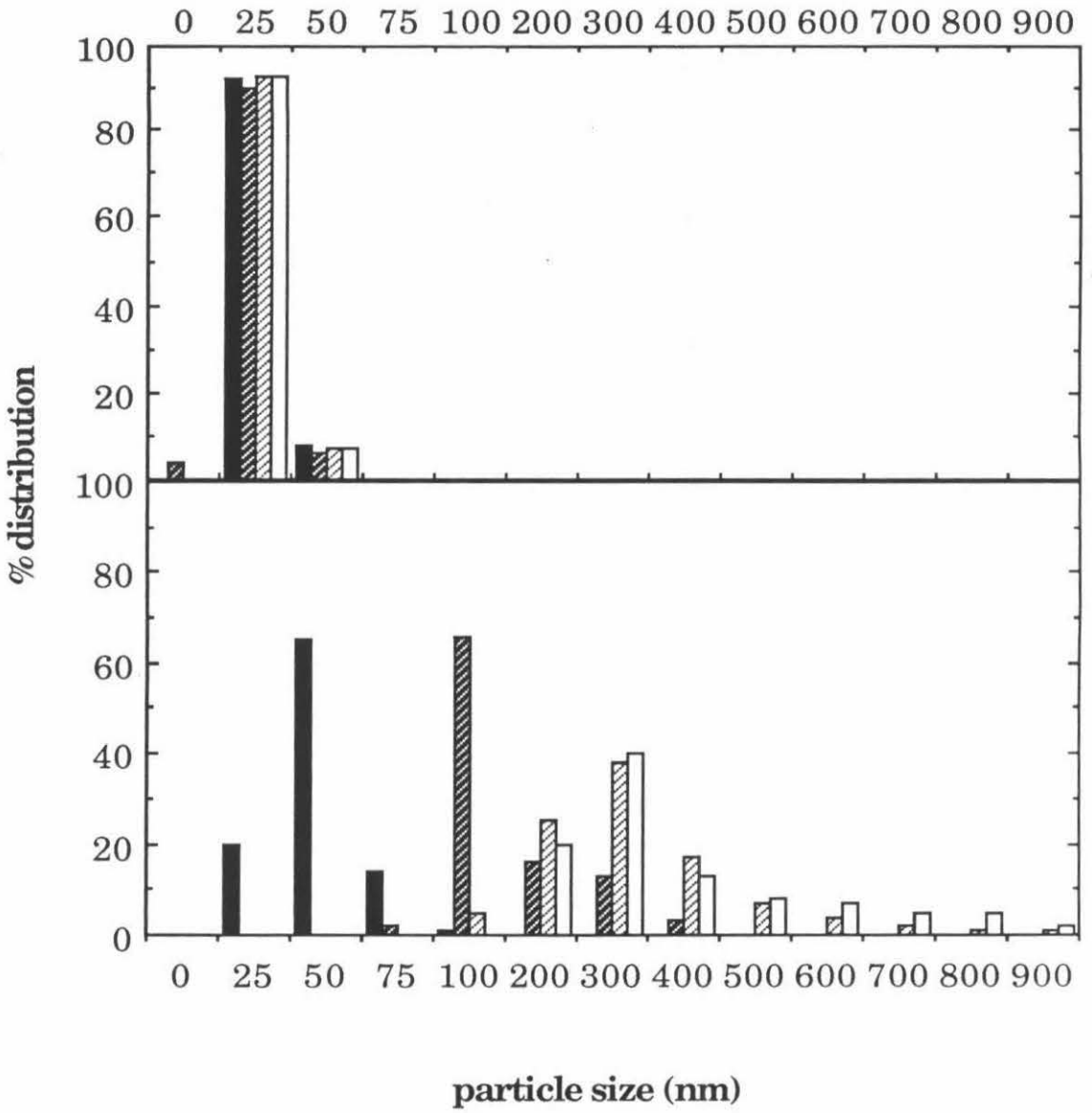
0 25 50 75 100 200 300 400 500 600 700 800 900
100
80
60
40
20
100
80
60
40
20
0
% distribution
0 25 50 75 100 200 300 400 500 600 700 800 900
particle size (nm)

FIGURE 3: Effect of pH on lipid intermixing of EPC vesicles (MLV, LUV, SUV) with PAA addition (1:1 w/w) at t=0.

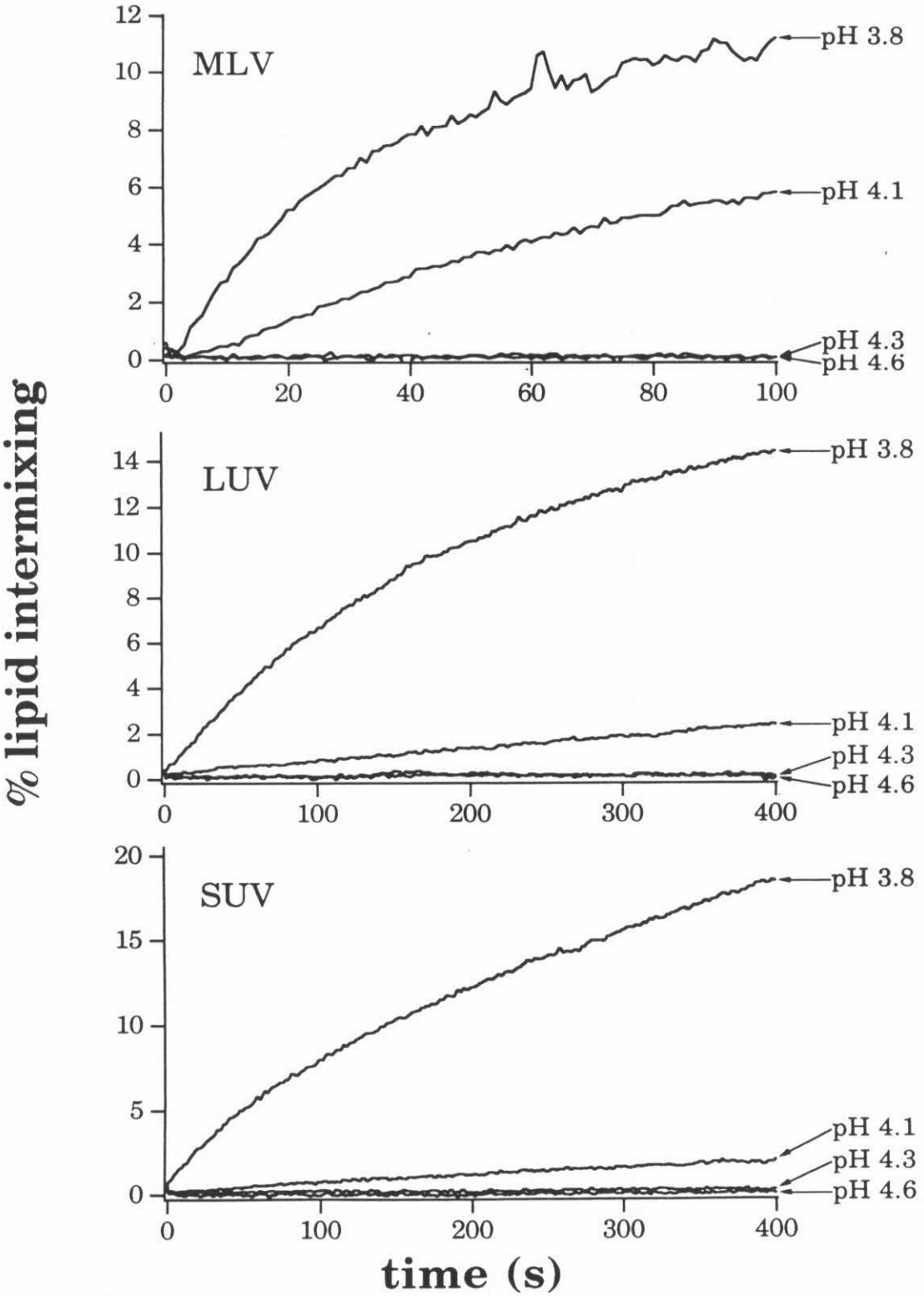
% lipid intermixing
MLV
pH 3.8
pH 4.1
pH 4.3
pH 4.6
LUV
pH 3.8
pH 4.1
pH 4.3
pH 4.6
SUV
pH 3.8
pH 4.1
pH 4.3
pH 4.6
time (s)

FIGURE 4: Effect of PAA concentration on EPC vesicle lipid intermixing at pH 3.8. o indicates the extent of lipid intermixing of LUV at 400 sec. • indicates the extent of lipid intermixing of MLV at 100 sec.

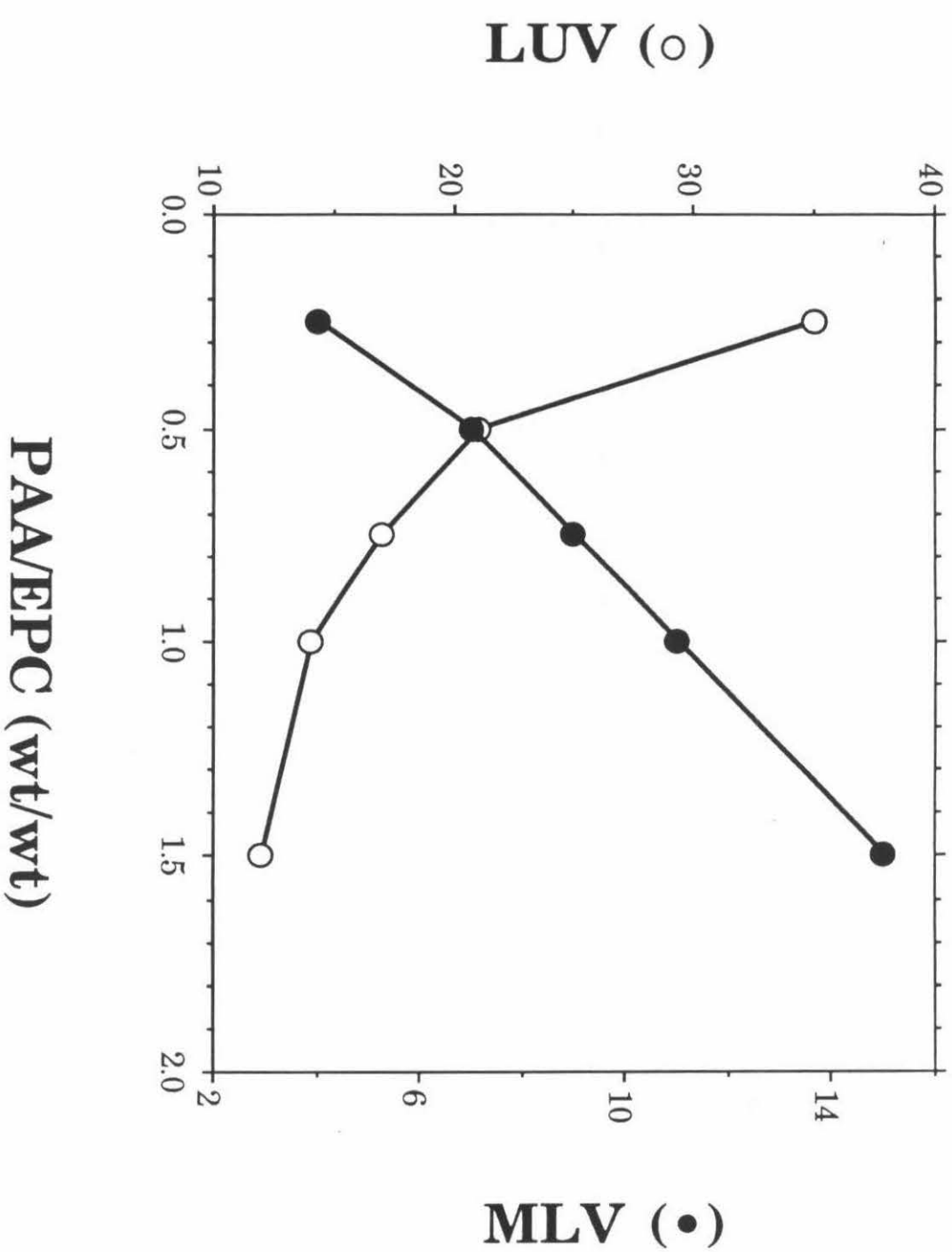
LUV (○)
40
30
20
10
0.0
0.5
1.0
1.5
2.0
PAA/EPC (wt/wt)
2
6
10
14
MLV (●)

FIGURE 5: Effect of pH on lipid intermixing of EPC-MLV made *in situ* with PAA (1:1 w/w). pH was adjusted with 0.5 N HCl. PAA-induced lipid intermixing of preformed EPC-MLV (o) is plotted for comparison.

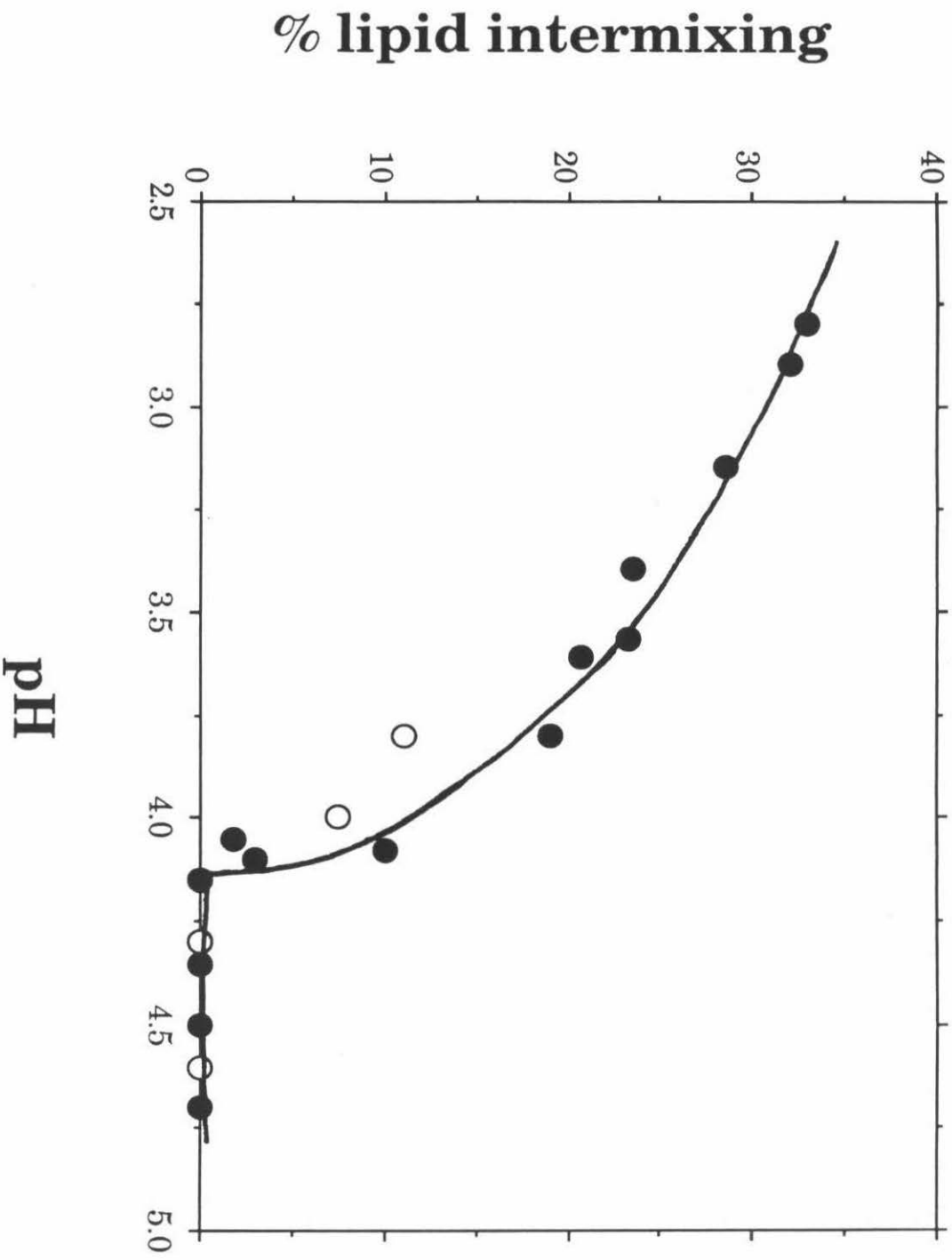
% lipid intermixing
0
10
20
30
40
pH
2.5
3.0
3.5
4.0
4.5
5.0

FIGURE 6: Temperature dependence of PAA-induced lipid intermixing of DPPC-MLV at pH 3.8. Lipid intermixing was measured 100 s after PAA addition (1:1 w/w).

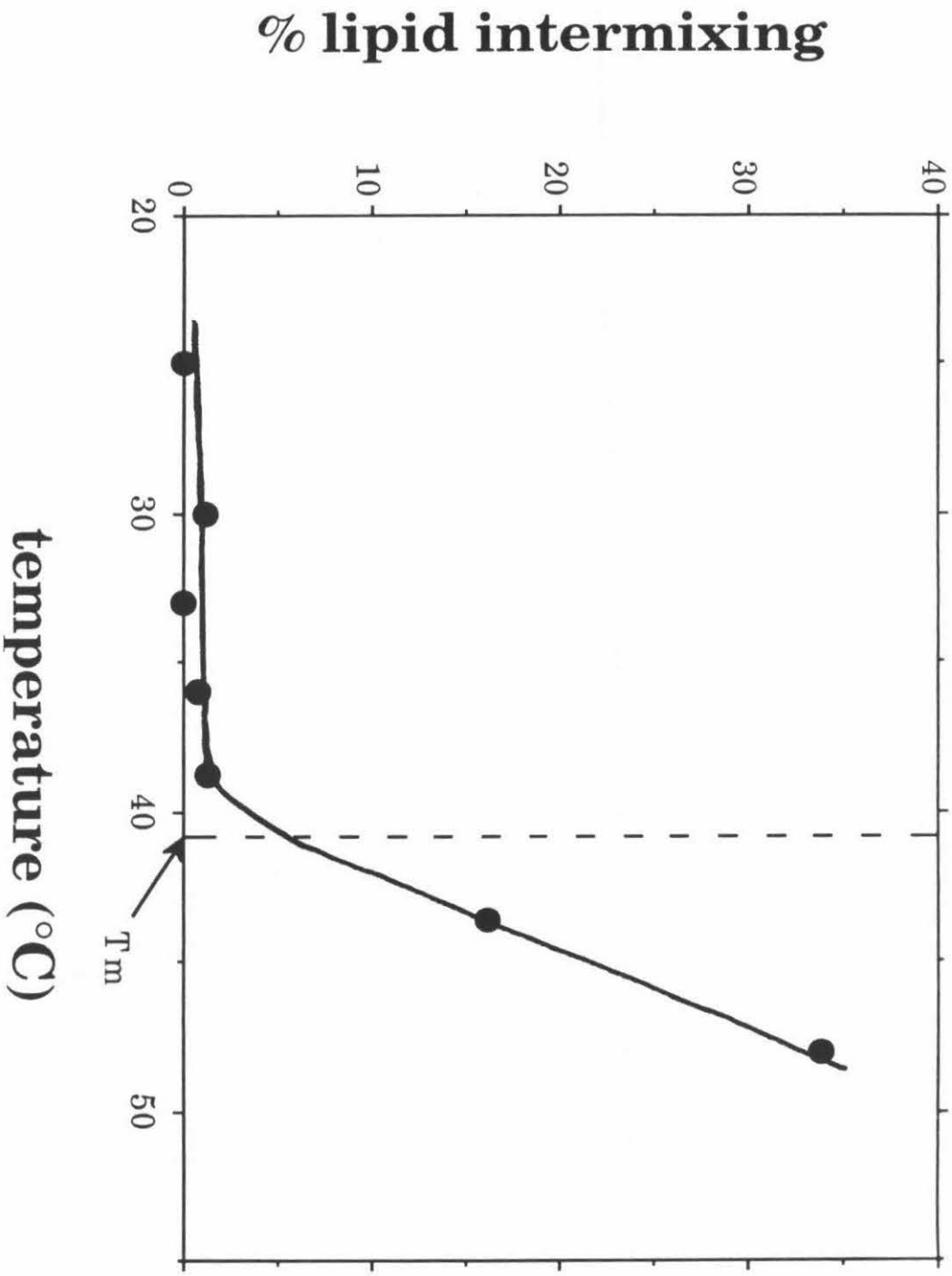
% lipid intermixing
0
10
20
30
40
20
30
40
50
Tm
temperature (°C)

FIGURE 7: Effect of pH on Lucifer Yellow release from EPC vesicles after PAA addition (1:1 w/w) at t=0. a) SUV and LUV b) Lucifer Yellow-dextran release from EPC-LUV.

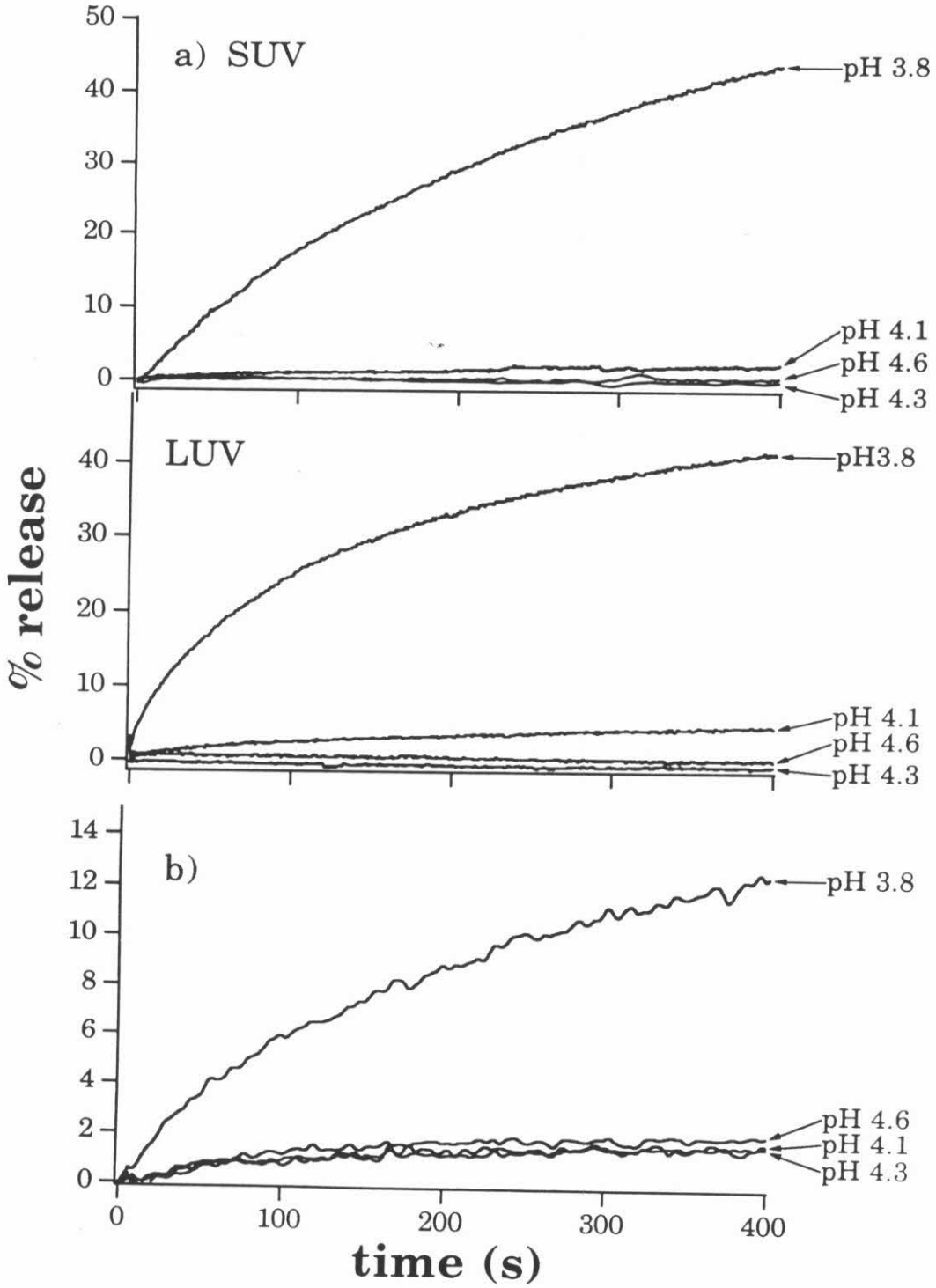
a) SUV
pH 3.8
pH 4.1
pH 4.6
pH 4.3
LUV
pH3.8
pH 4.1
pH 4.6
pH 4.3
b)
pH 3.8
pH 4.6
pH 4.1
pH 4.3
% release
time (s)
0
100
200
300
400

FIGURE 8: a) Emission spectra of excess MC-540 incubated with EPC-LUV (78 μM) in the presence of PAA (1:1 w/w) at various pH. b) A plot of MC-540 maximum emission fluorescence with varying EPC concentration at pH 3.8. o indicates EPC-LUV. • indicates EPC-LUV with PAA (1:1 w/w).

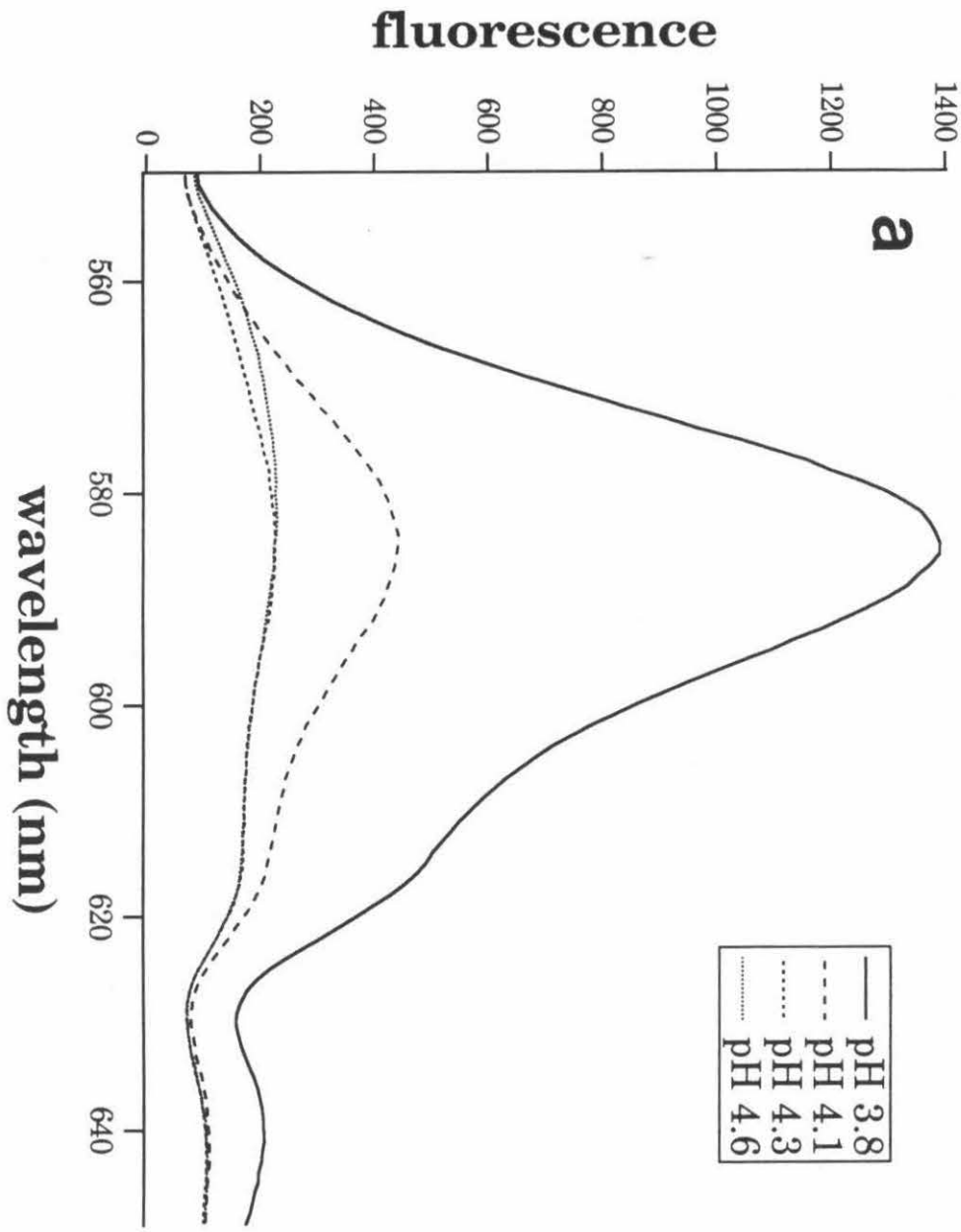
fluorescence
1400
1200
1000
800
600
400
200
0
a
pH 3.8
pH 4.1
pH 4.3
pH 4.6
560
580
600
620
640
wavelength (nm)

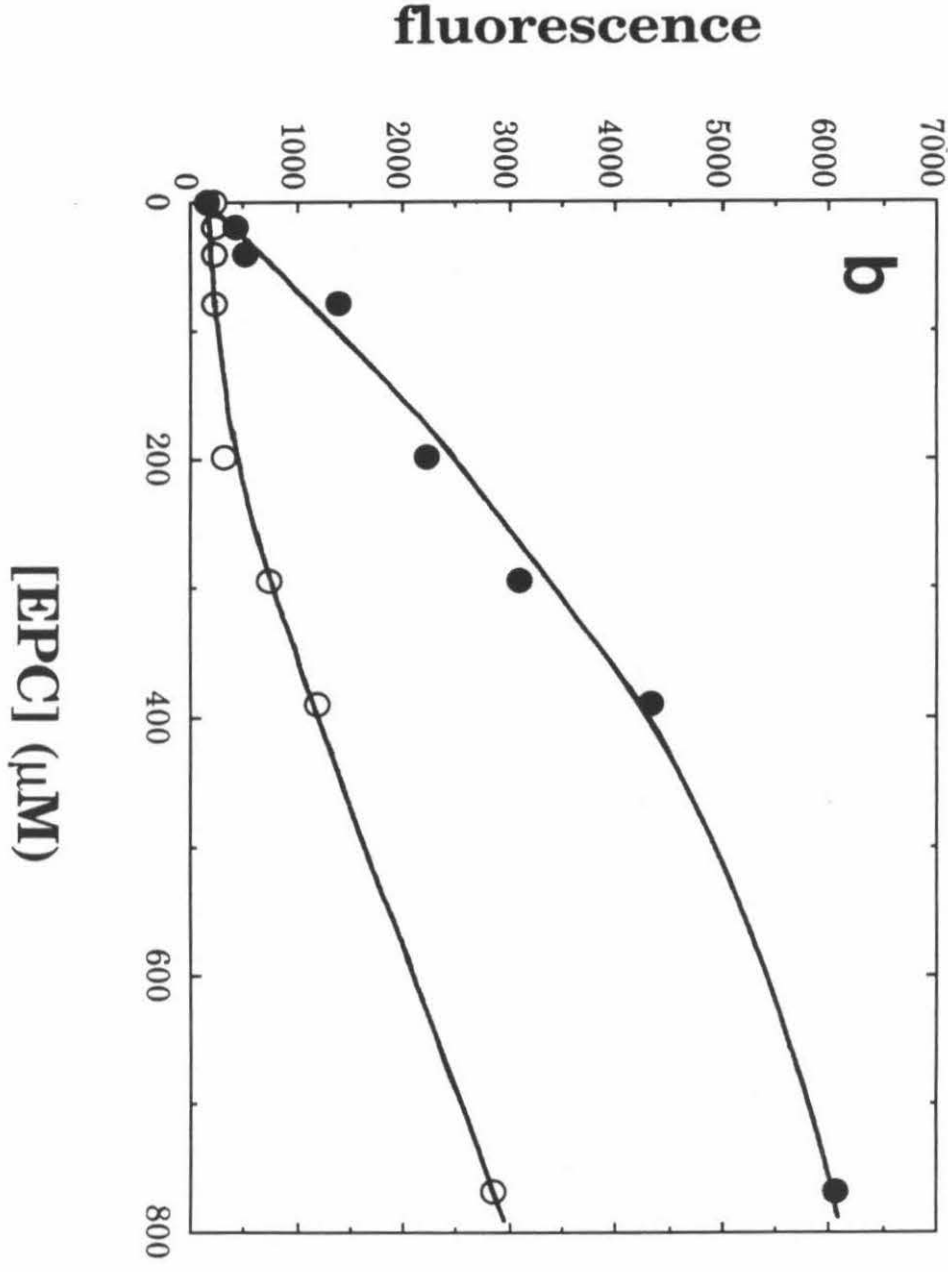
fluorescence
b
[EPC] (μM)
0
1000
2000
3000
4000
5000
6000
7000
0
200
400
600
800

FIGURE 9: Freeze-fracture images of EPC-MLV vesicles. a) at pH 3.8 b) after PAA addition (1:1 w/w) at pH 3.8 c) after pH was increased to 6 in the presence of PAA. The bar indicates 1 μm for a) and c) and 0.5 μm for b).


A


B

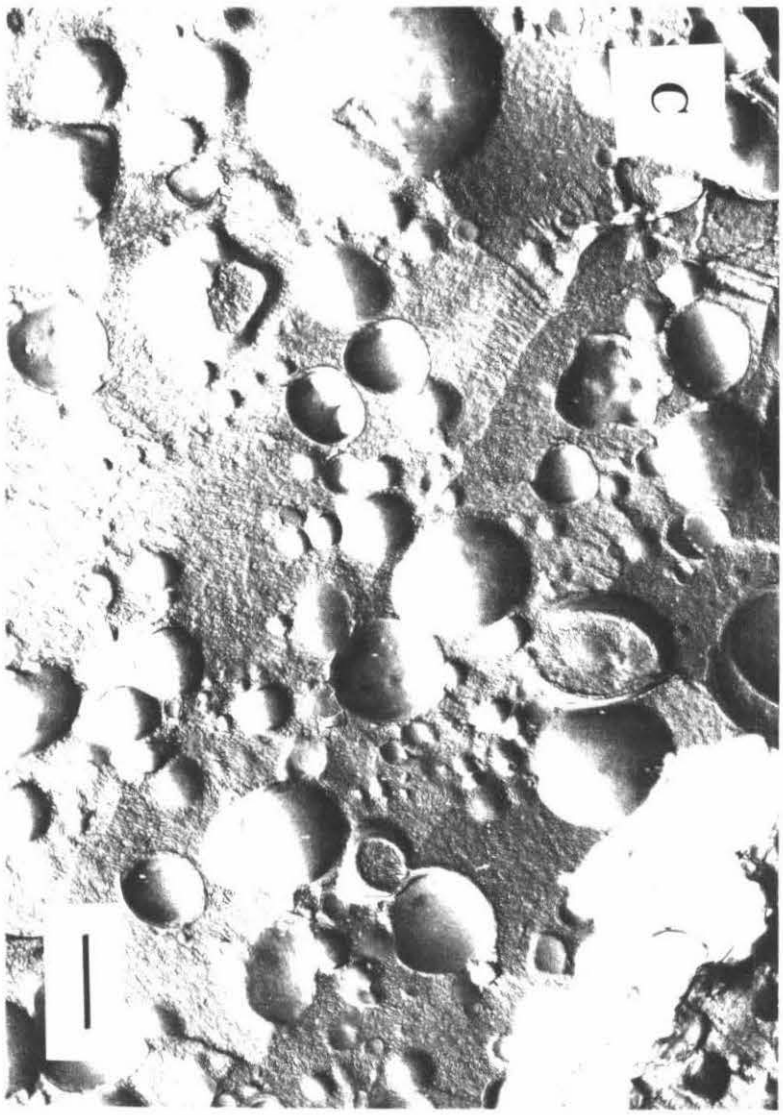
C

Chapter 3

Characterization of Vesicle Alterations Induced by Poly(Acrylic Acid) Using Calorimetric and Spectroscopic Techniques

Summary

Poly(acrylic acid) (PAA) have been shown to induce pH-dependent destabilization of phosphatidylcholine (PC) vesicles. Perturbations in the membrane structure resulting from PAA interactions with vesicles were characterized by DSC, FT-IR, fluorescence spectroscopy, and ^{31}P-NMR. PAA affects both the thermotropic and conformational properties of phospholipids. PAA-induced alterations in membrane properties of vesicles by PAA with changes in pH, lipid-polymer ratio, and temperature were studied. The effect of PAA on vesicle properties is minimal above pH 6. At low pH PAA induces an increase in the gel to liquid crystalline (LC) phase transition temperature (Tm) of the vesicles accompanied by an increase in the phase transition enthalpy (ΔH) and a decrease in the transition cooperativity. The interaction between PAA and vesicles is probably limited to the vesicle surface and the interface region. This suggests that any PAA-induced perturbation in the hydrocarbon region is due to an indirect effect resulting from perturbation in the headgroup regions. Drastic perturbations in phospholipid structure were detected upon investigation of the conformational properties of phospholipids. PAA-induces an increase in the disorder of hydrocarbon chain packing as evidenced by an increase in the peak positions and peakwidths of CH_2 asymmetric and symmetric stretching modes. The headgroup conformation and phospholipid phase behavior was investigated using ^{31}P-NMR. PAA-destabilized multilamellar vesicles showed ^{31}P-NMR spectra characteristic of multilamellar bilayer phase with decreased chemical shift anisotropy (CSA), indicative of increased headgroup packing disorder. PAA-induced destabilization

also results in increased hydrophobicity of the interfacial region and decreased mobility of the interfacial region as evidenced by fluorescence emission spectra and anisotropy measurements of phospholipid-conjugated dansyl probes incorporated in the vesicles.

Introduction

Even though many polyanions, such as PAA and pyran copolymer (DIVEMA), are shown to be biologically active,[1,2] the interaction of polyanions with model or cell membranes is not well understood. Contrary to polycations, which are known to electrostatically interact with negatively charged model membranes or cell membranes,[3] polyanion-membrane interaction is not obvious.

Tirrell has investigated the effect of pH on the interaction of vesicles and red blood cell ghosts with poly(carboxylic acid) derivatives.[4,5] Poly(ethacrylic acid) (PEAA) has been shown to induce micelle formation of multilamellar vesicles at a slightly acidic pH.[6] At low pH PEAA induced a broadening and an eventual loss of the main transition peak as evidenced by DSC.[4] Recently we have shown that PAA induces pH-dependent destabilization of PC vesicles (Chapter 2). PAA-induced vesicle aggregation occurred below pH 5 and lipid intermixing and release of vesicle contents occurred below pH 4.1. Formation of tubular structure was observed by freeze-fracture electron microscopy. Because of the difference in the hydrophobicity of the polymer, PEAA and PAA induce different vesicle behavior. However, both polymer seems to destabilize the bilayer membrane upon protonation. Though the polymer-induced vesicle interaction has been characterized, the mechanism of polymer-associated vesicle disruption has not been investigated.

Various spectroscopic and calorimetric methods were used to investigate the effect of PAA association on bilayer properties in an ongoing effort to understand the mechanism of pH-dependent vesicle destabilization induced by the polymer. Biophysical studies of phospholipid membranes were carried out to characterize the organization and dynamics of lipid matrix. DSC was used to study the gel to LC phase transition of phospholipid and the effect of PAA on the phospholipid phase transition. The CH_2 symmetric and antisymmetric stretching modes of the phospholipid was studied to characterize the changes

in the hydrocarbon chain packing. ^{31}P-NMR was used to probe the state of phospholipid phase and the headgroup packing behavior. Membrane fluidity was probed by measurements of the anisotropy of the phospholipid conjugated fluorescent probe, dansyl-phosphatidylenthanolamine (DPE).

Materials and Methods

Materials. EPC, DPPC, and DPE were obtained from Avanti Polar Lipids. PAA was obtained from Aldrich. Buffers were made from distilled deionized water.

Vesicle preparation. Vesicles were prepared as described previously (Chapter 2).

DSC. Calorimetry was conducted using a MC-2 scanning calorimeter (Microcal) heated at a rate of 60°C/h. A minimum of duplicate scans were made for each sample. Vesicle samples (1 mg/ml) were made in degassed acetate buffer (10 mM NaAcetate, 100 mM NaCl) of appropriate pH. Samples were scanned under nitrogen (10 psi) against the buffer as its reference. The data analysis was done by a DA-2 data aquisition and analysis system assuming a two-state reversible transition.

^{31}P-NMR. The spectra were recorded at 202.5MHz on Bruker AM500 NMR spectrometer equipped with a broad-band probe and interfaced to a computer. Inverse-gated broad-band ^{1}H-decoupling was applied to minimize sample heating. The chemical shift is measured relative to H_3PO_4 (85%) as an external standard. Spectral parameters are as follows, sweep width 40 KHz, pulse width 23 μs (90° flip angle), 200 Hz line broadening, and data set 16K. A lipid concentration of 50-100 mg/ml in acetate buffer containing 50% D_2O was used for all samples.

FT-IR. Temperature-dependence spectra of pelleted DPPC-MLV were recorded with FT-IR spectrophotometer (Perkin-Elmer 1600 series) with a resolution of 4 cm^{-1}. A CaF_2 cell (Beckman) was placed in a sample holder connected to a water bath, and the temperature of the cell was monitored with a thermocouple.

Fluorescence. Measurements of polarized fluorescence and fluorescence spectra were recorded on SLM spectrofluorometer. For polarization measurements DPE was excited with vertically polarized light at 340 nm with a slitwidth of 8 nm. The vertically and horizontally polarized fluorescence were measured at 90° configuration at 515 nm using a GG385 filter (Schott). The fluorescence anisotropy (r) was calculated as follows,

$$r = \frac{I_{//} - I_{\perp}}{I_{//} + I_{\perp}}$$

where $I_{//}$ and $I_{\perp}$ are the emission intensity through polarizer parallel and perpendicular to the excitation beam, respectively. Emission spectra of DPE (0.5 %) in EPC-LUV (1 mg/ml) in acetate buffer were obtained by excitation at 340 nm with excitation and emission bandwidths of 8 nm using a GG385 filter (Schott).

Results

DSC. Changes in the phase transition behavior from gel (Lβ) to LC (Lα) phase were studied. Since the pH range studied included low pH values, DSC scans of DPPC-MLV at low pH were obtained to insure that the low pH does not affect the vesicles. Tm of DPPC-MLV remained constant with a slight increase in the peak width ($T_{1/2}$) at pH 3.8. DSC thermograms exhibited by DPPC-MLV in the presence of PAA are resolvable into two components, a peak corresponding to the pure vesicles and a broad peak at a higher Tm with increased ΔH. As the pH was lowered, the DSC sans showed a gradual disappearance of the pretransition peak at 35°C and the main transition peak at 41°C with an accompanying appearance of a peak at 44°C (Fig. 1). At pH 3.8 only the latter peak is observed. The combined ΔH of all three peaks remains constant within the limit of experimental error at all pH. The fractional contribution of the original component to the total ΔH decreased with decreasing pH and increasing polymer concentration. PAA

induced an increase in Tm by approximately 3°C, accompanied by a loss of pretransition. A decrease in phase transition cooperativity is manifested in the broadening of the phase transition peak.

FT-IR. Changes in the behavior of acyl chains were investigated using the CH_2 asymmetric stretching mode. The frequency of this band is conformation-sensitive and responds to temperature-induced changes of the *trans/gauche* ratio in the acyl chains, such as gel to LC phase transition.[7] Changes in frequency and bandwidth can be semiquantitatively correlated with a change in the population of *gauche* conformers in the chain and the chain packing disorder. The frequency and the bandwidth of CH_2 asymmetric stretch of DPPC-MLV were measured as a function of temperature through the gel to LC phase transition. DPPC-MLV at pH 7.4 and 3.8 with and without PAA were examined (Fig. 2). The value for Tm, taken at the midpoint of the transition region in the IR spectra agreed with DSC values. The IR transition also showed a decrease in cooperativity in the presence of PAA at low pH. The increase in wavenumber of the CH_2 stretch suggests an increase in the proportion of *gauche* conformer. Therefore PAA induces an disorder in hydrocarbon chain packing at low pH. The change in the bandwidth at Tm is directly related to the disorder introduced in the acyl chains and is proportional to ΔH of the transition. The larger change in bandwidth observed with PAA at low pH compared to without PAA suggests an increase in ΔH, which is consistent with the DSC results.

The PO_4^- stretch is sensitive to headgroup conformation and hydration.[8] Investigation of the PO_4^- stretch of lyophilized and nonlyophilized samples of DPPC-MLV showed that no effect on the PO_4^- stretch was detected upon PAA addition within experimental limits.

Fluorescence. The effect of PAA adsorption on the phospholipid interface region was investigated using DPE. The dansyl probe, covalently attached to the lipid headgroup, is

located in the glycerol region and sensitive to the environment.[9] The emission maximum of the probe is related to its local dielectric constant as long as the excitation spectra remains the same.[10] Excitation spectra of DPE were independent of the pH in the range studied. Since the excitation is independent of the presence of PAA, the local dielectric constant was evaluated from the Stoke's shifts of DPE incorporated into PC vesicles. Changes in the emission spectra of DPE incorporated into EPC-SUV were measured at various pH in the presence of PAA (Fig. 3). An increase in emission maximum was observed, indicating an increase in the hydrophobicity at the interfacial region of the vesicle. DPE has also been used to detect lipid dynamic structure by fluorescence depolarization techniques, which give the motional and structural state of the chromophore and its environment.[11] An increase in anisotropy, which is correlated with a decrease in the probe mobility or the fluidity of the phospholipid, was observed upon PAA addition at low pH (Fig. 4).

^{31}P-NMR. ^{31}P-NMR spectra of EPC-MLV in the presence of PAA were acquired at various pH (Fig. 5). At all pH values, the phospholipids exhibited typical ^{31}P-NMR spectra of MLV with or without PAA. Nonbilayer phases, such as H_{II}, were not detected. This is consistent with the freeze-fracture images (Chapter 2). A decrease in the chemical shift anisotropy (CSA) of the powder pattern was observed with decreasing pH in the presence of PAA. A slight downfield shift of the main peak was also detected with decreasing pH. These values remained constant at these pH values without addition of PAA.

Discussion

We showed previously that PAA could induce extensive lipid intermixing and destabilization of PC vesicles at low pH, but not a true fusion with intermixing of the encapsulated aqueous space as well (Chapter 2). The effect of PAA on vesicle properties is minimal around neutral pH probably due to electrostatic repulsion. At neutral pH PAA is

highly negatively charged. At low pH its anionic character decreases and its hydrophobic character increases due to protonation of the carboxyl groups. As vesicles interact with protonated PAA, two populations of vesicles are observed with DSC, 1) the vesicles with high Tm and low cooperativity of transition and 2) the vesicles which exhibits properties similar to those of the pure lipid. The heterogeneous population of vesicles could be the result of the formation of a population of vesicles that have undergone lipid intermixing through interaction with PAA and a population of bulk lipids, or could be due to polymer-induced phase separation in all or some of the vesicles.

There are three possible contributions to induce this phase transition behavior: 1) changes in the hydrocarbon chain interactions 2) expansion of the lipid vesicles and 3) changes in the headgroup conformation. The gel to LC phase transition involves increased volume of lipid vesicles, increased hydration, increased surface area of phospholipid headgroup, increased bilayer thickness, and conformational changes in the headgroup and the hydrocarbon chains.[12,13] A general correlation have been made regarding protein-vesicle interaction and changes in the phase transition behavior of vesicles.[14,15] Hydrophobic proteins that tend to interact with the hydrophobic domain of the lipid bilayer have no effect or slight effect on the Tm, but produce a decrease in ΔH proportional to their concentration in the membrane. Proteins that bind to the interface and do not penetrate into the bilayer have either no effect or increase Tm and produce a large increase in ΔH. The proteins do not induce permeability increase or monolayer expansion. Proteins that bind and expand phospholipid monolayer produce a decrease in Tm and ΔH indicating a marked fluidizing effect. From DSC results PAA seems to fall in the second category; however, PAA binds to vesicles and also induces monolayer expansion (Chapters 4 and 5).

Increased Tm is caused by increased van der Waals interactions between the lipid acyl chains and usually results from interaction between the polar head groups of phospholipids.[16] Through modification of the headgroup hydrogen-bonding, PAA affects

the lipid headgroup conformation and the acyl chain packing, without direct interaction with the acyl chains. The effect on the pretransition peak also supports headgroup interaction. The pretransition peak disappears with the main transition. This suggests that the lipid headgroup conformation is altered by PAA since pretransition is associated with long axis rotation of PC molecules.[17] However, the possibility of the pretransition peak being hidden beneath the higher temperature transition cannot be discarded.

Dehydration of liposomes also causes an increase in Tm. PAA may affect Tm by competing with the phospholipid polar group for water of hydration. PAA induced dehydration was not detected by IR spectra. possibly because the phosphate stretching frequency is sensitive to the degree of hydration only at a low level of hydration (less than 10 water molecules per phospholipids).[8] Other methods, such as D-NMR, might be useful in determining the effect of PAA on vesicle hydration (see Chapter 7). Changes in hydration result in changes in Tm of 6-8 ^{o}C while changes in the hydrogen bonding result in 1-3 ^{o}C.[18] The increase in Tm produced may also be the result of a reduction of the surface charge density of the bilayer.[19] ΔH depends on the number of gauche conformers and the distance between the hydrocarbon chains. The 2 kcal increase in the ΔH indicates the decreased packing density of hydrocarbon chains from increased packing disorder. This is also supported by IR results.

Increased disorder and motion of the headgroup of phospholipid lead to a reduction in the CSA.[21] However, for polymerized vesicles, a reduction in CSA resulted from a change in headgroup orientation and reduced motion of the headgroup as supported by the T_1 and cross polarization measurements.[22] Therefore, with PAA-vesicle system, the reduction in CSA upon polymer binding is due to headgroup orientation change and packing disorder. Due to lack of T_1 and cross polarization results, we are not able to state about the change in the motion of the phospholipid headgroup.

A decrease in probe motion and increased hydrophobicity of the probe environment suggest dehydration of phospholipid surface and increased rigidity at the interface region. A correlation between membrane fusion and decreased dielectric constant, or increased hydrophobicity, of DPE incorporated in the vesicles has been obtained. It could also have resulted from changes in the location of the probe. Due do the increased permeability of the liposomes, the probe location could have moved toward the hydrocarbon chain, giving similar results. Because of the ambiguity associated with the analysis of the results, the DPE experiment was not pursued further. The motional and structural state of DPE and its environment has been investigated.

Formation of polymer bridges between apposed vesicles leads to vesicle aggregation and subsequent lipid mixing. The bridging mechanism explains the close apposition of vesicles, but the polymer molecule must be separated from the contact region. Since polymer adsorption results in polymer repulsion, the contact regions of the bilayer must be at the membrane surface not covered with PAA.

References

1. Breslow, D.S. *Chemtech.* **15**, 302 (1985).
2. Anionic Polymeric Drugs Donaruma L.G. et al. eds. Wiley-Interscience, New York, 1980.
3. Schuler, F. *Biochem J.* **260**,1 (1989).
4. Seki, K. and Tirrell, D.A. *Macromolecules* **17**, 1692 (1984).
5. Tirrell, D.A., Takigawa, D.Y. and Seki, K. *Ann. N.Y. Acad. Sci.* **446**, 237 (1985).
6. Schroeder, U.K.O. and Tirrell, D.A. *Macromolecules* **22**,765 (1989).
7. Casal, H.L. and Mantsch, H.H. *Biochim. Biophys. Acta* **779**, 381 (1984).
8. Chapman, D. *Chem. Phys. Lipids* **1**, 445 (1967).
9 Waggoner A.S. and Stryer, L. *Proc. Natl. Acad. Sci.* **67**, 579 (1970).
10 Kimura, Y. and Ikegami, A. *J. Membr. Biol.* **85**, 225 (1985).
11. Kimura, Y. *J. Membr. Biol.* **96**, 187 (1987).
12. Levin, I. in Advances in Infrared and Raman Spectroscopy vol. 11 , Clark, R.J.H. and Hester, R.E. eds. Wiley-Interscience, New York, 1984.
13. Mabrey-Gaud, S. in Liposomes from Physical Structure to Therapeutic Applications Knight C.G. ed. Elsevier, New York, 1981.
14. Papahadjopoulos, D. *J. Coll. Int. Sci.* **58**, 459 (1977).
15. Marrow, M.R. and Davis, J.H. *Biochim. Biophys. Acta* **904**, 61 (1987).
16. Susi, H., Sampugna, J., Hampson, J.W. and Ard, J.D. *Biochemistry* **18**, 297 (1979).
17. Marsh, D. *Biochemistry* **19**, 1632 (1980).
18. Cevc, G. and Marsh D. in Phospholipid Bilayers Wiley-Interscience, New York, 1987.
19. Boggs, J.M. Rangaraj, G. and Kosby, K.M. *Chem. Phys. Lipids* **40**, 23 (1986).
20. Ohki, S. and Arnold, K. *J. Membr. Biol.* **114**, 195 (1990).

21. Cullis, P.R., deKruijff, B. and Richard, R.E. *Biochim. Biophys. Acta* **426**, 433 (1976).

22. Handel, T.M. in Disulfide Polymerizeable Phosphatidylcholine: Characterization of Membrane Physical Properties and Investigations of in vivo Behavior (Thesis) California Institute of Technology, California, 1989.

Figure 1. DSC profiles and the corresponding table of DPPC-MLV phase transition with PAA addition (1:1 w/w) at various pH. Units for Tm and $T_{1/2}$ are ^{o}C and for ΔH is cal/mol.

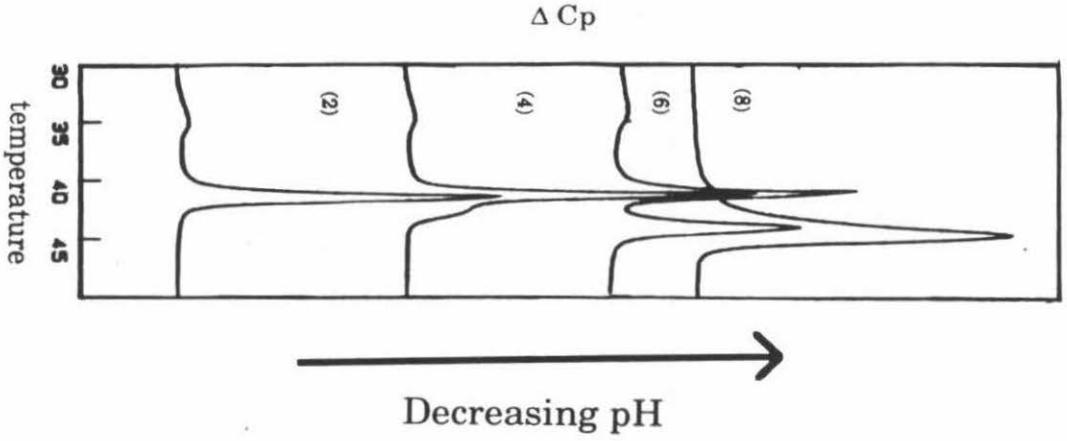

	sample	pH	Tm	ΔH°	$\Delta T_{1/2}$
1	DPPC	7.6	40.9	7250	0.56
2	DPPC + PAA	7.6	41.1	6400	0.89
3	DPPC	6.6	41.2	11550	0.54
4	DPPC + PAA	6.6	41.2	11300	0.66
5	DPPC	4.6	41.1	9300	0.61
6	DPPC + PAA	4.6	41.1	1700	0.64
			44.2	10250	1.25
7	DPPC	3.8	41.3	9500	0.80
8	DPPC + PAA	3.8	44.5	10700	1.58

Units for Tm and $\Delta T_{1/2}$ are (°C) and for ΔH^{o} is (cal/mol).

Figure 2. Vibrational frequency and peakwidth for CH_2 asymmetric stretch as a function of temperature.

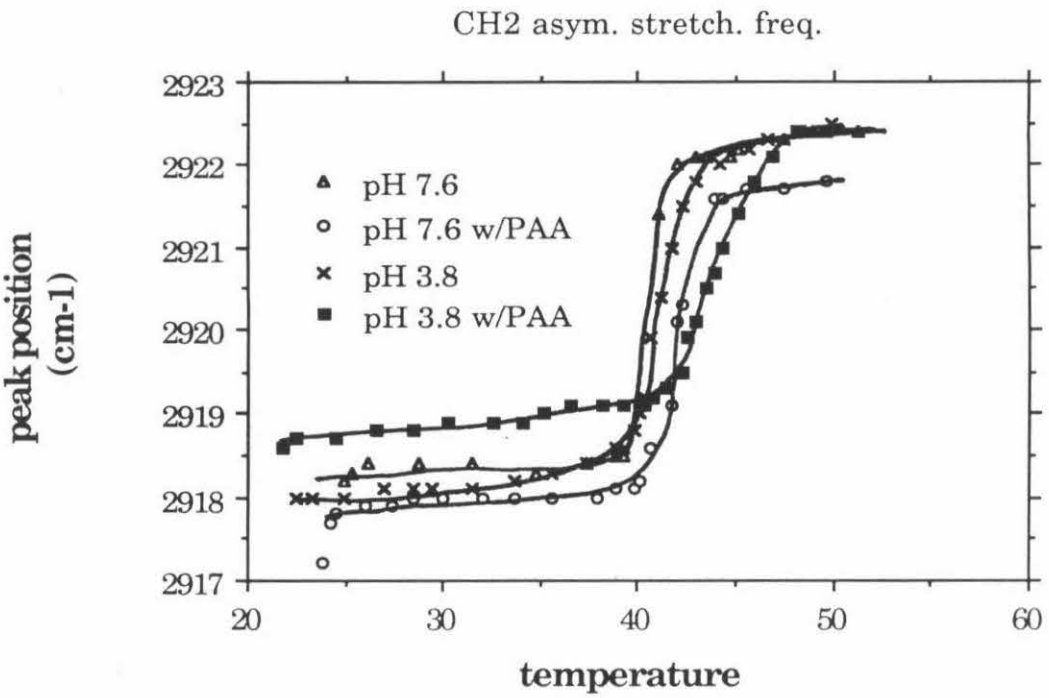
CH2 asym. stretch. freq.
peak position (cm-1)
2923
2922
2921
2920
2919
2918
2917
pH 7.6
pH 7.6 w/PAA
pH 3.8
pH 3.8 w/PAA
20
30
40
50
60
temperature

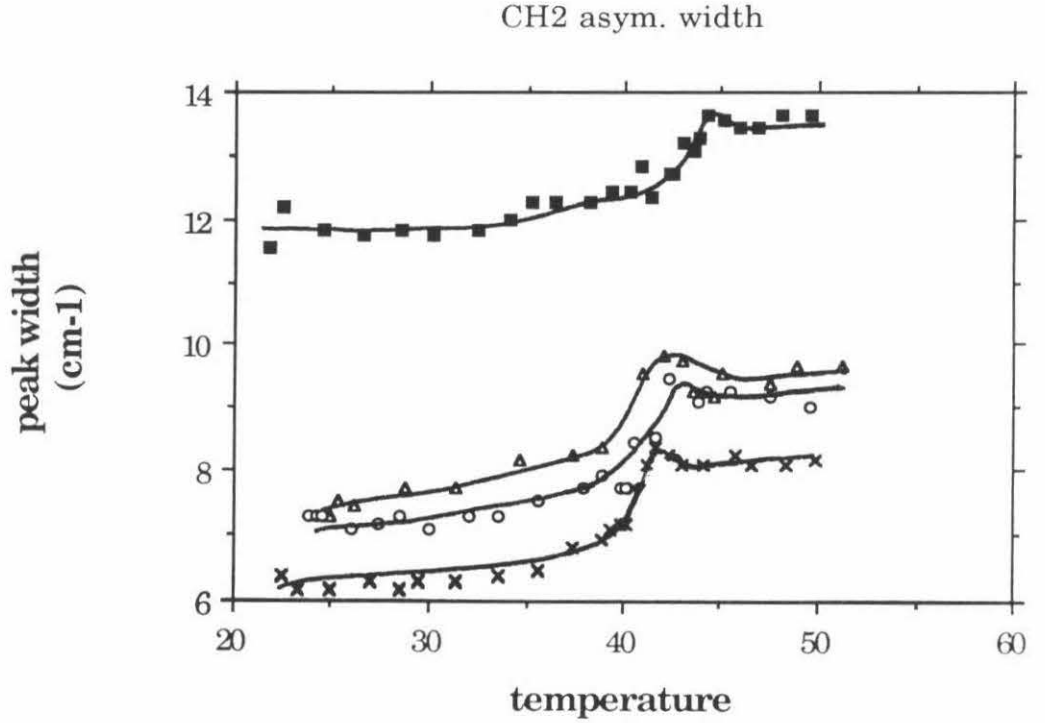
CH2 asym. width
peak width (cm-1)
14
12
10
8
6
20
30
40
50
60
temperature

Figure 3. Effect of PAA addition on fluorescent emission spectra of DPE in EPC-SUV.

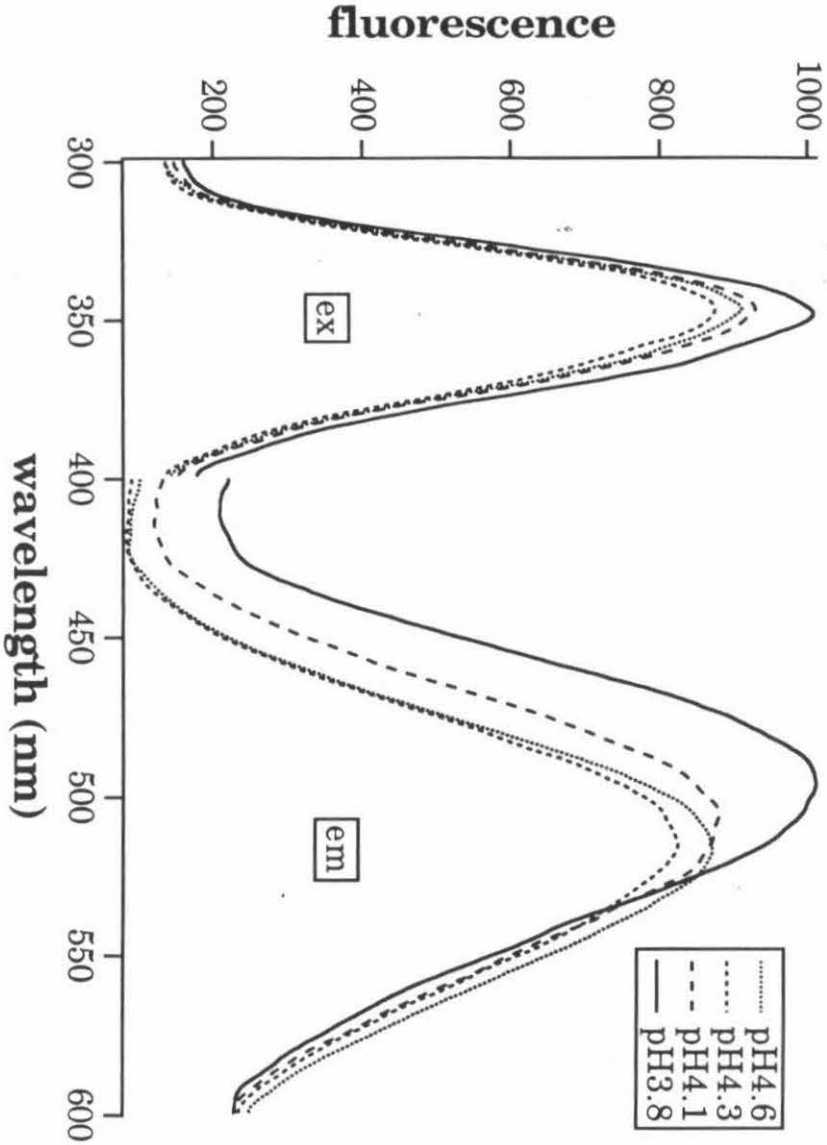
fluorescence
1000
800
600
400
200
300
350
400
450
500
550
600
wavelength (nm)
ex
em
pH4.6
pH4.3
pH4.1
pH3.8

Figure 4. Effect of PAA addition on fluorescence anisotropy of DPE in EPC-SUV.

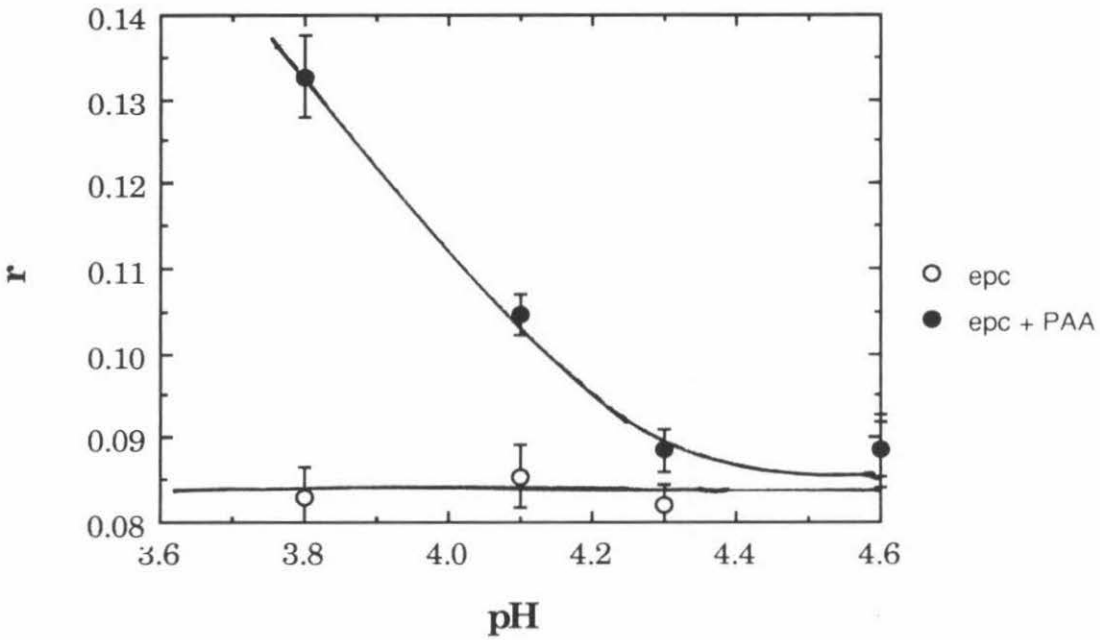
0.14
0.13
0.12
0.11
0.10
0.09
0.08
r
3.6
3.8
4.0
4.2
4.4
4.6
pH
epc
epc + PAA

Figure 5. ^{31}P-NMR spectra of EPC-MLV at various pH a) without and b) with PAA.

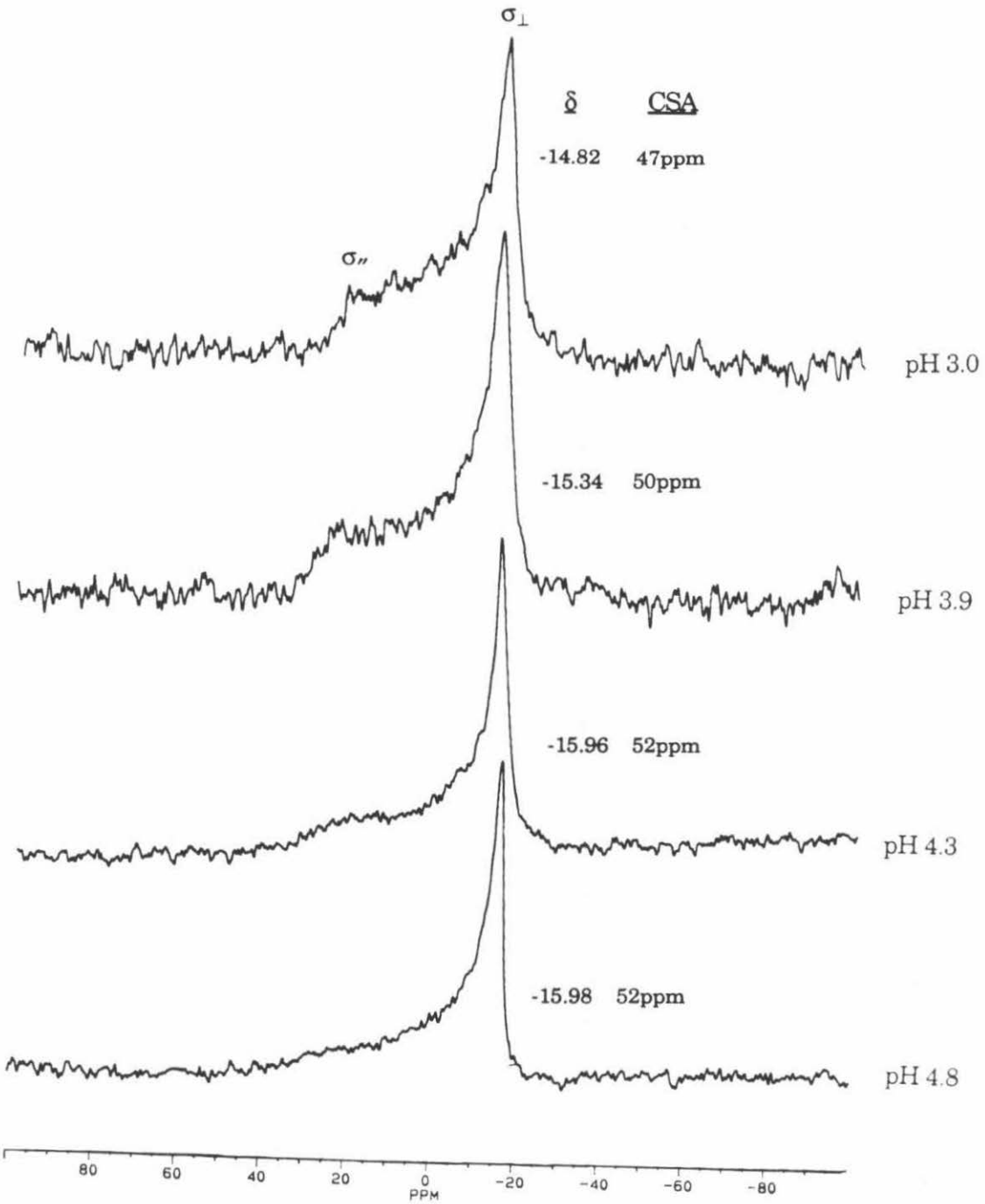
σ⊥
δ
CSA
-14.82
47ppm
σ//
pH 3.0
-15.34
50ppm
pH 3.9
-15.96
52ppm
pH 4.3
-15.98
52ppm
pH 4.8
80
60
40
20
0
PPM
-20
-40
-60
-80

Chapter 4

Fluorescence Studies of PAA Complexation With Phospholipid Vesicles

Summary

Complex formation of poly(acrylic acid) (PAA) with phospholipid vesicles was characterized by the change in the polarization of acenaphthylene molecules attached to the polymer backbone. The complexation was pronounced below pH 4, when the polymer carboxyl groups are protonated, as observed by a decrease in the probe mobility and an increase in polymer binding to vesicles. Complexation was strong at low polymer to vesicle ratios and was weaker at high polymer to vesicle ratios possibly due to different interactions of polymers with the vesicle surface. This model is used to explain the observed negative cooperativity of PAA binding to vesicles.

Introduction

Cooperative complexation between water soluble polymers has been investigated because of its wide application in the areas of mineral processing, filtration, batteries, and a model of the interaction of biological macromolecules.[1] Proton donating polymer, such as PAA, is known to form a complex with proton accepting polymer, such as poly(ethylene oxide) (PEO) and poly(vinyl pyrrolidone) (PVP)[1,2] (Fig. 1). Polymer complexes are formed by the association of two or more complementary polymers and may arise from electrostatic forces, hydrophobic interactions, hydrogen-bonding, van der Waals or combinations of these interactions.[1] Due to the long-chain structure of the polymers, once one pair of complementary repeating units associate to form a segmental complex, many other units may readily associate without significant loss of translational

degrees of freedom. Hence, the complexation process is cooperative, and stable polymer complexes may form even if segmental interaction energy is relatively small.[1]

Poly(carboxylic acid)s have been shown to interact with phospholipid vesicles at acidic pH.[3] It has been suggested that the interaction of poly(carboxylic acid) with phospholipid possibly involves a H-bonding between the phosphate group of the lipid and the carboxyl group of the polymer.[3] PAA has been shown to destabilize phosphatidylcholine (PC) vesicles at pH below 4.1 and change vesicles properties, such as phase transition temperature, permeability, particle size, etc. (Chapters 2 and 3). Complexation of PAA with PC vesicles were studied using acenaphthylene modified PAA (ace-PAA).

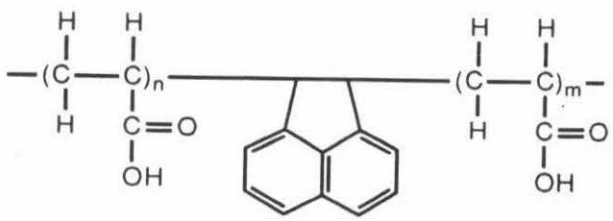

(ace-PAA)

Fluorescence depolarization of ace-PAA has been used to study the behavior of polymer during complexation with PEO.[4] The associated chains are believed to be stiffer as observed by the decrease in the segmental motion of the polymer chain. The advantage of using acenaphthylene, which is incorporated in the backbone, as opposed to a sidechain probe is that it minimizes the motion independent of polymer backbone and is a true measure of polymer segmental motion.[5]

Behavior of polymer chain during PAA complexation with PC vesicles was investigated by fluorescence deploratization measurements at various pH and polymer/lipid ratios and from binding studies.

Materials and Methods

Materials. Acenaphthylene (Aldrich) was recrystalized three times from methanol. AIBN (Fluka) was recrystallized three times from acetonitrile/water. Acrylic acid (Aldrich) was passed through inhibitor remover column (Aldrich). 2-Butanone was dried over $CaSO_4$ and vacuum distilled. All other materials were reagent grade or better and used as received.

Ace-PAA Synthesis. Ace-PAA was synthesized as described previously.[6] Acenaphtyhlene (10 mg) and acrylic acid (1 g) were polymerized with AIBN (100mg) in 2-butanone under Ar at 60°C for 90 min. Precipitated polymer was washed with ether, dissolved in water and repeatedly dialyzed (molecular weight cut off 1000) against water to remove low molecular weight materials and freeze-dried. Molecular weight of Ace-PAA (43,000) was determined by viscosity measurement in 2N NaOH at 25°C using k = 42.2 x 10^3 and a = 0.64[7] in the following equation,

$$[\eta] = kM^a$$

where h is the viscosity, M is the molecular weight, and k and a are experimentally determined constants. One acenaphthylene molecule per 323 monomers was incorporated. This corresponds to less than 2 acenaphthylene molecule per polymer strand.

Binding Studies. Large unilamellar vesicles of egg-PC (EPC-LUV) of 200 nm in diameter were prepared as described previously (Chapter 2). EPC-LUV (830 μM) in acetate buffer (50 mM NaAcetate, 150 mM NaCl) was incubated with ace-PAA (15 μM) overnight at 25 °C at various pH. Vesicles were separated from free ace-PAA by ultracentrifugation at 84,000 x g for 30 min using L5-56 Beckman Ultracentrifuge with an SW 50.1 rotor. The amount of ace-PAA bound was determined from fluorescence emission intensity at 340 nm with 295 nm excitation using an ace-PAA calibration curve. The extent of polymer binding to vesicles at varied polymer/lipid ratios was determined

at pH 3.8, and a corresponding Scatchard plot was obtained. All polymer/lipid ratios are wt/wt.

Fluorescence Polarization. Anisotropy (r) of ace-PAA was obtained with 295 nm excitation and 340 nm emission using a WG320 filter (Schott). Anisotropy values were calculated as described previously (Chapter 3). Anisotropy of ace-PAA (1.15 μM) with and without EPC-LUV (63 μM) in acetate buffer were obtained at various pH. Dilute concentration of EPC-LUV was used to reduce the effect of light scattering on the polarization measurements. Anisotropy of ace-PAA in the presence of EPC-LUV at varied polymer/lipid ratios were obtained at pH 3.8.

Fluorescence Lifetime. "Apparent" lifetimes of Ace-PAA were measured by phase modulation method using SLM 4800 spectrofluorimeter.[8] Phase (τ_p) and modulation (τ_m) lifetimes were obtained at various pH in the presence of EPC-LUV in acetate buffer at a modulation frequency of 18 kHz. Lifetimes were determined from the following equation,

$$\tau_p = \omega^{-1}\tan \phi$$

$$\tau_m = \omega^{-1}[(1/m^2)^{-1}]^{1/2}$$

where ω is the modulation frequency, ϕ is the phase delay, and m is the demodulation factor.

Results

Binding Study. The amount of ace-PAA bound to EPC-LUV at various pH was determined (Fig. 2a). The extent of Ace-PAA binding to EPC-LUV increased dramaticaly at pH below 4.5. The amount of ace-PAA bound to EPC-LUV at different polymer/lipid ratio were measured at pH 3.8 (Fig. 2b). The amount of ace-PAA binding to vesicles increased with increasing polymer concentration and saturated at high polymer concentration. At saturation 1 mg of ace-PAA was bound per 1.5 mg of phospholipid,

which corresponds to approximately 4600 polymer strands bound per vesicle, or 7 acrylic acid monomer units associated per phospholipid. The calculations were made using 60 $Å^2$ for phospholipid surface area and 200 nm for vesicle diameter. At low polymer concentration (limiting condition), where 99 % of the polymer is bound, approximately 690 polymer strands are bound per vesicle, which corresponds to 1 acrylic acid per phospholipid. Scatchard plot at pH 3.8 showed a negative cooperativity for ace-PAA binding to EPC vesicleswith a binding constant (K_b) of 1.5×10^6 M^{-1} (Fig. 3).

Fluorescence Polarization. Anisotropy (r) of ace-PAA at various pH were determined and compared to values in the presence of EPC vesicles (Fig. 4a). Anisotropy increased with deacreasing pH in the presence of vesicles, and remained constant at these pH in the absence of vesicles. The effect of EPC-LUV on the anisotropy of ace-PAA at varied polymer/lipid ratios was studied at pH 3.8 (Fig. 4b). The anisotropy was largest at low polymer concentrations and decreased with decreasing polymer concentration. The anisotropy of the control ace-PAA samples without vesicles remained constant within experimental limits. The low anisotropy values at high polymer concentrations are due to the presence of free PAA which lowered the average anisotropy values. At 1.5 ace-PAA/lipid ratio, only 46 % of ace-PAA was bound. The anisotropy value (0.10) obtained at 0.1 ace-PAA/lipid ratio, where over 99% of the polymer is bound, is closer to the true anisotropy value of the bound polymer.

Fluorescence Lifetime. "Apparent" lifetimes (τ_p and τ_m) of ace-PAA with and without EPC-LUV were measured at various pH (Table). For single exponential decay,

$$\tau_p = \tau_m = \tau$$

where τ is the actual fluorescence lifetime. Since $\tau p \neq \tau m$ for ace-PAA, the lifetime of ace-PAA seems to follow a more complex decay law. Lifetime values of 33.6 and 39.5 have been obtained for ace-PAA (MW 550,000) and for ace-PAA PEO complex, respectively, by other methods.[4] The lifetime values obtained by phase modulation

measurement are indirect and are sensitive to small measurement errors. Therefore extensive analysis of lifetime results are not possible, and lifetimes measured are listed here only for reference. However, within experimental limits, the lifetime of ace-PAA remained relatively constant at different pH in the presence and absence of EPC vesicles.

Discussion

PAA-phospholipid vesicle complexation was investigated using fluorescence techniques widely used for studying PAA-PEO complexation. First, dansyl-conjugated PAA was used to study polymer complexation with EPC vesicles. Since the emission spectra of dansyl probe is sensitive to the dielectric constant of the environment, it has been used to measure the extent of dehydration upon PAA complexation with PEO.[9] Fluorescence enhancement of dansyl-PAA resulting from water displacement has been observed upon complexation with PEO. However, in the presence of EPC vesicles the excitation maximum of dansyl-PAA changed drastically upon varying the pH. Therefore no correlation could be made between the emission maximum and the polarity of the polymer environment. Therefore, ace-PAA was used to study the complexation behavior.

A reduction in polymer mobility was observed at low pH only in the presence of EPC-vesicles. At these pH values, the carboxyl groups of the polymer are protonated (pKa 4-4.5).[10] Reduced mobility of the polymer is most likly due to complexation of PAA with phospholipid vesicles through H-bonding and hydrophobic interactions. Even though the reduction of depolarization of fluorescence on complexation does not require an intimate contact between the polymer and the vesicles, the binding study supports that there is complexation between ace-PAA and the vesicles.

The strength of a single H-bond is very low. Therefore the total strength of a PAA-PEO complex will depend upon the number of H-bonds as well as the distance between the two H-bonded groups. The concept that polymer complexation in an

aqueous solution by cooperative H-bonding requires the interaction of long sequences of contiguous monomer has been questioned and is believed to be improbable.[11] With the phospholipid-PAA interaction, there are more than one monomer units associated per phospholipids under all conditions. The number of monomer units calculated is underestimated because there are phospholipids which are inside the bilayer and are unavailable for interaction with the polymer even after destabilization. Therefore PAA-vesicle interaction does not seem to require a long sequence of contiguous monomer H-bonding. Also, with phospholipid vesicles, it would be sterically impossible for contiguous PAA monomer to hydrogen-bond to phospholipid headgroups.

The negative cooperativity can be explained by changes in the strength of PAA complexation at different polymer concentrations. At low polymer concentration, the complexation is strong most likely because a longer segment of a polymer is associated to the vesicles. At higher polymer concentration, different polymer strands compete for the same surface, and a shorter segment of a polymer can associate to the vesicles. Therefore the strength for complexation would be weaker at high polymer concentration. It is also possible that once the phospholipid surface is covered with polymer, more polymer associate to the vesicles indirectly through the bound polymer (Fig. 5). If the association of polymer with bound polymer is weaker than polymer-vesicle association, similar results would be obtained.

Weaker complexation at high polymer concentration is also supported by the polarization data. The theoretical anisotropy value is 0.059 as opposed to 0.048 at saturation condition, where 54 % of the polymer is free, and when r = 0.01 and 0.10 are used in the calculation for free and bound polymer, respectively. At all polymer concentrations, except the limiting condition, the experimental value is less than the theoretical value. This suggests that at polymer concentrations, except the limiting condition, the average segmental motion of the bound polymer is higher than that of the

bound polymer in the limiting condition. The higher mobility can be explained by weaker complexation of ace-PAA to vesicles. The polarization measurements do not yield any information about the fraction of polymer carboxylate groups that are H-bonded to vesicles. This could by obtained by measuring the change in pH of PAA solution upon complexation with phospholipid. An increase in pH should be observed upon complexation because H^+ is abstracted from solution for H-bond formation.[12]

References

1. Tsuchida, E. and Abe, K. *Adv. Polym. Sci.* **1**, 45, 1982.
2. Chen, H.L. and Morawets, H. *Eur. Polym. J.* **19**, 923, 1983.
3. Seki, K. and Tirrell, D.A. *Macromolecules* **17**, 1692, 1984.
4. Heyward, J.J. and Ghiggino, K. P. *Macromolecules* **22**, 1159, 1989.
5. Kettle, G.J. and Soutar, I. *Eur. Polym. J.***14** , 895, 1978.
6. Heyward, J.J. and Ghiggino, D.P. *Macromolecules* **22**, 1159, 1982.
7. Polymer Handbook Brandrup, J. and Immergut, E.H. eds. third ed. Wiley-Interscience, New York, 1989.
8. Lakowicz, J.R. in Principles of Fluorescence Spectroscopy, Plenum Press, NY, 1983.
9. Bednár, B. et al. *Macromolecules* **18**, 1829, 1985.
10. Pradip et al. *Langmuir* **7**, 2108, 1991.
11. Wang, Y. and Morawets, H. *Macromolecules* **22**, 164,1989.
12. Iliopoulos, I. and Audebert, R. *Polym. Bull.* **13**, 171, 1985.

Figure 1. Association between the ether oxygen of PEO and carboxyl groups of the PAA.

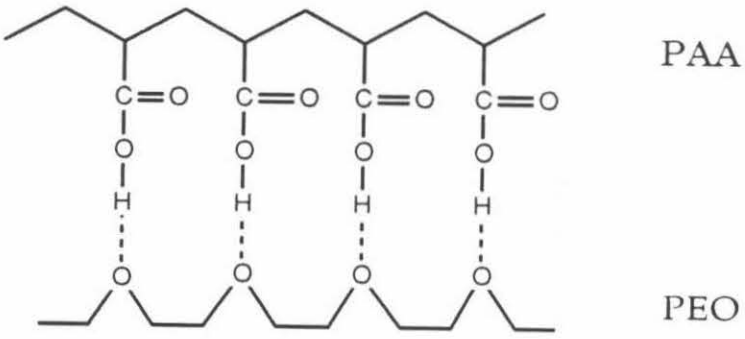
PAA
PEO

Figure 2. top) Plot of ace-PAA binding to EPC-LUV at varying pH. bottom) Plot of ace-PAA binding to EPC-LUV at pH 3.8 with varying polymer/lipid ratio.

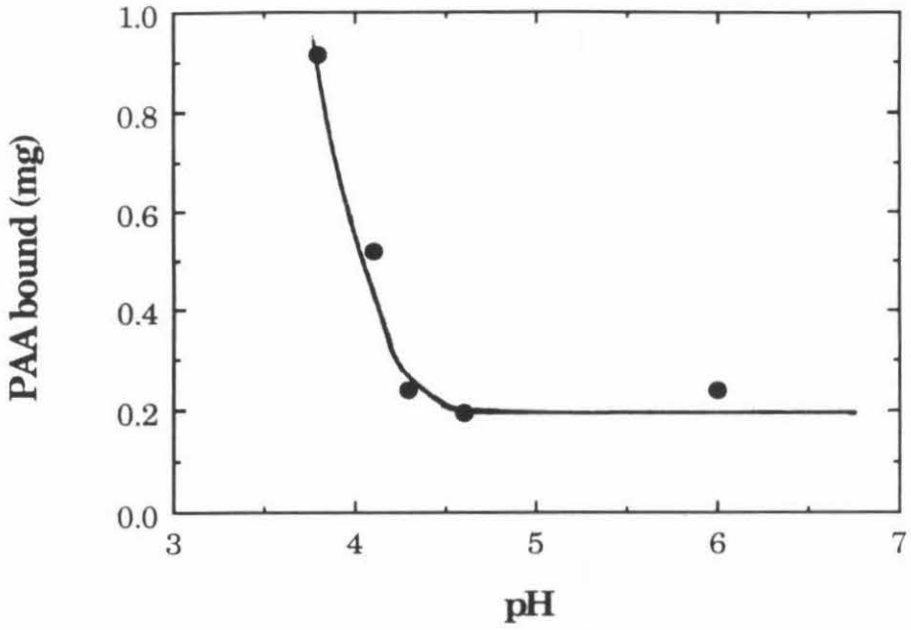
PAA bound (mg)
1.0
0.8
0.6
0.4
0.2
0.0
3
4
5
6
7
pH

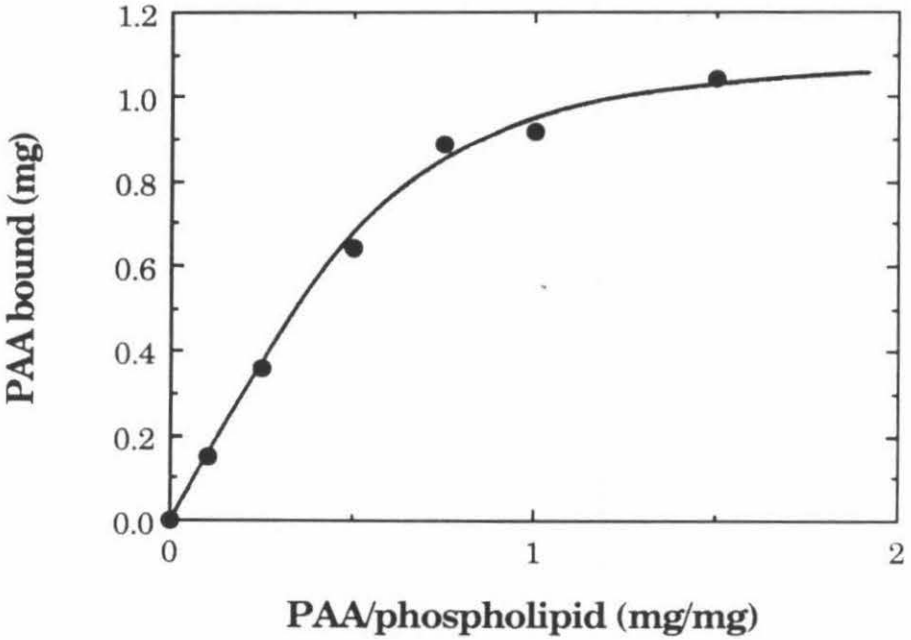
PAA bound (mg)
1.2
1.0
0.8
0.6
0.4
0.2
0.0
0
1
2
PAA/phospholipid (mg/mg)

Figure 3. Scatchard plot of ace-PAA binding to EPC-LUV at pH 3.8

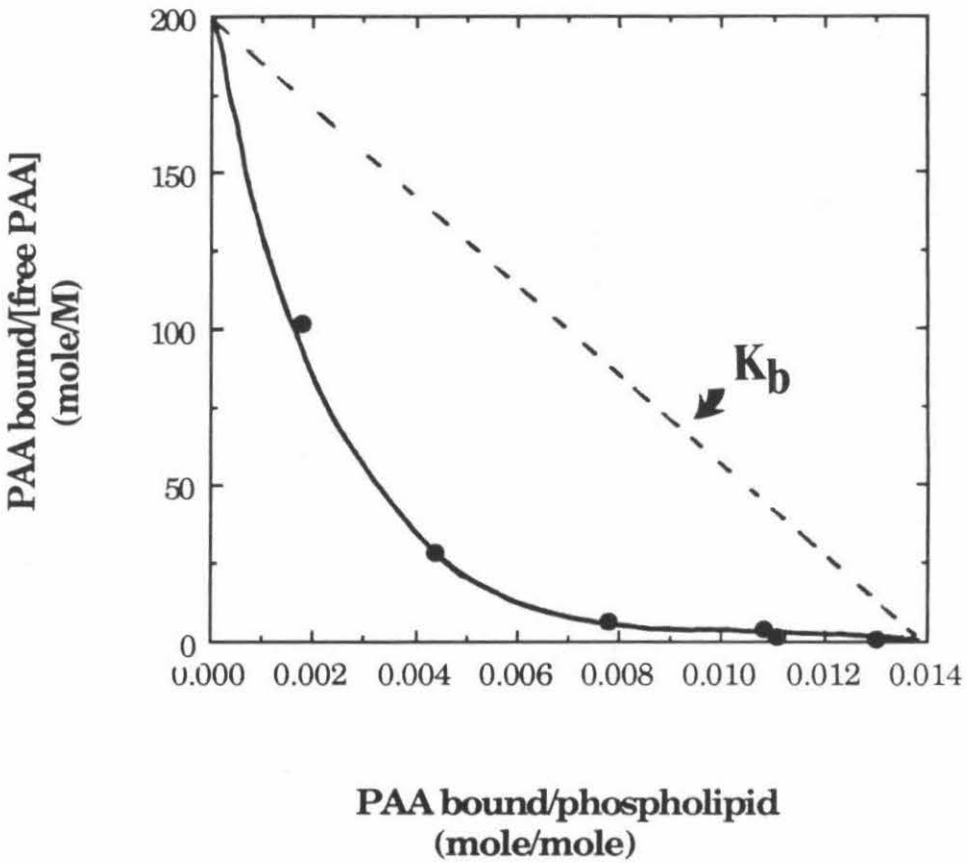
200
150
100
50
0
0.000
0.002
0.004
0.006
0.008
0.010
0.012
0.014
K_b
PAA bound/[free PAA]
(mole/M)
PAA bound/phospholipid
(mole/mole)

Figure 4. top) Plot of anisotropy of ace-PAA at various pH with and without EPC-LUV addition. bottom) Plot of anisotropy of ace-PAA at varied polymer/lipid ratio at pH 3.8. Anisotropy of ace-PAA without EPC-LUV is plotted for comparison.

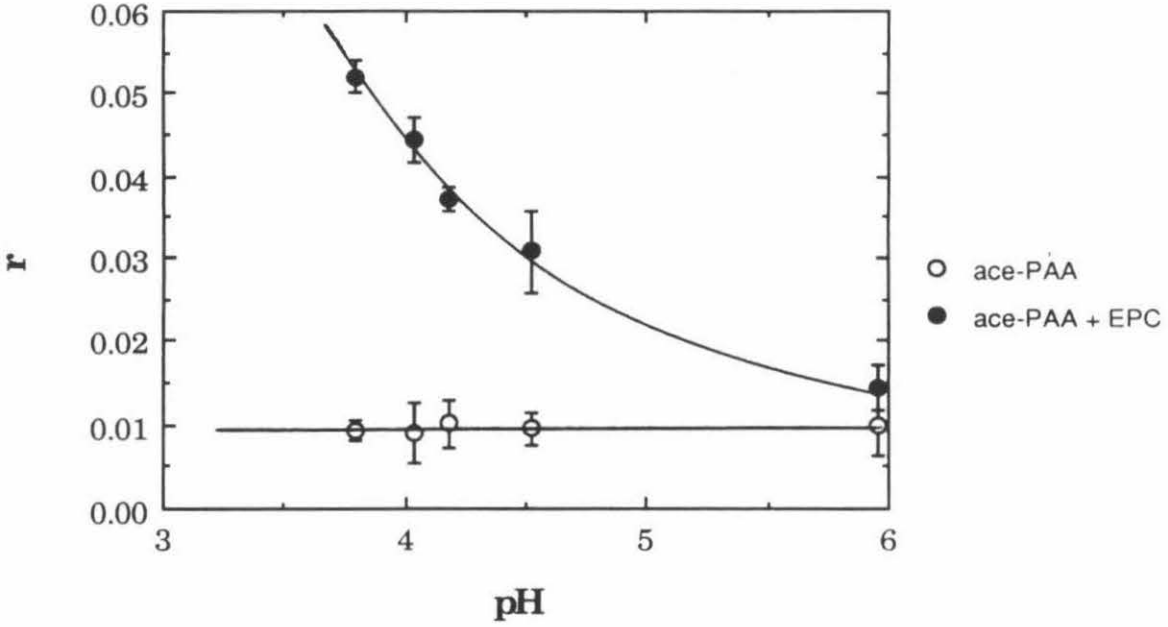
r
0.06
0.05
0.04
0.03
0.02
0.01
0.00
3
4
5
6
pH
ace-PAA
ace-PAA + EPC

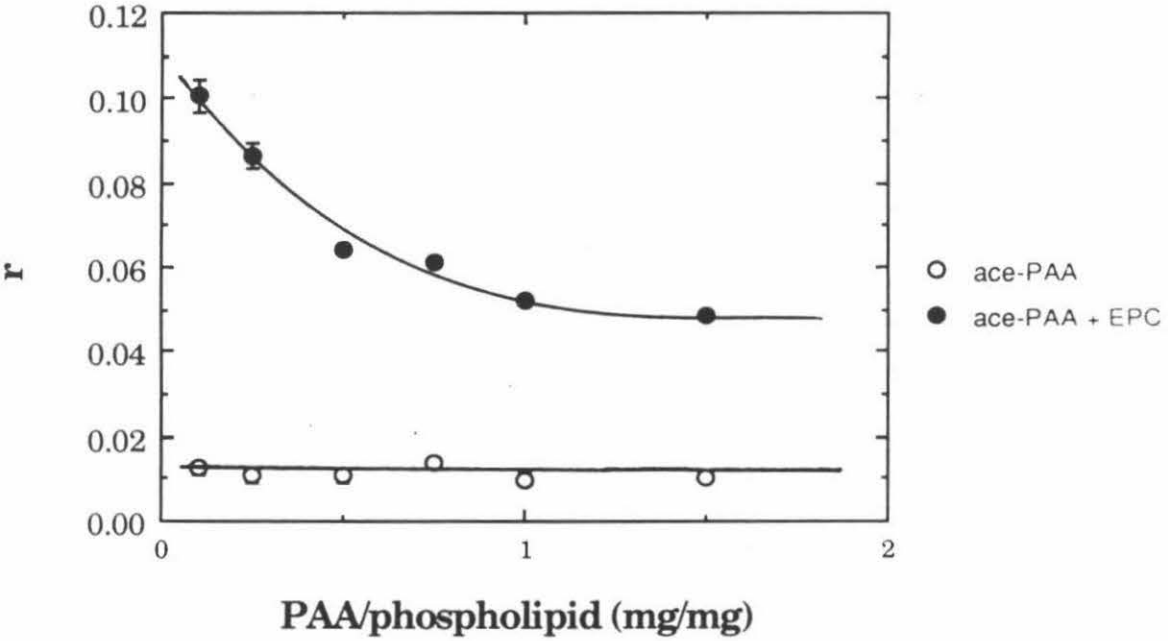
r
0.12
0.10
0.08
0.06
0.04
0.02
0.00
0
1
2
PAA/phospholipid (mg/mg)
ace-PAA
ace-PAA + EPC

Table. Phase modulation lifetime measurements of ace-PAA and ace-PAA with EPC-LUV at various pH.

pH	sample	τ_p (ns)	τ_m (ns)
5.7	PAA	22.3 ± 1.2	27.1 ± 0.6
	PAA + EPC	16.8 ± 1.3	28.7 ± 0.3
4.4	PAA	26.1 ± 2.5	28.4 ± 0.8
	PAA + EPC	24.2 ± 2.3	32.2 ± 1.1
4.2	PAA	24.8 ± 3.0	29.7 ± 0.8
	PAA + EPC	25.5 ± 1.3	33.9 ± 2.0
4.0	PAA	30.0 ± 1.3	32.5 ± 0.3
	PAA + EPC	22.5 ± 1.7	38.4 ± 2.1
3.7	PAA	23.3 ± 1.9	33.0 ± 1.3
	PAA + EPC	22.4 ± 2.7	35.2 ± 0.6

Figure 5. Schematic drawing of possible models for ace-PAA association with phospholipid vesicles at varying polymer/lipid ratio.

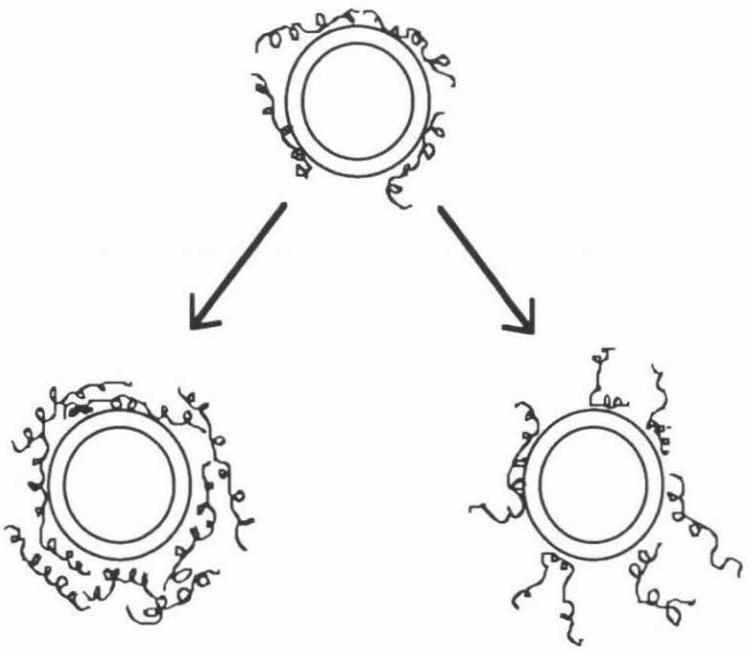

Limiting condition
(low polymer concentration)

Saturation
(high polymer concentration)

polymer associated
with bound-polymer

smaller polymer segment
associated with vesicles

Chapter 5

pH-Dependent Adsorption of Poly(Acrylic Acid) to Phospholipid Monolayer

Summary

Phospholipid monolayers at the air-water interface provide a two-dimensional model membrane system suited for studying membrane surface interactions. Poly(acrylic acid) (PAA) destabilizes phosphatidylcholine (PC) vesicles at low pH. The pH-dependent interaction of PAA to PC monolayer was investigated using monolayer techniques to elucidate the mechanism of polymer adsorption on phospholipid membranes and the consequent membrane disruption. The ability of PAA to penetrate the membrane was determined by the measurement of the lateral compressibility of the monolayer. An increase in surface area was observed below pH 3.8 upon addition of PAA to monolayer subphase at a constant pressure of 30 mN/m due to lateral expansion of the monolayer. This is attributed to a spontaneous penetration of PAA between the phospholipid molecules upon protonation of the polymer. Level of PAA insertion increased with decreasing monolayer packing density as evidenced by a larger relative area increase at lower surface pressure. The effect of pH on the limiting surface pressure of the polymer was investigated. The ability of the polymer to penetrate into the monolayer increased with decreasing pH probably due to increased hydrophobicity of the polymer upon protonation. The information is correlated with complementary biophysical data obtained from vesicle studies.

Introduction

pH-sensitive phospholipid vesicles, or liposomes, have been investigated as drug delivery vehicles for acid-induced cytoplasmic delivery via endosomes.[1] Poly(carboxylic acid) derivatives (PCA) have been shown to render vesicles sensitive to pH and are possible candidates to control drug release from vesicles. Poly(ethylacrylic acid) (PEAA) has been successful in inducing the release of vesicle contents at slightly acidic pH.[2] Poly(acrylic acid) (PAA) not only induces the release of vesicle contents but also the intermixing of phospholipids of different vesicles at low pH.[3] This pH-dependent PAA-vesicle interaction mimics the fusion step required for the transmission of genetic material during viral infection and has implication in elucidating the mechanisms of membrane fusion, an essential step for many biological processes. These polymers alter vesicle properties at acidic pH through adsorption onto the membrane surface. In an acidic environment, PCA derivatives are more hydrophobic due to protonation of the carboxylate groups. It has been postulated that hydrogen bonding between the carboxylic group of the polymer and the phosphate group of the phospholipid is the driving force for polymer adsorption on the vesicles.[4] The mechanism for destabilization of vesicles by polymer adsorption is not known.

The best method to study interface systems is via the investigation of self-assembled monolayers at an air/water interface. Monolayer techniques provide useful information on a molecular scale and are suitable for studies of structure-function relationships of the adsorption of pH-sensitive polymers at phospholipid membranes. Conventional bilayer studies do not permit the study of the effects of polymer adsorption on membrane surface packing because polymer-induced side effects also alter membrane packing. By using a monolayer, it is possible to exclude the effects of membrane packing from vesicle intermixing or vesicle disruption. Phospholipid monolayers provide a simple model for studying the interaction between polymer and phospholipid headgroups

at a more detailed molecular level. Therefore the effect of PAA on molecular packing of model membrane lipids was studied using monolayer techniques.

Langmuir-Blodgett Technique

Phospholipids spontaneously form monomolecular films at an air/water interface so that the phospholipid molecules are oriented with polar headgroups facing the aqueous phase and the hydrocarbon chains extending into the air[5] (Fig. 1). The hydrocarbon chains lie parallel to each other and perpendicular to the surface plane. After formation of the initial monomolecular film, additional components can be injected in the subphase. Phospholipid headgroups, which are in contact with the aqueous media, contribute largely to the interfacial properties of such surfaces. Monolayer techniques permit the study of the association of specific molecules in considerable detail.

By using a Langmuir film balance,[6] the interaction of the monolayer components with the polymers in the aqueous subphase may be examined. Information that can be obtained from monolayer studies includes surface area of a molecule, surface pressure, and force-area curves. The surface area of a molecule is obtained by dividing the total surface area of the film (A) by the number of molecules on the surface and is equal to the reciprocal of the surface concentration of the molecules. The minimum molecular surface area achieved corresponds approximately to the area of a phospholipid molecule in the membrane.

The surface pressure (π) corresponds to the lowering of surface tension of the aqueous solution upon film formation and is given by the following equation,

$$\pi = \gamma_o - \gamma_m$$

where γ_o and γ_m are the surface tensions in the absence and presence of the monolayer respectively.[5] The surface pressure is proportional to the number of molecules in a dilute monolayer and is sensitive to the temperature, ionic strength of the subsolution, and subphase components. The surface pressure is affected by altering the conformation of

the molecule at the interface or by interfering directly with intermolecular interactions within the film. The Wilhelmy plate or Langmuir-float methods are generally used for determining surface pressures.[7]

The relationship between surface concentration and surface pressure is represented in the force-area curve (Fig. 2). The "collapse pressure" is the maximum packing that can be achieved while maintaining the monolayer organization. Changes in the slope represent transitions between closely related phases in which the orientation of lipid molecules varies either from differences in the order of hydrocarbon chains or separation of components into domains.

Materials and Methods

Materials. Palmitoyl-oleoyl phosphatidylcholine (POPC) was obtained from Avanti Polar Lipids (Birmingam, AL). The purity of the lipid was checked with thin layer chromatography. Deionized distilled water was used for all experiments. Methanol (HPLC grade) and PAA (250,000 MW) was obtained from Aldrich. PAA was dialyzed as described in chapter 2. All other reagents obtained were the highest grade.

Monolayer Experiments. Monolayer experiments were carried out on a KSV5000 microtrough (KSV). The surface pressure was measured by the Wilhelmy method using a platinum plate. POPC (1mg/ml) was dissolved in chloroform:methanol (3:1) and 15 µl was spread at the air/water interface using a Hamilton syringe equipped with a small Teflon tube. The monolayer was compressed at a barrier speed of 25 mm/min. Small amounts of PAA (1mg/ml) were injected with a Hamilton syringe into the buffer phase (10 mM NaAcetate, 100 mM NaCl). The buffer phase was stirred by a tiny magnet to attain an homogeneous distribution of PAA. Stirring did not disturb the monolayer that had formed. All measurements were carried out at 25 ^{o}C.

Results

POPC monolayer was formed on acetate buffer at pH 7.0, 4.6, 4.3, 4.1, and 3.8 (Fig. 3). These monolayers were stable for at least 1 hr as evidenced by constant surface area. Time-dependent changes in the surface area of POPC molecules at a constant surface pressure of mN/m were recorded upon addition of 45 μl of PAA solution to the subphase (Fig. 4). The effect of pH on the ability of PAA to induce monolayer expansion was investigated at a constant surface pressure of 20 mN/m (Fig. 5). A monolayer expansion was observed below pH 4.3. The change in surface area (ΔA) increased with decreasing pH. An increase in surface area was induced below pH 3.8 at a surface pressure of 30 mN/m, which is close to the lateral pressure well suited to mimic bilayer membrane.[8]

The relative area increase (ΔA/A) was highly pressure dependent, and the monolayer expansion is increasingly difficult with increasing packing density of the lipid molecules. Plots of relative area increase is linear as a function of surface pressure in the pressure range of 15 - 30 mN/m at pH 3.5 (Fig. 6). One can extrapolate from such plots the limiting surface pressure, the pressure above which the polymer can no longer incorporate into the monolayer.[8] At pH 3.5 the limiting surface pressure was determined to be about 35 mN/m. The limiting surface pressure is a measure of the polymer's ability to penetrate into the membrane. The limiting surface pressure decreased with increasing pH. At pH 3.8 and 4.3, the limiting surface pressure was below 30 mN/m and below 25 mN/m, respectively.

PAA dissolved in buffer solution did not show any surface activity at above pH values. In the pressure-area isotherm of PAA between 160 Å and 40 Å, the maximum surface pressure observed was 0.7 mN/m, which is well below the surface pressure of the lipid monolayer.

Discussion

The pH-dependent interaction of PAA with POPC monolayers at the air-water interface was investigated. When PAA was injected underneath a POPC monolayer kept at a constant surface pressure, a film expansion was observed at low pH values when PAA is protonated. This is probably due to PAA adsorption to or insertion in the monolayer surface. From the DSC studies (Chapter 3), it was established that PAA is most likely interacting with the phospholipid headgroup and not the hydrocarbon chains. Therefore polymer insertion is believed to be limited to the headgroup region or the interface region. Polymer adsorption to or insertion in the vesicle surface separates the lipid headgroups. The resulting decrease in the van der Waals attraction between the phospholipids renders the membrane prone to disruption.

The ability of PAA to induce monolayer expansion depends on the packing density of the monolayer and the pH. Increased monolayer packing density rendered polymer adsorption more difficult. This agrees with the fluorescence destabilization studies of vesicles (Chapter 2). PAA induced destabilization of vesicles only above the lipid phase transition temperature where the phospholipids are less closely packed. Increased disorder in surface packing of phospholipid bilayer was observed at low pH as evidenced by the increased binding of the MC540 probe (Chapter 2). The results from monolayer studies also showed an increased surface packing at those pH values.

Monolayer studies and vesicle studies are complementary techniques; some information that cannot be obtained from vesicle studies can be obtained from monolayer studies. The advantage of using monolayer techniques to study polymer adsorption to membrane surfaces is its ability to distinguish direct effects of polymer adsorption on membrane packing from indirect effects arising from vesicle disruption and aggregation.

References

[1]Connor, J.; Huang, L. *J. Cell Bio.* **1985**, *101*, 582.

[2]Eum, K. M.; Langley, K. H.; Tirrell, D. A. *Macromolecules* **1989**, *22*, 2755.

[3]Fujiwara, M.; Baldeschwieler, J. D.; Grubbs, R. H. submitted for publication.

[4]Seki, K.; Tirrell, D. A. *Macromolecules* **1984**, *17*, 1692.

[5]Rothfield, L. I.; Fried, V. A. in "Methods in Membrane Biology"; Korn, E. D., ed.; Plenum Press: New York, 1975; p. 277.

[6]Fromherz, P. *Rev. Sci. Instrum.* **1975**, *46*, 1380.

[7]Fendler, J. H. "Membrane Mimetic Chemistry"; John Wiley & Sons: New York, 1982; Ch. 4.

[8]Seelig, A. *Biochim. Biophys. Acta* **1987**, *899*, 196.

Figure 1. Phospholipid monolayer at an air-water interface with polymer injected in the subphase.

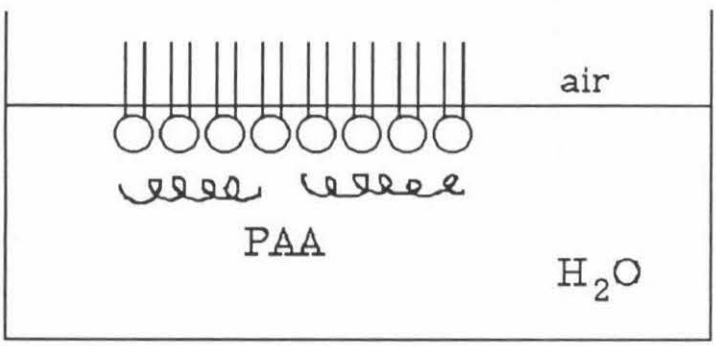
air
PAA
H_2O

Figure 2. Schematic representation of a surface pressure-surface area isotherm.

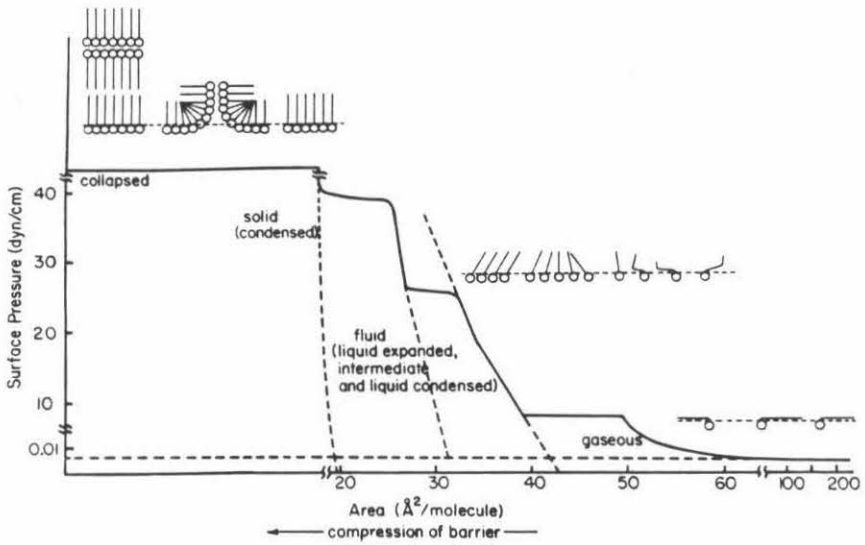
collapsed
solid
(condensed)
fluid
(liquid expanded,
intermediate
and liquid condensed)
gaseous
Surface Pressure (dyn/cm)
40
30
20
10
0.01
20
30
40
50
60
100
200
Area (Å²/molecule)
compression of barrier

Figure 3. Surface pressure-area isotherm of POPC monolayer.

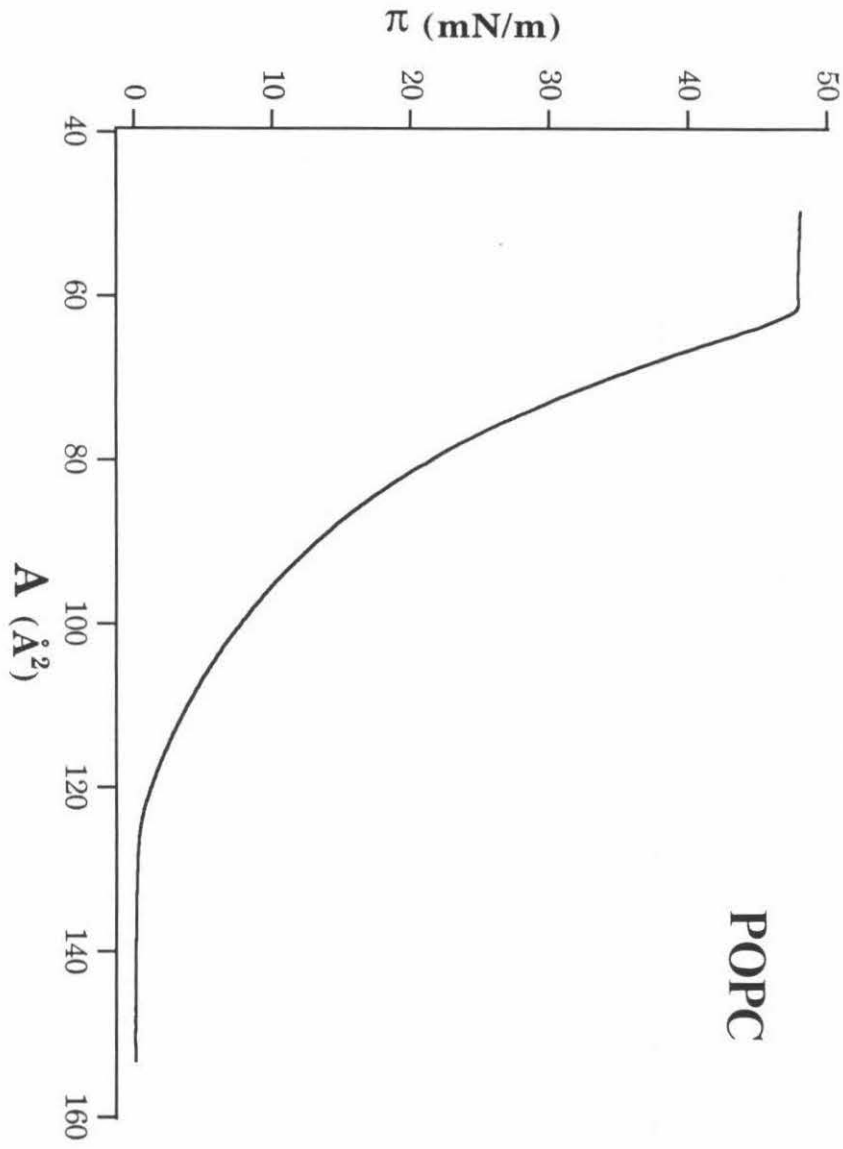
π (mN/m)
0
10
20
30
40
50
40
60
80
100
120
140
160
A (Å²)
POPC

Figure 4. Area increase (ΔA) of POPC monolayer at 20 mN/m induced by the addition of PAA as a function of time. (pH 3.5)

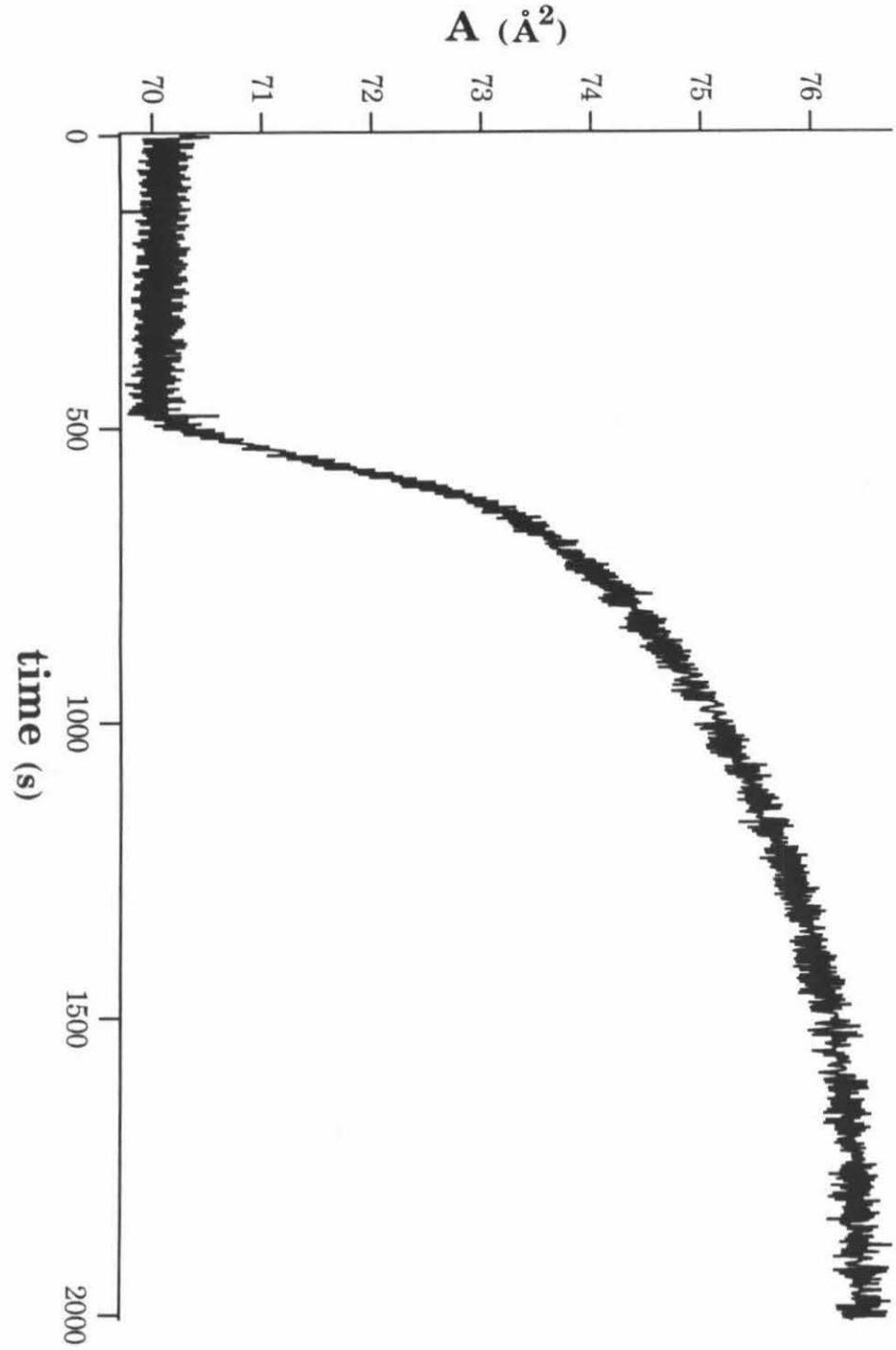
A (Å²)
70
71
72
73
74
75
76
0
500
1000
1500
2000
time (s)

Figure 5. Relative area increase ($\Delta A/A$) as a function of pH at a surface pressure of 20 mN/m.

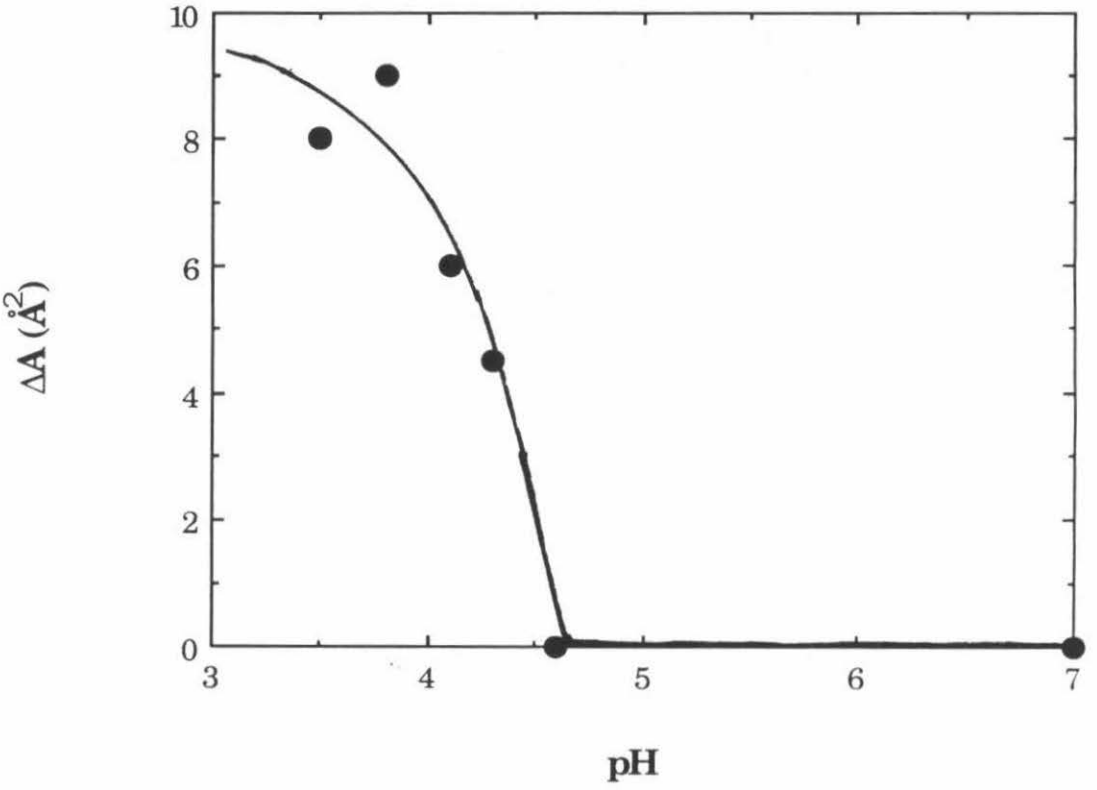
10
8
6
4
2
0
3
4
5
6
7
ΔA (Å²)
pH

Figure 6. Relative area increase ($\Delta A/A$) as a function of surface pressure at pH 3.5. Limiting surface pressure was determined from extrapolation to x-axis intercept.

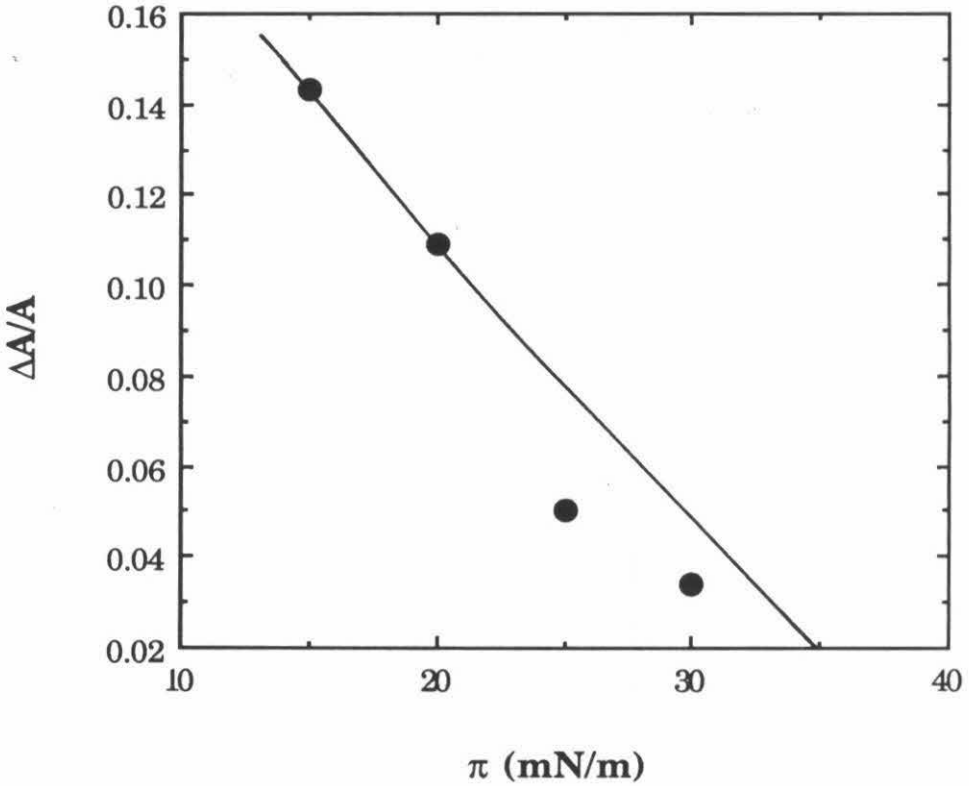
0.16
0.14
0.12
0.10
0.08
0.06
0.04
0.02
ΔA/A
10
20
30
40
π (mN/m)

Chapter 6

Receptor-Mediated Endocytosis of Poly(Acrylic Acid)-Conjugated Liposomes by Macrophages

Summary

The cell uptake characteristics of polymer-conjugated liposomes by the RAW cell line of mouse macrophages were studied and compared to the uptake of unmodified liposomes. An over 5-fold increase in the uptake of phosphatidylcholine (PC) liposomes was obtained by poly(acrylic acid) (PAA) conjugation. PAA-conjugated liposomes were internalized and digested in an acidic compartment at a faster rate than unmodified liposomes. Less than 15 % of the aqueous content and 3 % of the lipid probe were exocytosed after 12 hrs. The high affinity binding of PAA-conjugated liposomes to macrophages is very similar to macrophage binding by scavenger receptors. Cross-competition experiments showed that PAA-liposomes inhibited the uptake of acetylated-low density lipoprotein (acetyl-LDL) by RAW cells and vice versa. PAA-liposome uptake was also inhibited by dextran sulfate and maleylated-bovine serum albumin (maleyl-BSA), which are known to bind to scavenger receptors. Native LDL, Poly(C) and BSA competed poorly with PAA-liposome uptake. The data obtained indicate that the primary macrophage receptor responsible for PAA-liposomes uptake is probably the scavenger receptor.

Introduction

Liposomes are one of the most effective carriers for the introduction of various agents into cells in *in vitro* experiments. Liposome interactions with various cells have been investigated. Lipid components and compounds entrapped in the aqueous compartment of the vesicles can be transferred into cells by various mechanisms. It has been shown that cells capable of phagocytosis, such as macrophages, endocytose liposomes readily.[1] In order to improve cell uptake and specificity, ligand-conjugated liposomes, such as IgG-coated liposomes, have been examined.[2] Poly(ethacrylic acid) (PEAA) has been shown to induce vesicle to micelle transition at acidic pH.[3] PEAA conjugation to liposomes has been introduced as a way to render liposomes sensitive to pH.[4] The interaction of cell with some intinsically unstable pH-sensitive liposomes, which release their contents rapidly in an acidic environment, have been studied.

PAA renders liposomes sensitive to pH by destabilizing the liposomes below pH 4.1 (Chapter 2). The PAA-conjugated liposomes and control unmodified liposomes were compared with respect to macrophage the endocytosis and exocytosis. The extent of endocytosis and exocytosis were measured by the amount of radiolabelled-liposomes incorporated into and released from the macrophages. Liposomes labeled with a pH-sensitive fluorescent probe (HPTS) were used to study the fate of liposomes inside the cell. Competition and cross competition studies were carried out with various reagents to determine the receptor responsible for increased uptake of PAA-liposomes.

Materials and Methods

Materials. Egg phosphatidylcholine (EPC), bovine brain phosphatidylserine (PS), and N-[4-(p-maleimidophenyl)butyryl-dimyristoyl phosphatidylethanolamine (MPB-PE) were obtained from Avanti Polar Lipids (Alabaster, AL). The purity of the lipids was checked with thin layer chromatography, and they were used without further purification. ^{3}H-

cholesterylhexadecylether (^{3}H-cholether) was obtained from New England Nuclear. ^{3}H-inulin (MW 5,600) and Na^{125}I were obtained from Amersham (Arlington, heights, IL). Maleic anhydride, pyruvate, acridine orange, ethidium bromide, LDL, BSA, heparin, and dextran sulfate (MW 500,000) were obtained from Sigma (St. Louis, MO). 2-Aminoethanethiol (AET) and dicyclohexylcarbodiimide (DCC) were obtained from Aldrich (Milwaukee, WI). 4-pyrrolidinopyridine (4-pp) was obtained from Fluka (Ronkonkoma, NY). Poly(C) was obtained from Calbiochem (San Diego, CA). 8-hydroxypyrene-1,3,6-trisulfonic acid (HPTS) was obtained from Molecular Probes (Eugene, OR). Dimethylformamide (DMF) was vacuum distilled. All other reagents were reagent grade or better. Distilled deionized water was used.

Liposome preparation. A lipid solution in chloroform was dried under N_2 and further under vacuum overnight. The lipid film was hydrated with phosphate buffered saline (PBS, pH 7.4) or by Tris buffer (50 mM Tris, 10mM NaCl, pH 7.4). SUV were made by probe sonication (Heat Systems) of the aqueous lipid solution under N_2. Ti particles and large liposomes were removed by centrifuging the SUV solution for 5 min. at 12,000 x g in a Beckman Microfuge 11. All liposome solutions were sterilized by passing through a 0.2 μm filter prior to incubation with macrophages. The phosphate content was determined by Böttcher modification of Bartlett assay.[5]

PAA Conjugation. Acenaphthalene-labeled PAA (ace-PAA) was synthesized (Chapter 4), thiolated, and conjugated to EPC-SUV.[4] Briefly, PAA was reacted with AET in the presence of 4-pp and DCC in DMF for 24 h at room temperature. The reaction mixture was filtered and precipitated into ethyl acetate. PAA-AET was reduced with DTT under N_2 for 15 min and passed through Sephadex G-50 (Sigma) equilibrated with 0.9 % saline. Polymer fractions collected were immediately reacted with EPC-SUV containing 5 % MPB-PE for 4 hrs. Free PAA-AET was separated from liposomes using a Bio-Gel A-5m column equilibrated with Tris buffer.

Cell Cultures. RAW264.7 macrophages (ATCC, Rockville, MD) were cultured in RPMI1640 media containing glutamine (Hyclone, Logan, UT) supplemented with 1 mM pyruvate, Fungi-Bact solution (Irvine Scientific, Santa Ana, CA), and 10 % fetal bovine serum (Hyclone). Cells were incubated at 37°C in a humidified 5 % CO_2 atmosphere. Cell concentration was determined by cell counting using a hemocytometer (American Optical).

Endocytosis Assay. Liposomes were labeled with ^{3}H-cholether or with ^{3}H-inulin. ^{3}H-cholether (4.5 μCi) in toluene was added to a lipid solution (10 mg) in chloroform, and SUV were made as described above. ^{3}H-inulin (25 mCi) in buffer (1 ml) was added to dry lipid (20mg) during the hydration step. The solution was passed through five freeze-thaw cycles to maximize inulin encapsulation prior to sonication.[6] Excess ^{3}H-inlulin was removed after sonication by passing through a Bio-Gel A-5m (Bio-Rad, Richmond, CA) column equilibrated with Tris buffer. The liposomes were incubated with macrophages at 37 °C or at 4 °C in a 6-well tissue culture plate (Becton Dickinson, Lincoln Park, NJ) in a 5% CO_2 atmosphere for the desired incubation times. For time-dependent assays, 51 nmol phospholipid was added to each well containing 1 x 10^6 cells. After varying time intervals, the cells were washed twice with cold PBS, scraped off the plates, and centrifuged at 3,500 x g for 3 min. in the Beckman Microfuge 11. The pellets were dissolved in 0.5M NaOH/0.5% SDS solution prior to scintillation counting. For each experiment all samples were done in triplicate.

Exocytosis Assay. Radiolabeled liposomes were incubated with macrophages as described above for 24 hrs. The cells were washed twice with cold PBS to remove free liposomes and further incubated in media for varying periods of time. The cells were scraped off the plates, and both the pellets and supernatants were collected by centrifugation and counted for radioactivity.

HPTS Assay. HPTS assay was carried out as described previously.[1] Briefly, HPTS (35 mM) in Tris buffer was added to dry lipid during the hydration step, and EPC-SUV were prepared as described for ^{3}H-inulin liposomes. After incubation with HPTS liposomes, cells were washed twice with cold PBS and incubated further for 5 min. at 37 ^{o}C. Cells were dislodged, and excitation spectra were recorded at 510 nm emission with 8 nm bandwidth using a SLM spectrofluorometer. The fraction of HPTS endocytosed in acidic compartment was calculated as follows,

$$\text{fraction endocytosed} = \frac{R_{7.4}-R_{measured}}{R_{7.4}-R_{low}}$$

where $R_{7.4}$, $R_{measured}$, and R_{low} are the 460/413 nm ratio of HPTS-liposomes at pH 7.4, liposome treated cells, and HPTS pinocytosed, respectively.

Competitive Assays. LDL was radioiodinated with Na^{125}I using the iodine monochloride method.[7] LDL was acetylated using acetic anhydride.[8] The extent of modification was determined by amine assay,[9] which indicated that over 90% of the amine groups in LDL were acetylated. Maleyl-BSA was prepared as described previously.[10] Over 95% of the amino groups in BSA were maleylated. The uptake of ^{3}H-cholether labeled EPC-PAA liposomes was measured at various concentrations of the following reagents: PS-SUV, EPC-SUV, EPC-PAA, free PAA, acetyl-LDL, maleyl-BSA, LDL, poly C, heparin, and dextran sulfate. For cross competition experiments, the extent of ^{125}I-acetyl-LDL and ^{3}H-cholether labelled PS-SUV uptake were measured in the presence of EPC-PAA.

Cytotoxicity Assay. Cells were exposed to varied concentrations of EPC-PAA (0, 2.5, 5, 25, 50 μg phospholipid) and free PAA (0, 50, 100, 500 μg) in tissue culture plates. The cell viability after 24 hrs was determined using an acridine orange/ethidium bromide assay.[11] Cells were incubated with 1 ppm solution of acridine orange and ethidium bromide (15 μl/well) for few a minutes and were examined under fluorescence microscope.

Viable cells were stained green and nonviable cells appeared orange. The total cell proteins of cell cultures incubated with EPC-PAA were compared to that of cell culture grown without EPC-PAA. The cell protein concentration was estimated by the Peterson's modified Lowry assay using BSA as a standard.[12]

Results

EPC-PAA preparation. 4 % of the monomers in PAA were modified by AET as determined by thiol analysis.[13] The extent of polymer conjugation to liposomes was determined by the emission intensity of ace-PAA at 340 nm with 295 nm excitation using a calibration curve. Approx. 150 polymer strands were conjugated to the SUV (170 mol phospolipid/mol polymer) using 30 nm as the vesicle diameter and assuming 60 % of phospholipid molecules reside on the outer monolayer. The particle sizes of control liposomes and PAA-liposomes were determined using laser light scattering. The mean liposome size was 28.8 nm ± 7.5 and increased slightly to 42.2 nm ± 9.7 after PAA conjugation.

Endocytosis. Uptake of EPC-PAA by the RAW mouse macrophages was studied and compared to EPC-SUV (Fig. 1). PAA-conjugated liposomes showed an increased uptake of both the aqueous and lipid phase liposome markers. ^{3}H-inulin, a nondegradable aqueous marker, and ^{3}H-cholether, a lipid marker, were used to quantitate aqueous content uptake and phospholipid uptake, respectively. Increased uptake was not observed when free PAA is added to EPC-SUV with or without 5 % MPB-PE, indicating that PAA conjugation to liposomes is necessary for improved uptake. Uptake processes showed saturation at high vesicle concentration with a maximum uptake value of 10 nmol phospholipid/10^{6} cells.

The extent of liposome binding to cell surface receptors was obtained by incubating the cells with liposomes at 4 ^{o}C, where endocytosis is inhibited. At 4^{o}C internalization is

prevented, but cells are capable of ligand binding to their receptors. Increased binding of EPC-PAA to macrophage receptors was found.

Exocytosis. The release of endocytosed liposomal aqueous and lipid marker was measured with time (Fig. 2). After 12 hrs. 13 % of ^{3}H-inulin was released while only 3 % of ^{3}H-cholether was released. The increased release of the aqueous probe from cells compared to the lipid probe is similar to the exocytosis behavior observed with Kupffer cells.[2]

HPTS. The intracellular fate of endocytosed liposome contents was studied using HPTS (Fig. 3). Over 95 % of PAA-liposomes were endocytosed into an acidic compartment as opposed to 88 % for EPC-liposomes in the first 3 hrs.

Competitive assay. In order to determine the receptors responsible for PAA-liposome uptake, inhibition of liposome uptake by various substances was investigated (Fig. 4). Poly(C) and BSA did not compete with EPC-PAA uptake. Heparin, LDL, and EPC-SUV inhibited EPC-PAA uptake slightly. Acetyl-LDL, dextran sulfate, maleyl-BSA, and free PAA competed efficiently with EPC-PAA uptake. Unlabeled EPC-PAA competed with labeled EPC-PAA uptake in a linear manner. To make sure that these inhibitors were acting by binding to the cells and not by binding to EPC-PAA, cells were incubated with acLDL at 4 ^{o}C prior to incubation with EPC-PAA. Subsequent EPC-PAA binding was inhibited by 80 %. EPC-PAA competed efficiently with PS-SUV and acetyl-LDL uptake. PS-SUV and acetyl-LDL uptake values were suppressed by 58 % and 77 %, respectively.

Cell Cytotoxicity. After 24 hrs of incubation with EPC-PAA, both cells without EPC-PAA and with EPC-PAA addition showed greater than 98% viability. The protein content of cells was the same within experimental error for cells with and without EPC-PAA addition.

Discussion

The mechanism of liposome-cell interaction is an important factor in liposomal drug delivery. Liposomes interact with cells by such mechansims as fusion with the cell membrane, phagocytosis, and receptor-mediated endocytosis, and the mechanism of uptake is dependent on the liposome formulation (Fig. 5). Neutral liposomes are believed to bind nonspecifically to clathrin-coated pits and subsequently endocytosed.[14] It has been shown that liposomes containing negatively charged lipids (e.g., PS) are more efficiently endocytosed than liposomes containing neutral lipids.[15] PAA conjugation is responsible for the improved uptake of EPC-PAA since free PAA inhibited the uptake of EPC-PAA and did not alter the uptake of unmodified liposome. The increased recognition of PAA-liposomes by the macrophages is most likely due to the negative charges on the polymer which are recognized by certain receptors on the macrophages. It is believed that improved uptake of the negatively-charge liposomes is due to scavenger receptor recognition.[16]

Scavenger receptors have been implicated in the development of atherosclerosis and other macrophage-associated functions.[17] The expression of scavenger receptor is limited to macrophages, monocytes, and endothelial cells.[18] Macrophages in cell culture accumulate large quantities of lipid if presented with certain chemically modified forms of LDL, such as acetylated LDL, resulting in the development of foam cells.[17] The uptake of acLDL is mediated by the scavenger receptor which is distinct from the high specificity LDL receptor. The scavenger receptor exhibits a broad ligand specificity. AcLDL, poly (I), maleyl-BSA, and sulfated polysaccharides (dextran sulfate and fucoidan) are effective ligands whereas native LDL, BSA, and poly (C) are not. It is believed that negative charges and their presentation are important in the binding interaction.

Competitive assays suggest that PAA-liposomes are recognized by the scavenger receptor. LDL and EPC-SUV competed poorly while acetyl-LDL competed efficiently for the binding of PAA-liposomes by macrophages. PAA-liposomes are digested in an acidic

compartment, and their aqueous components are exocytosed. They showed rapid uptake and degradation kinetics, which are characteristic of scavenger receptor ligands. Other pathway and receptor involvement are not excluded but the major pathway for EPC-PAA seems to be through internalization by the scavenger receptor. Differences in the ability to compete for the same receptor suggests that more than one type of receptor is involved in EPC-PAA uptake. Recently, results have been obtained which suggests that the receptor involved in PS-SUV uptake is not the scavenger receptor as previously believed from cross competition experiments.[19] Therefore, cross competition assays do not prove that the receptor involved for EPC-PAA is the scavenger receptor and more experiments are needed to support the results. Competition experiment with macrophage antibody specific for scavenger receptor is needed.

References

1. Daleke, D.L., Hong, K. and Papahadjopoulos, D. *Biochim. Biophys. Acta* **1024**, 352, 1990.
2. Derksen, J.T.P., Morselt, H.W.M. and Scherphof, G.L. *Biochim. Biophys. Acta* **931**, 33, 1987.
3. Borden, K.A. et al. *Macromolecules* **21**, 2649, 1988.
4. Maeda, M., Kumano A, and Tirrell, D.A. *J. Am. Chem. Soc.* **110**, 7455, 1988.
5. Böttcher, C.J.F., van Gent, C.M. and Fries, C. *Anal. Chim. Acta* **24**, 203, 1961.
6. Mayer, L.D., Hope, M.J., Dullis, P.R., Janoff, A.S. *Biochim. Biophys. Acta* **817**, 193, 1985.
7. Goodstein, J.L., Basu, S.K., and Brown, M.S. *Methods Enzymol.* **98**, 241, 1983.
8. Brown, S.K. et al. *Proc. Natl. Acad. Sci.* **73**, 3178, 1976.
9. Lai, C.Y. *Methods Enzymol.* **47**, 236, 1977.
10. Takata, K., Horiudi, S. and Morino, Y. *Biochim. Biophys. Acta* **984**, 273, 1989.
11. Mishell, B. and Shiigi, S. eds Selected Methods in Cellular Immunology W.H. Freeman & Co., San Francisco, 1980.
12. Peterson, G.L. *Anal. Biochem.* **83**, 346, 1977.
13. Habeeb, A.F.S. *Methods Enzymol.* **25**, 457, 1972.
14. Straubinger, R.M. et al. *Cell* **32**, 1069, 1983.
15. Lee, K.-D., Hong, K. and Papahadjopoulos, D. *Biochim. Biophys. Acta* **1103**, 185, 1992.
16. Nishikawa, K., Arai, H. and Inoue, K. *J. Biol. Chem.* **265**, 5226, 1990.
17. Goldstein, J.L. et al. *Proc. Natl. Acad. Sci.* **76**, 332, 1979.
18. Pitas, R.E. *J. Biol. Chem.* **265**, 12722, 1990.
19. Lee, K.-D., Pitas, R.E. and Papahadjopoulos, D. *Biochim. Biophys. Acta* **1111**, 1, 1992.

Figure 1. Uptake of EPC-PAA at 37 ^{o}C and 4^{o}C over time is compared to EPC-SUV uptake in the presence of free PAA.

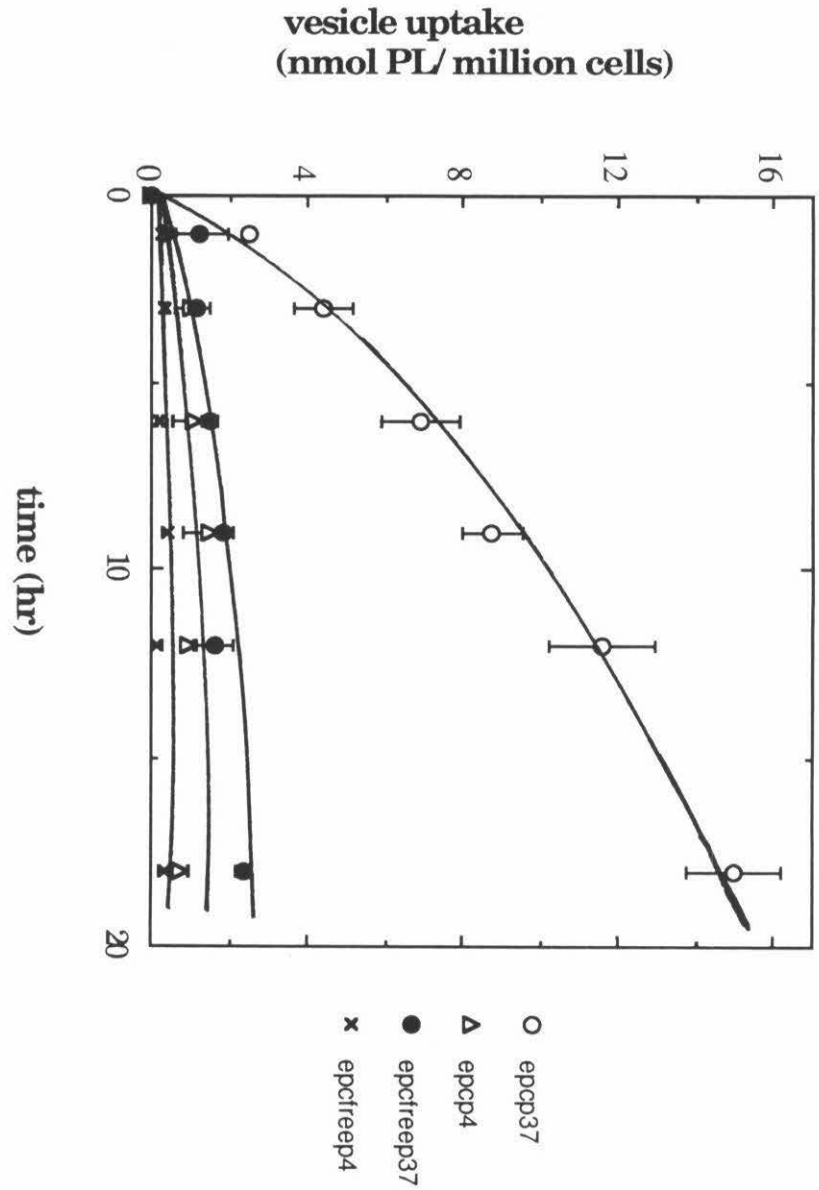
vesicle uptake
(nmol PL/ million cells)
0
4
8
12
16
0
10
20
time (hr)
epcp37
epcp4
epcfreep37
epcfreep4

Figure 2. Extent of EPC-PAA exocytosis measured with aqueous probe, ^{3}H-inulin, and lipid probe, ^{3}H-cholether.

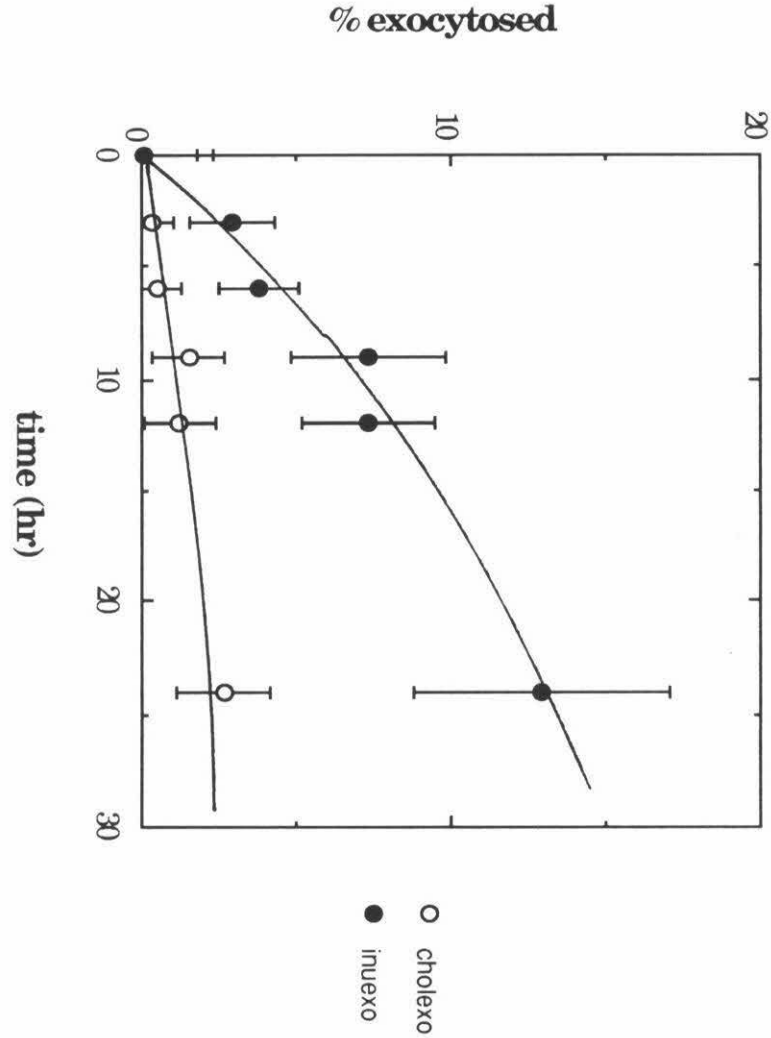
% exocytosed
0
10
20
time (hr)
0
10
20
30
cholexo
inuexo

Figure 3. Fraction of EPC-PAA and EPC-SUV endocytosed into an acidic compartment.

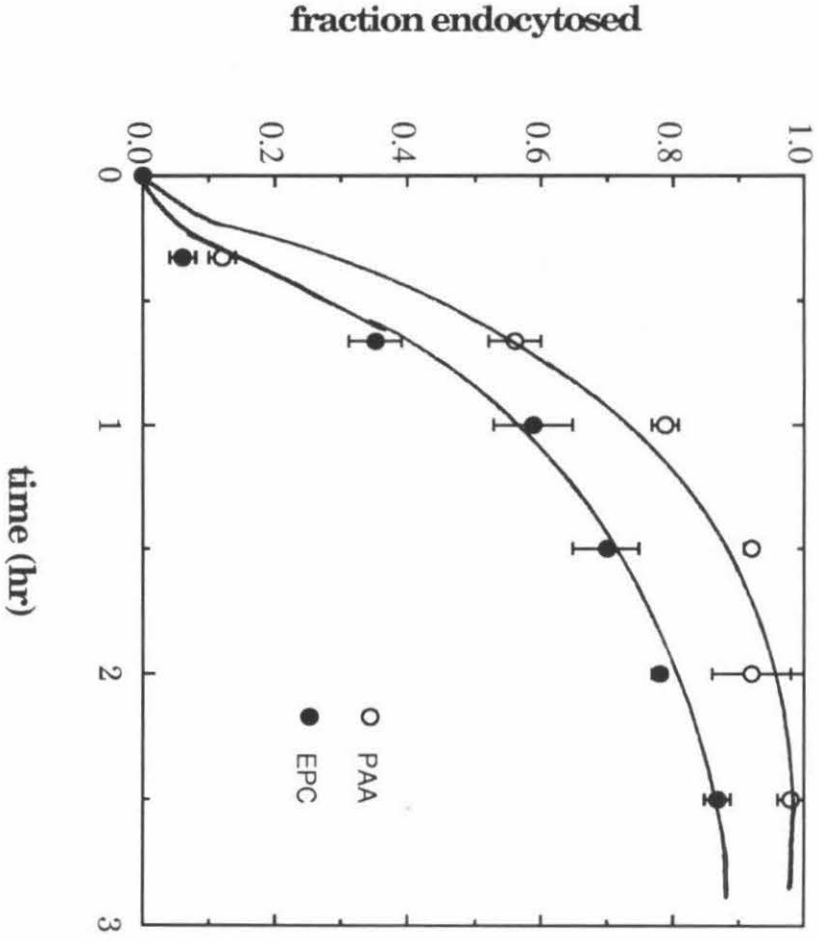
fraction endocytosed
0.0
0.2
0.4
0.6
0.8
1.0
0
1
2
3
time (hr)
PAA
EPC

Figure 4. Pattern of EPC-PAA uptake inhibition by various reagents.

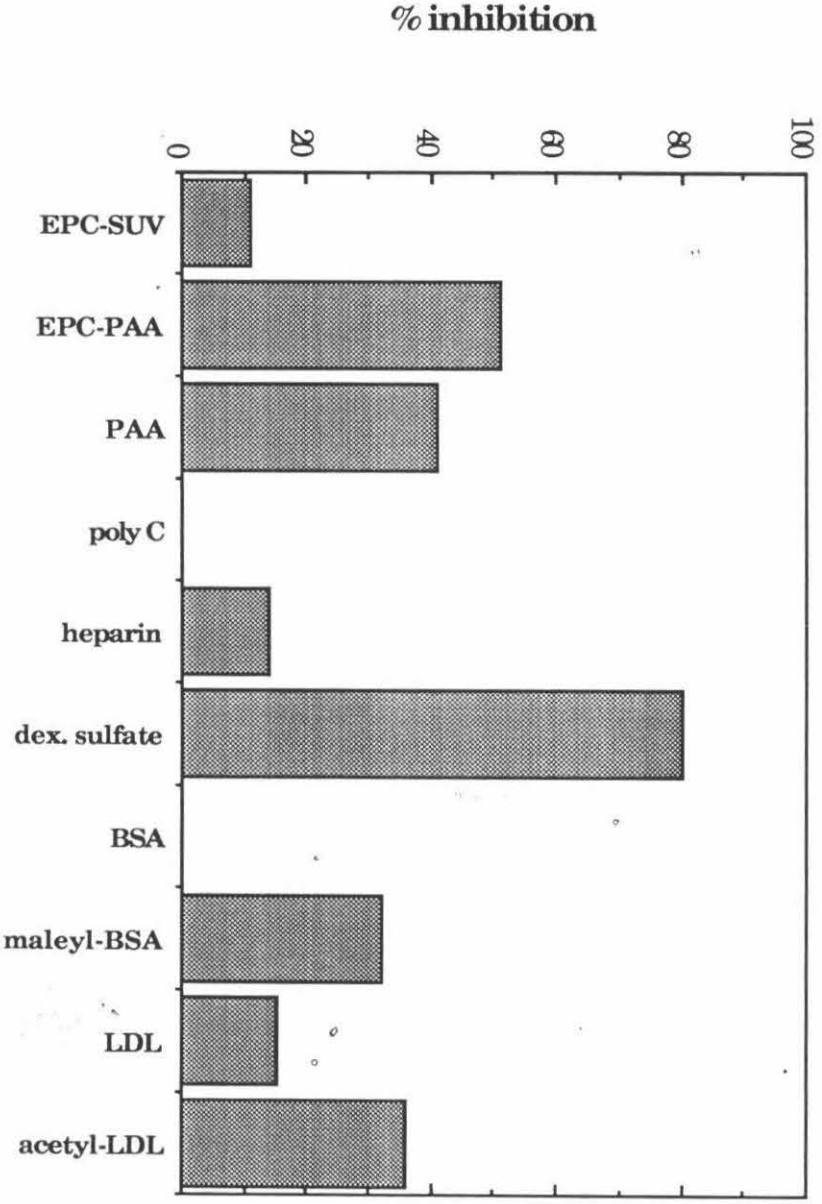
% inhibition
0
20
40
60
80
100
EPC-SUV
EPC-PAA
PAA
poly C
heparin
dex. sulfate
BSA
maleyl-BSA
LDL
acetyl-LDL

Figure 5. Schematic drawing of various mechanisms of liposome-cell interaction.

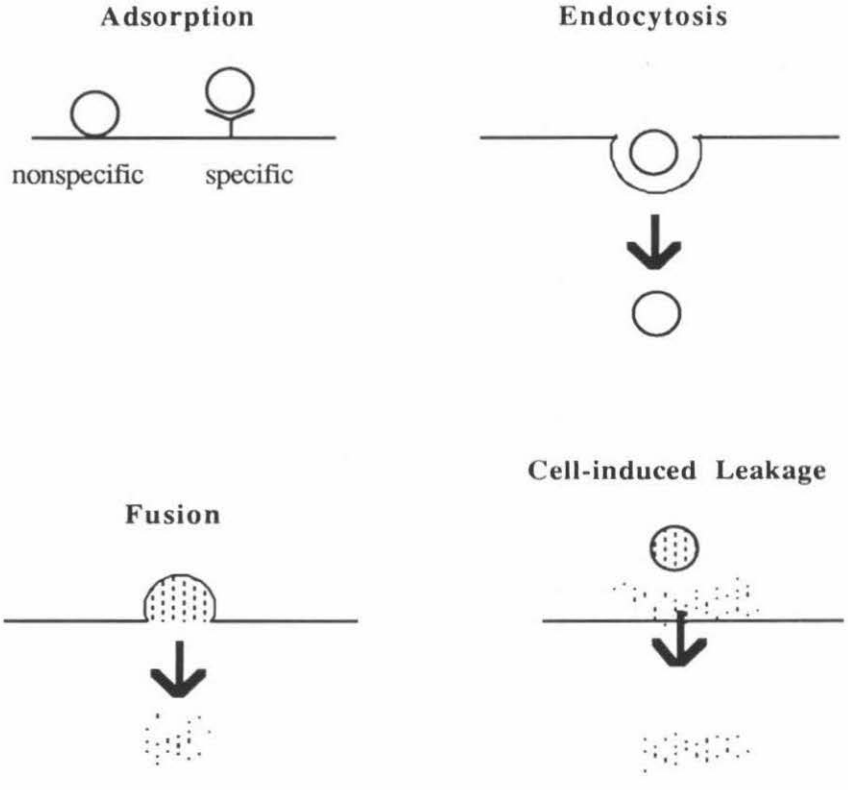
Adsorption
nonspecific
specific
Endocytosis
Fusion
Cell-induced Leakage

Chapter 7

Conclusion and Future Work

A general mechanism for pH-dependent PAA-induced vesicle destabilization was obtained from characterizing the interaction of PAA with phospholipid vesicles and monolayers using various analytical techniques. PAA induced vesicle aggregation of both multi- and unilamellar PC vesicles upon protonation, which resulted in the formation of hydrophobic sticky liposomes. Vesicle size increased with decreasing pH, and a flocculate formation was observed at low polymer concentrations due to bridging of vesicles by PAA molecules which brings the vesicles closer together. Vesicle aggregation occurred below pH 4.6, and lipid intermixing and content release was induced below pH 4.1. Since no content mixing was observed, the process is not considered to be a true membrane fusion. The increased permeability of vesicles is due to increased phospholipid packing disorder in the bilayer resulting from the collapse of vesicles into tubular, cylindrical structure. The reorientation of phospholipid headgroups caused by polymer complexation is associated with the increased phospholipid packing disorder. PAA is complexed to phospholipids through hydrogen-bonding at low pH when the polymer is protonated and more hydrophobic. Upon binding, PAA partially penetrates between the phospholipid molecule causing an expansion in the membrane packing. The increased lateral stress caused by membrane expansion probably rendered the membrane prone to aggregation and subsequent lipid intermixing.

As stated throughout the discussion sections in the previous chapters, there are many issues that can be further investigated. But rather than listing numerous possible experiments that can or should be done, two important issues that were not mentioned in detail in the chapters will be discussed. The first issue is the amount of polymer coverage

of the vesicle surface. The DSC thermograms, which show a one-phase transition peak for PAA-associated vesicles, seem to suggest that all phospholipids are associated with the polymer (Chapter 3). However, it is possible that the phase transition behavior is due to an averaging of phospholipids in different environments. Therefore, the extent of vesicle surface covered with PAA is not known. Three methods can be proposed to determine the extent of vesicle surface covered by PAA. ^{31}P-NMR can be used with paramagnetic cations, such as Mn^{+2}, to determine the percent of phospholipids on the outer surface.[1] Mn^{+2} quenches the ^{31}P-NMR signal upon binding to phosphate groups by broadening the resonance. Since Mn^{+2} does not readily cross the bilayer, only the outer membrane is bound, resulting in the phosphorous signal from the inner membrane only. Similarly, the surface area of vesicle unavailable to Mn^{+2} due to PAA complexation can be determined. However, since the PAA-complexed vesicle are very leaky (see Chapter 2), it can no longer be assumed that Mn^{+2} stays only on the outer membrane, and any results obtained would be ambiguous. The second possible method to solve the problem is by the use of a phospholipase to determine the amount of phospholipids which are not accessible to enzyme digestion due to PAA complexation. The method would work only if PAA complexation with phospholipids is strong enough that there is no exchange with unbound phospholipids. Otherwise, all phospholipids will be digested due to the rapid lateral diffusion of phospholipid membrane. (In LC phase the lateral diffusion constant is approx. 10^{-8} cm^2/s.[2]) The third method is the use of EPR spectroscopy using EPR probes covalently attached to phospholipid. If the signal from PAA-complexed phospholipids differs from that of unbound phospholipids, the percent of bound phospholipids can be determined. Since the probes are covalently attached, the problem of probe diffusion across the membrane would be circumvented. Therefore, ESR seems to be the most promising method to determine the amount of polymer surface coverage.

Membrane hydration provides a critical structural stability to the integrity of the membrane. Hydration properties of MLV can be investigated by D-NMR measurements if the lipids are hydrated by D_2O. D_2O molecules near the membrane surface show a quadrupole splitting. Because of fast exchange between the water in layers far from the membrane surface with the water at the membrane surface, the quadrupole splitting decreases with increasing water concentration. The quadrupole splitting of free water increased upon addition of PEG to vesicles.[3] This indicates a decrease in the amount of water incorporated between the lamellar and is therefore a measurement of membrane dehydration. By using this method, one can determine if bound water is partially extracted by PAA resulting in membrane dehydration or if membrane hydration is increased upon PAA-induced membrane expansion.

The results obtained in this study are limited in their general applicability to all polymers since each polymer has different characteristics. With PAA, a monolayer expansion seems to lead to vesicle destabilization. However, it is not known whether this is a general characteristics of polymers or it is limited to polymers capable of hydrogen-bonding to phospholipids. We also don't know whether all polymers capable of hydrogen-bonding would induce a monolayer expansion. It would be of general interest to find a correlation between the effect of a polymer on monolayer surface packing and the polymer's ability to destabilize or stabilize the membrane.

References

1. Mayer, L.D. et al. *Biochim. Biophys. Acta* **817**, 193 (1985).

2. Devaux, P.F. and McConnell, H.M. *J. Am. Chem. Soc.* **94**, 4475 (1972).

3. Arnold, K. Pratsch, L. and Gawrisch *Biochim. Biophys. Acta* **728**, 121 (1983).